ELASTIC ANALYSIS OF AN INHOMOGENEOUS MEDIUM WITH APPLICATIONS TO GEOMECHANICS

by

Amirabbas Katebi

July, 2014

Department of Civil Engineering and Applied Mechanics

McGill University, Montreal

A thesis submitted to

McGill University

in partial fulfillment of the requirements of the degree of

Doctor of Philosophy

To my wife and my parents

ABSTRACT

This thesis presents analytical and computational analysis of boundary value problems and mixed boundary value problems for incompressible non-homogeneous elastic geomaterials. The study of the mechanics of non-homogeneous elastic media has always occupied a prominent position in the literature in mechanics. Quite apart from the intrinsic mathematical interest, the non-homogeneity problem in elasticity has applications to many problems of technological importance. In this thesis, two types of elastic non-homogeneity in the shear modulus are considered; one with exponential variation of shear modulus over the entire halfspace region and the other one with exponential variation of shear modulus over a finite depth, beyond which the shear modulus is assumed to be constant. The choice of exponential variation of shear modulus stems from the experimental evidences related to measurement of elastic properties of British Clays in which it is shown that elastic modulus of elasticity increases with depth.

The general equation governing the axisymmetric elastic non-homogeneity is presented for both types of the non-homogeneity considered in this thesis. The thesis, in general, deals with two types of problems, (i) boundary value problems (ii) mixed boundary value problem or contact problems. In both cases, the influence of non-homogeneity on the response of the halfspace was clearly shown by numerical results presented. Furthermore, where applicable, the results have been used to verify the finite elements analysis results which can be used ultimately as a benchmark to solve more complex problem encounters in geomechanics.

Boundary value problems includes, (i) the interior loading problem of an incompressible isotropic elastic halfspace where the shear modulus varies exponentially over the entire depth, or the shear modulus varies exponentially over the finite region, beyond which it is constant (ii) the surface loading problem of a non-homogeneous elastic medium where the medium is characterize as a

layer of finite depth *d* and of infinite lateral extends and the shear modulus has an exponential variation over the finite depth *d*. (iii) The axisymmetric distributed radial loading on the surface of an incompressible non-homogeneous elastic halfspace where the shear modulus varies exponentially with depth.

Mixed boundary value problems includes, (i) the axisymmetric smooth and adhesive indentation problem for a rigid circular plate and an incompressible elastic halfspace with exponential variation of shear modulus. The method of solution is based on the discretization technique in which the contact normal and contact shear stress distributions are approximated by their discretized equivalents. (ii) The indentation problem of flexible circular plate with an incompressible non-homogenous elastic halfspace using the energy method where the shear modulus of elasticity varies exponentially with depth. The contact between the flexible plate and the elastic halfspace is solved using a variational approach in which the deflected shape of the plate is represented in the form of a power series expansion which satisfies the kinematic constraints of the plate deformation.

RÉSUMÉ

Cette thèse présente l'analyse analytique et numérique de problèmes aux limites et problèmes aux limites mixtes de géomatériaux incompressibles, non homogènes et élastiques. L'étude de média non-homogène et élastique a toujours occupée une place importante dans les publications traitant de la mécanique. Mis à part l'intérêt qu'y accordent les mathématiques intrinsèques, le problème de non-homogénéité en élasticité s'applique à de nombreux problèmes d'importance technologique. Dans cette thèse, deux types de non-homogénéités élastiques sont considérés; la variation exponentielle du module de cisaillement sur toute la région du demi-espace et la variation exponentielle du module de cisaillement selon une profondeur déterminée, au-delà desquels le module de cisaillement est supposé demeurer constant. Le choix de la variation exponentielle est basé sur des analyses expérimentales de mesures d'élasticités menées sur des échantillons d'Argile Anglaise pour lequel il a été démontré que le module d'élasticité augmente avec la profondeur.

L'équation générale qui gouverne la non-homogénéité élastique et axisymétrique est présentée pour les deux cas de non-homogénéité considérés dans cette thèse. D'un point de vue général, la thèse traite de deux types de problèmes : (i) les problèmes aux limites et (ii) les problèmes aux limites mixtes ou problèmes de contact. Dans les deux cas, l'influence de la non-homogénéité sur la réaction du demi-espace est clairement démontrée par les résultats numériques présentés. De plus, là où applicable, les résultats obtenus ont été utilisés pour vérifier les résultats de l'analyse par la méthode des éléments finis qui peut être utilisée comme point de référence pour résoudre des problèmes plus complexes en mécanique des sols.

Les problèmes aux limites inclus, (i) le problème de charge interne d'un demi-espace incompressible, isotropique et élastique où le module de cisaillement varie exponentiellement selon la profondeur ou la région déterminée, au-delà desquels il est supposé demeurer constant. (ii)Le problème de charge en surface d'un média

non-homogène et élastique où le média est caractérisé par une couche d'une profondeur déterminée d et d'une étendue latérale infinie et où le module de cisaillement a une variation exponentielle sur toute la profondeur d. (iii) La charge radiale distribuée axisymétriquement sur la surface incompressible, non-homogène et élastique où le module de cisaillement varie exponentiellement selon la profondeur.

Les problèmes aux limites mixtes inclus, (i) le problème axisymétrique d'échancrure lisse et adhésive pour une plaque rigide et circulaire et un demi-espace incompressible et élastique et selon une variation exponentielle du module d'élasticité. La méthode de résolution de ce problème est basée sur la technique de discrétisation dans laquelle la contrainte normale et en cisaillement sont estimés par leur équivalent discret. (ii) Le problème d'échancrure d'une plaque flexible et circulaire et d'un demi-espace incompressible, non-homogène et élastique, en utilisant la méthode énergétique, où le module élastique de cisaillement varie exponentiellement selon la profondeur. Le contact entre la plaque flexible et le demi-espace élastique est résolue en utilisant une approche de calculs des variations dans lesquels la forme de la plaque en flexion est représentée par l'expansion d'une série de puissance qui satisfait les contraintes cinématiques de déformation de la plaque.

ACKNOWLEDGEMENTS

The author wishes to express sincere appreciation and gratitude to his doctoral research supervisor, Professor A.P.S. Selvadurai, *William Scott Professor and James McGill Professor*, Department of Civil Engineering and Applied Mechanics, McGill University, for suggesting the research topic, his extensive guidance, encouragement and support during this research. Professor Selvadurai's extensive corrections to the research papers resulting from the work are gratefully appreciated. The financial support provided by NSERC Discovery Grant awarded to Professor Selvadurai is also acknowledged.

Sincere thanks and appreciation also go to my colleagues in the Environmental Geomechanics group at Department of Civil Engineering and Applied Mechanics, McGill University for creating a friendly and supporting environment; namely, Mr. Cyrille Couture, Mr. Adrian Glowacki, Mr. B. Hekimi, Mr. L. Jenner, Mrs. Juen Kim, Dr. Meysam Najari, Dr. Alex Suvorov. The author wish also thanks Technical Staff of the Department Civil Engineering and Applied Mechanics at McGill University, notably Mr. Gerard Bechard, Mr. John Bartczak, Dr. Bill Cook and Mr. Jorge Sayat. Special thanks are due to Mrs. Sally Selvadurai for her extensive editorial correction of drafts of the research papers and the thesis. Sincere thanks and appreciation goes to Mr. Cyrille Couture for his assistance in translating the abstract of this thesis into French.

Finally, the author wishes to express his deepest thanks to his wife, Ghazaleh Tasoji Azar, his Parents, Mr. Mohammadali Katebi and Mrs. Fatemeh Forghani Ramandi and his brothers and sister, Mr. Mohammad Katebi, Mr. Mohsen Katebi and Miss Maryam Katebi for their prolonged understanding, support and encouragement during the course of this work.

CONTRIBUTIONS AND STATEMENTS

a. Articles published in refereed journals

- Katebi A., Selvadurai A.P.S. (2014) A frictionless contact problem for a flexible circular plate and an incompressible non-homogeneous elastic halfspace. International Journal of Mechanical Sciences, 90, 239-245. doi:10.1016/j.ijmecsci.2014.10.017
- Selvadurai A.P.S., Katebi A. (2014) An Adhesive Contact Problem for an Incompressible Non-homogeneous Elastic Halfspace. Acta Mechanica, 226, 249-265. http://dx.doi.org/10.1007/s00707-014-1171-8
- Katebi A., Selvadurai A.P.S. (2013) Undrained behaviour of a non-homogeneous elastic medium: the influence of variations in the linear elastic shear modulus. Géotechnique, 63, 1159-1169. http://dx.doi.org/10.1680/geot.12.P.164
- Selvadurai A.P.S., Katebi A. (2013) Mindlin's problem for an incompressible elastic halfspace with an exponential variation in the linear elastic shear modulus. International Journal of Engineering Science, 65, 9-21. http://dx.doi.org/10.1016/j.ijengsci.2013.01.002

b. Most significant contributions to research and development

The thesis presents an analysis of the axisymmetric adhesive contact problem for a rigid circular plate and an incompressible elastic halfspace where the linear elastic shear modulus varies exponentially with depth. To the author's knowledge, this problem has not been investigated in the literature on contact problems. In particular, the method of solution is based on the discretization of the contact normal stresses and the contact shear stresses in the bonded region. This technique yields a set of algebraic equations that can be solved to develop results of engineering interest. In the classical problem for the adhesive indentation of an isotropic homogeneous elastic halfspace, the indentational stiffness is controlled by Poisson's ratio for the deformable medium and, in the case of an *incompressible homogeneous elastic halfspace region*, the interface conditions (either frictionless or fully bonded) have no influence on the elastic stiffness. This is due to the zero radial displacement at the surface of the halfspace for Boussinesq's problem for the concentrated normal force acting on an

incompressible halfspace. It is observed that for the exponential variation in shear modulus in an incompressible elastic halfspace, the contact constraints, either adhesive contact or frictionless, also have very negligible influence on the indentational stiffness of the rigid circular indenter and for the exponent in the exponential variation $\tilde{\lambda} \in (0, 0.25)$ .The discrepancy is of the order of 10% for $\tilde{\lambda} \approx 2$.

The contact problem was extended to examine, using a variational technique, the axisymmetric smooth contact between a flexible plate and an incompressible isotropic non-homogeneous elastic halfspace in which the shear modulus varies exponentially with depth. This problem has not investigated in the literature in the case where shear modulus of elasticity varies non-linearly with depth. The effect of relative rigidity of the plate as well as the non-homogeneity of the incompressible elastic halfspace on the flexural response is clearly demonstrated in the numerical results.

TABLE OF CONTENTS

LIST OF TABLES

LIST OF FIGURES

CHAPTER 1

INTRODUCTION AND LITERATURE REVIEW

1.1 General

This thesis presents analytical and computational solutions to traction and mixed boundary value problems for an inhomogeneous medium with applications to geomechanics. The term analytical solution, in the engineering context, refers to the use of advanced mathematical techniques to develop a solution to problems encountered in engineering. Geotechnical engineers have used analytical solutions to examine a variety problems in soil mechanics and geomechanics. One of the advantages of the analytical solutions is that they can provide/have provided reliable, convenient and speedy preliminary estimates to a large number of problems in geomechanics. Secondly, these solutions are not only usable for the problems encountered in geomechanics but also give insight into the behavior and mechanics of the problem; this helps the researchers reach a better understanding of the problem. These two aspects together, a quick and reliable estimation and insight into the behavior and mechanics of the problem, can provide engineers with the basis to make sound engineering judgments. The other advantage of

analytical solutions is that they can be used as a check on more sophisticated computer-based solutions. Due to the increasing use of computational methods to solve a wide range of problems, it is very important and valuable for users, in view of uncertainties of input data, to see that the software is able to give accurate results to the problems under investigation, a check that can be provided by analytical solutions.

Boussinesq's fundamental solution (Boussinesq, 1885) dealing with the action of a concentrated normal force on the surface of an isotropic homogeneous elastic halfspace represents a solution that is widely applied in geomechanics (see also Selvaudrai, 2001a, 2007). The use of mathematical theories of elasticity in geomechanics dates back to the fundamental solution of Boussinesq (1885) in which he considered an isotropic homogeneous elastic halfspace subjected to a concentrated force acting normal to a traction free surface. This problem can be solved using several techniques and approaches and, for those interested in the mathematical procedures of these approaches and boundary conditions of the problem, it is well documented in the literature (Michell, 1900; Love, 1927; Westergaard, 1952; Sokolnikoff, 1956; Lur'e, 1964; Timoshenko and Goodier, 1970; Podio-Guidugli, 2004). Following Boussinesq (1885), Flamant (1892) investigated the problem of a line load acting on an isotropic elastic halfspace using Boussinesq's solution along with the principal of superposition. The problem of a horizontal point load acting at the surface of an elastic halfspace was first considered by Cerrutti (1882) in which the displacements and stresses are presented in Cartesian coordinates due to the absence of radial symmetry. Mindlin (1936) considered the point load problem (either vertical or horizontal) in which the load is acting in the interior of an elastic halfspace. The literature pertaining to this class of problems is quite extensive and no attempt will be made to provide a comprehensive bibliography. The reader is referred to the references (Sneddon, 1951; Goodier, 1958; Koronev, 1960; Rakov and Rvachev, 1961; Gurtin, 1972; Gladwell, 1980; Selvadurai, 1979a, 1996, 2000b) for adequate coverage of the topic. There are also two extensive reviews of the topic "analytical methods in geomechanics" given by Booker (1991) and Selvadurai (2007). Selvadurai (2007)

presents an extensive review on the application of analytical methods in the theory of elasticity and poroelasticity to solve boundary value problems encountered in geomechanics.

2.1 Elastic non-homogeneity

The mechanics of non-homogeneous elastic media has been a topic of continuing interest to theoretical and applied solid mechanics. The non-homogeneity problem in elasticity has applications to many problems of technological importance. Non-homogeneity is generally attributed to an alteration of the elastic properties of the body due to mechanical working and, on occasion, to chemical action (Selvadurai, 2007). In the context of geomechanics, the inhomogeneous medium serves as a model for the study of soil and rock media that exhibit spatial variations in their elastic properties.

Studies of specific interest to the elastomechanics of non-homogeneous media date back to the early studies by Klein (1956), Korenev (1960), Mossakovskii (1958), Popov (1959) and Rostovtsev (1961, 1964). Reviews of the subject are also given by Rakov and Rvachev (1961), Olszak (1959) and Popov (1973). The type of problems discussed in these developments mainly focused on elastic contact problems referred to halfspace regions, where the elastic modulus varied with the axial coordinate and Poisson's ratio was assumed to be constant. Also, the specific forms of elastic non-homogeneity dealt with either a linear, an exponential or a power law variation in the elastic modulus with the axial coordinate. The resulting solutions have been applied quite extensively in contact and indentation problems with application to the engineering sciences.

Korenev (1957) examined the problem of the axisymmetric indentation of a rigid smooth indenter and an isotropic elastic halfspace, whose modulus of elasticity varied exponentially with depth. This problem was also examined by Mossakovskii (1958) who gives a corrected result for the contact stress distribution. The interaction between an unbounded plate and a non-homogeneous medium whose elastic modulus varies with depth according to a power law was

considered by Popov (1959). Rostovtsev (1961) also examined the variation in the elastic modulus of the halfspace in the form of a power law and developed results applicable to elliptical indentation regions. Ter-Mkrtch'ian (1961) presents the development of the elastic non-homogeneity where the shear modulus varies with depth according to a power law. Lekhnitskii (1962) developed solutions to the half plane problem where the elastic modulus varies with the r and θ coordinates. The study by Rostovtsev (1964) also examines both two-dimensional and axisymmetric problems related to the loading of a half plane. Zarestsky and Tsytovich (1965) investigated contact stresses beneath a rigid strip in which the elastic modulus varies according to a power law variation. Belik and Protsenko (1967) also examined the two-dimensional contact problem for a half plane where the elastic modulus varies as a power law for the depth variable. Kassir (1970) solved the Reisssner-Sagosi problem for a non-homogeneous halfspace with power law variation in the elastic modulus. Boussinesq's problem for a non-homogeneous medium where the elastic modulus varies exponentially with the axial spatial variable was presented by Plevako (1971). A solution to Boussinesq's problem for a halfspace with an exponetial variation in the elastic modulus was presented by Rostovtsev and Khranevskaia (1971). The axisymmetric loading of a non-homogeneous elastic layer with a hyperbolic depth-dependent variation in the elastic modulus and underlain by a homogeneous elastic halfspace was examined by Plevako (1972). Other studies by Plevako (1973a,b) considered the shear loading of a non-homogeneous elastic halfspace with a hyperbolic variation in the elastic modulus. The surface loading of the halfspace with a power law non-homogeneity was examined by Plevako (1973c), who also investigated the interior loading of a non-homogeneous elastic layer underlain by a homogeneous elastic halfspace (Plevako, 1974). Puro (1973) presents a Hankel transform development of three-dimensional problems where the modulus of elasticity varies as a power function of depth. The axisymmetric adhesive contact problem for a non-homogeneous elastic halfspace was presented by Popov (1973). Kassir and Chuaprasert (1974) present the surface displacement and stresses for the torsional indentation of a non-homogeneous halfspace in

which the elastic modulus varies according to a power law. Kassir and Chuaprasert (1974) also examined the axisymmetric problem of a rigid punch in which the elastic modulus varies as a power law in depth. Dhaliwal and Singh (1978) investigated torsion of a circular die in a non-homogeneous elastic layer that is bonded to a non-homogeneous halfspace, where it is assumed that the shear modulus is different in the elastic layer and in the halfspace and it varies according to a power law.

The renewal of interest in the application of the theory of elasticity for a non-homogeneous elastic medium commenced with the seminal paper by Gibson (1967) who examined a model of an incompressible elastic halfspace where the shear modulus varies linearly with depth. Gibson (1967) showed that when the shear modulus of the incompressible medium varied linearly from zero at the surface of the halfspace, the surface displacement profile exhibited a discontinuous form with displacements restricted only to the loaded region. Furthermore, the magnitude of the deflection within the loaded region was directly proportional to the intensity of stress at the loading point and inversely proportional to the linear increase in the elastic shear modulus with depth. Gibson's research provided a definitive explanation for a Winkler medium (Winkler, 1867; Hetényi, 1946; Selvadurai, 1979a), which is comprised of a series of closely spaced independent springs with identical stiffness. The elastic stiffness for the spring elements can be interpreted in terms of the linear variation of the shear modulus with depth for the specific case where the surface shear modulus is zero. The elastic halfspace with this particular variation in shear modulus is referred to as a 'Gibson soil', and has been extensively studied by a number of researchers. Gibson et al. (1971) examined the behaviour of an incompressible layer of finite depth of resting on a rough rigid base in which the elastic modulus in the finite layer varies linearly with depth. Brown and Gibson (1972) studied the surface displacement of an elastic halfspace whose Young's modulus increases linearly with depth, and is subject to a uniform strip or circle load.

Awojobi and Gibson (1973) investigated the influence of a linear variation in the shear modulus with depth on the stresses and displacements of a halfspace subjected to normal loading of a traction free surface. Alexander (1977) presented the stresses and displacements in an incompressible isotropic elastic halfspace in which the Young's modulus varies linearly in depth and which is subject to a load normal to its plane boundary.

Calladine and Greenwood (1978) examined line and point loads applied to the surface of an elastic non-homogeneous isotropic halfspace with a linear variation of the shear modulus. The torsional problem of a rigid foundation embedded in a non-homogeneous soil with a weathered crust, in which the shear modulus of the elastic soil increases linearly with depth while the shear modulus of the weathered crust decreases, was investigated by Rajapakse and Selvadurai (1989). The application of a concentrated load to the interior of an elastic halfspace where the linear elastic shear modulus varies linearly with depth was examined by Rajapakse (1990a) while Rajapakse and Selvadurai (1991) examined the mixed boundary value problem related to the interior loading of a non-homogeneous isotropic elastic halfspace by a flexible plate.

As described above, the majority of the theoretical developments prior to Gibson's studies have focused on power law or exponential variations in the linear elastic shear modulus, which lead to significant simplifications in the solution of the associated elasticity problem. The idealization of the elastic non-homogeneity in either a linear or an exponential form restricts its applicability to the study of boundary value problems relevant to halfspace regions. In particular, both exponential and linear variations in the shear modulus with depth give rise to unbounded values of the shear modulus when the theoretical developments are applied to semi-infinite regions. This limitation was first addressed by Selvadurai et al. (1986), who examined the torsional indentation of an inhomogeneous elastic halfspace with an exponential but bounded variation in the shear modulus. The accurate representation of both the near surface non-homogeneity and far-field variation are important for estimating the undrained displacements of

inhomogeneous soils that are subjected to surface and interior loads. Selvadurai (1996) also examined the problem of the smooth indentation of an incompressible inhomogeneous elastic halfspace where the shear modulus exhibits a bounded exponential variation.

The studies by Selvadurai and Lan (1997, 1998) consider contact and crack problems where the elastic shear modulus exhibits a harmonic variation. A more generalized approach to the formulation of spatial inhomogeneity is described by Spencer and Selvadurai (1998), who examine the problem of anti-plane shear in cracks and edge dislocations in a non-homogeneous elastic solid. An alternative approach to modeling the depth-dependent non-homogeneity in a halfspace is to use a layered system approach to represent the variation in the elastic moduli (Yue et al., 1999) or the more generalized approach that was presented by Spencer and Selvadurai (1998). Selvadurai (2000c) have also considered the exponential variation in the linear shear modulus to examine penny shaped inclusion problem. The analysis of elastic non-homogeneity is not limited to analytical solutions; numerical approaches are also considered by some researchers (such as Carrier and Christian, 1973a,b; Chow, 1987; Dempsey and Li, 1995; Aliabadi and Brebbia, 1993; Jeng and Lin, 1999).

1.3 Incompressibility

In this thesis, it is assumed that the material of the halfspace is incompressible, which simulates immediate (undrained) deformation of saturated elastic soils. In other words, at the start of the consolidation the behavior of the poroelastic medium at time zero corresponds to the incompressible behavior of an elastic medium.

Geotechnical engineers, in particular foundation engineers, are often interested in determining the profile of the surface displacement and, in general, to estimate the magnitude of the settlement during construction. This immediate settlement (or elastic settlement) occurs based on the fact that the clay, which is usually saturated, does not have the opportunity to consolidate in the short term.

Compression of saturated soil elements is caused by deformation of the soil skeleton or expulsion of water from the void space. For saturated soil in practice, it is usually found that the water in the pores is almost incompressible in comparison with the grain skeleton of the solid and any compression must be accompanied by expulsion of water from the pore space; therefore, the immediate displacement takes place without any volume change.

Numerous studies, which were mentioned in the previous section, have considered the material of the halfspace to be incompressible (see e.g. Zarestsky and Tsytovich, 1965; Gibson, 1967; Gibson et al., 1971; Carrier and Christian, 1973a; Alexander, 1977; Calladine and Greenwood, 1978; Rajapakse, 1990a,b; Rajapakse and Selvadurai, 1991; Yue et al., 1999).

1.4 Objectives and scope of the research

This thesis presents the analytical and computational solutions to traction and mixed boundary value problems of inhomogeneous media with applications to problems encountered in geomechanics.

The second chapter provides the justification for considering incompressible elastic non-homogeneity, which stems from the results of experimental investigations where it has been shown that the shear modulus of many soils increases with depth. Also, a number of commonly used testing methods to determine the elastic moduli as well as terrain formations are briefly discussed.

In chapter 3, the development of the partial differential equations governing the incompressible elastic non-homogeneity problem is presented.

The axisymmetric interior loading problem for an incompressible isotropic elastic halfspace where the linear elastic shear modulus varies with depth is investigated in chapter 4. In particular, the non-homogeneity has an exponential variation either over the entire depth of the halfspace, or over a finite depth beyond which it is constant. The mathematical formulation of the traction boundary value problem is developed through the application of integral transform techniques, and the

numerical results are presented to show the influence of the non-homogeneity on the responses of an incompressible elastic halfspace. The numerical results are also used to establish the accuracy of finite element results for the analogous problems.

The axisymmetric smooth/adhesive contact problem for a rigid circular plate and an incompressible elastic halfspace where the linear elastic shear modulus varies exponentially with depth is examined in chapter 5. The analytical solution of the mixed boundary value problem entails a set of coupled integral equations that cannot be solved easily through conventional techniques proposed in the literature. A discretization scheme is adopted where the contact normal and contact shear stress distributions are approximated by their discretized equivalents. The consideration of compatibility of deformations due to indentation by a rigid indenter in adhesive contact gives a set of algebraic equations that yield the discretized equivalents of the contacts stresses and the axial stiffness of the rigid indentor.

In chapter 6 A departure from this model, a smooth contact problem for an isotropic elastic halfspace indented by a flexible circular plate, is examined using an energy method. The contact between the flexible plate and the elastic halfspace is solved using a variational approach. This method is an extension to the variational approach first adopted by Selvadurai (1979c) for examining the static contact between flexible plate and an isotropic homogeneous elastic halfspace. The Poisson-Kirchhoff thin plate theory is used to describe the flexural behaviour of the plate. The results for the maximum deflection, the relative deflection, and the maximum flexural moment in the circular plate are presented and the influence of non-homogeneity on the results investigated. In addition, the results obtained using this technique is compared with equivalent results derived from the finite element approach.

CHAPTER 2

DEPTH VARIATION OF ELASTIC MODULI

2.1 Introduction

Reliable estimates of the geotechnical properties and deformation parameters of the ground surface are a fundamental requirement of any foundation design. Deformation parameters of the ground surface are generally related to the small strain shear moduli, Poisson's ratio and Young's modulus.

There is extensive literature related to the classification, deformability and other geotechnical properties of Clays and mudrocks found in UK. It should be mentioned that there is little information in the literature regarding deformation parameters of clay formations other than UK Clays. The main focus of the chapter is to collect the published values regarding depth variation of the shear modulus for different territory formations and briefly discuss the various test procedures. Determinations of elastic moduli in the literature were made using different testing methods, such as the triaxial compression test, in-situ pressuremeter test and plate loading test, on materials from various locations and territories.

Consequently, the values presented here are only used to show the ranges and averages of the parameters and cannot necessarily be considered as typical values for the formation as a whole.

The properties of overconsolidated clays and mudrock in the UK generally depend on the lithology, geological loading history, degree of weathering, and testing methods. In most classifications, there is no geological distinction between mudrocks and overconsolidated clays since both contain more than 50% particles with a diameter of over 60μm (the effective size of clay particles in UK). The definition of modulus of elasticity in this review refers to the secant modulus for the initial stress-strain curve at 50% ultimate load in undrained triaxial compression tests.

Because of the importance of the testing method on the determination of the elastic moduli, a number of commonly used methods will be discussed briefly in the following section.

2.2 Testing methods

The type and method of the test is one of the important factors that will affect the accuracy and reliability of the each experimental result. The most common laboratory and in-situ tests used in the literature to determine the elastic moduli of Clay and mudrocks from the UK are the triaxial compression test, plate loading test and in-situ pressuremeter test.

The undrained triaxial test is one of the most commonly used laboratory tests to determine the elastic moduli of overconsolidated clays and mudrocks. The moduli determined from laboratory tests on highly fissured Clays from the UK are considerably lower than those obtained from large in-situ plate tests (Marsland, 1973a). The elastic moduli determined from triaxial tests are very variable and difficult to interpret and they are dependent on factors such as the amount of disturbance of the clay during sampling, the time between the test and sampling, the size of the spicemen and the reduction of the overburden pressure. A full

description of the sampling methods and triaxial test procedure on London Clay can be find in Marsland (1973 a,b).

The most common in-situ tests for determining deformation moduli are the plate loading test and pressuremeter test. The plate loading test and pressuremeter test have been employed to measure deformation moduli in order to mitigate the effect of sample disturbance and sample size and consequently give more reliable results. Details of the test procedure are given in the paper by Marsland (1973b). Marsland (1973c) conducted an extensive series of in-situ plate loading test with different plate dimensions, up to 865 mm, to a depth 25 m in order to make a comparison and also validate the results determined from triaxial tests. Marsland (1973c) considered the different factors affecting triaxial and plate loading tests, such as the sample size, disturbance of the clay, interval time between the sampling and testing for triaxial tests and the interval time between excavation and loading for the plate loading tests. Although the disturbance of the clay has a significant effect on the results of the laboratory tests, the most important factor affecting the triaxial test was the interval time between the sampling and testing. On the other hand, the size of the plate and method of site preparation were more important in the plate loading tests. Figure 2.1 (Marsland, 1973c) shows the variation of the elastic moduli for London Clay from Hendon; the results are from triaxial tests on 38 and 98 mm diameter samples and a 865mm diameter plate loading tests.

As can be seen from Figure 2.1, the results determined from the triaxial tests are variable and hard to interpret and are considerably lower than those determined from the plate loading tests. By comparing the triaxial tests conducted on 38 and 98 mm diameter specimens, it can be seen that the elastic moduli of the 38mm diameter specimen gave average moduli up to 1.3 times higher than for the 98mm diameter specimen.

Marsland concluded that the average elastic moduli determined from large plate loading tests were more compatible with the observations of ground movements and the analysis of settlement records, such as given in Hooper (1973), in

comparison with the results of laboratory tests and small plate loading tests. The comparison between the results from an analysis of settlement records (Hooper, 1973) and those determined from laboratory and in-situ tests (Marsland, 1973c) is given in Figure 2.2. Furthermore, it can be noted from Figures 2.1 and 2.2 that the in-situ plate loading tests are also sensitive to experimental procedures and should only be used with complete information of the test conditions.

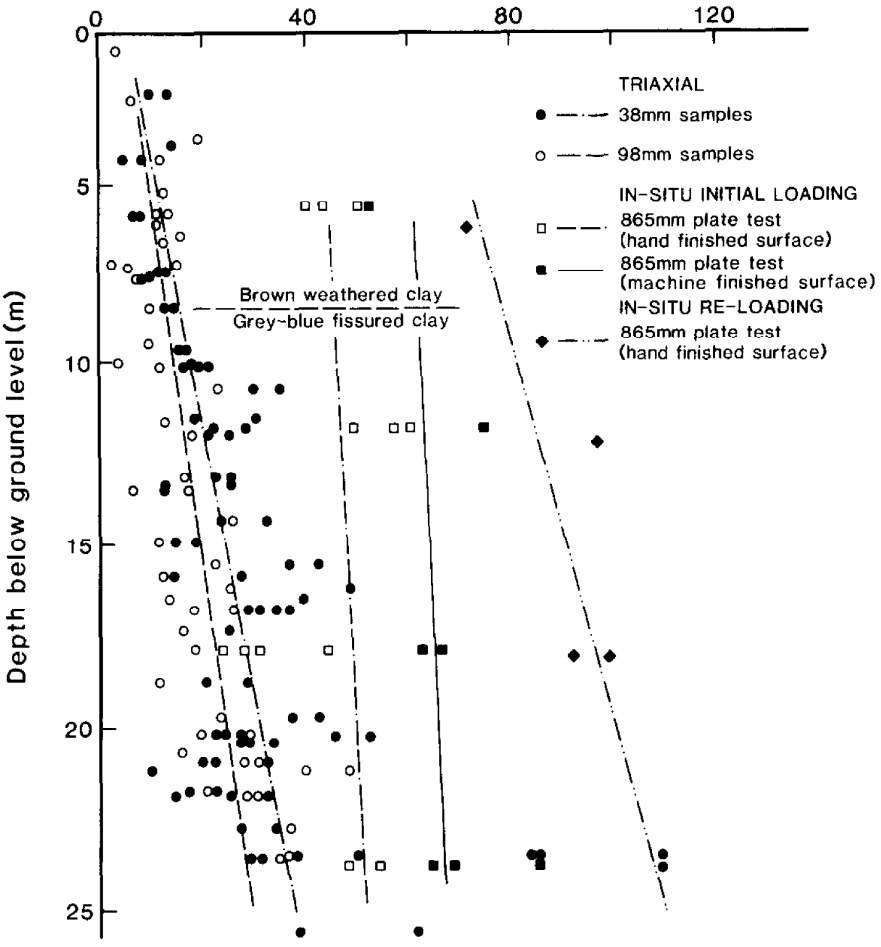

Figure 2.1: Modulus of elasticity of London Clay from Hendon (after Marsland, 1973c)

The other common in-situ test is the pressuremeter test. The general test procedures and equipment descriptions are presented by Marsland and Randolph (1978) for pressuremeter tests. Marsland and Randolph (1978) conducted a comparison between the results determined from plate loading tests using a 865 mm diameter plate and a pressuremeter test using a 60 mm diameter probe, to a depth of 25 m in London Clay. The results for the variation of shear modulus with depth for the plate loading and pressuremeter tests on London Clay are presented by Marsland and Randolph (1978) for initial loading as well as re-loading cycles.

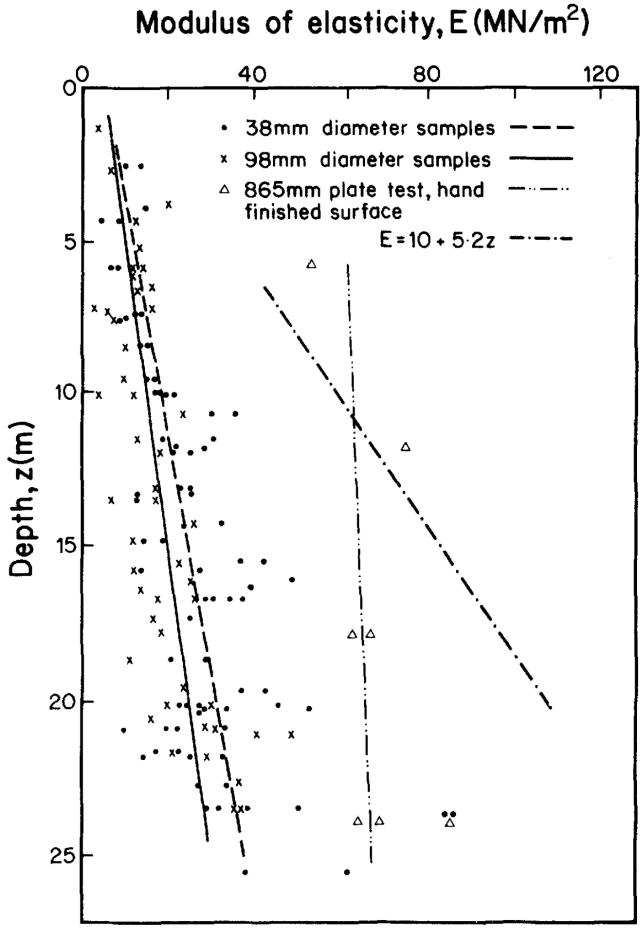

Figure 2.2: Initial secant moduli of London Clay from Hendon; (triaxial and plate loading tests); (Marsland, 1973c) and the modulus of elasticity of London Clay from Hyde Park interpreted from settlement calculation (Hooper, 1973)

Marsland and Randolph (1978) concluded that the shear moduli obtained from pressuremeter tests are considerably lower than those obtained from plate loading tests, especially for initial loading. There is a large difference between the values obtained for the initial loading and re-loading cycles that can be attributed to softening of the clay at the sides of the borehole during drilling and during the unloading period. The shear modulus determined from the unloading cycles in the pressuremeter tests give more reasonable values, which are much closer to the values obtained from the plate loading tests. The results obtained from both tests showed that the shear modulus increases with depth and is considerably higher at greater depths. These tests were performed at depths of 6.1, 12.2, 18.3 and 24.4 m below ground level. Since these tests encompass a volume of soil that has enough fissures and other planes of weakness, they can be considered as representative of the full scale.

2.3 Variation of modulus of elasticity with depth

In this thesis the half-space is considered to be elastic and non-homogeneous. The justification for considering elastic non-homogeneity stems from results of experimental investigations (see e.g. Skempton and Henkel, 1957; Ward et al., 1965; Hooper and Butler, 1966; Burland and Lord, 1969; Simons and Som, 1969; Cooke and Price, 1973; Marsland, 1973 a,b,c; Butler, 1974; Hobbs, 1974; Atkinson, 1975; Burland et al., 1977; Abbiss, 1979; Simpson et al., 1979; Costa Filho and Vaughan, 1980), in which it is shown that the shear modulus of many soils generally increases with depth, although not always systematically. The early work by Skempton and Henkel (1957) on London Clay suggested that the modulus of elasticity increases with depth. Ward et al. (1965) conducted a series of in-situ and laboratory test to obtain the geotechnical properties of London Clay at Ashford Common at different depths, varying from 30ft to 140ft; they reported that the modulus of elasticity increases with depth, but the rate of the increase is more rapid at larger depths. He observed from the test results that the secant moduli increase after 91 ft (27.7368 m).

Similar observations by Marsland (1973 a,b,c) on London Clay using both triaxial and plate loading tests show that the elastic modulus increases with depth; however, it can be observed from these and other studies that the triaxial test results are very variable. The results from large in-situ plate load tests are more consistent and are also typically higher than those obtained from laboratory triaxial tests. By comparing the laboratory values with the plate load test results, Marsland (1973c) noted that the modulus of elasticity values given by the plate tests are much closer to those derived from the analysis of settlement records (Hooper, 1973). Instrumented pile test results presented by Cooke and Price (1973) also support this view.

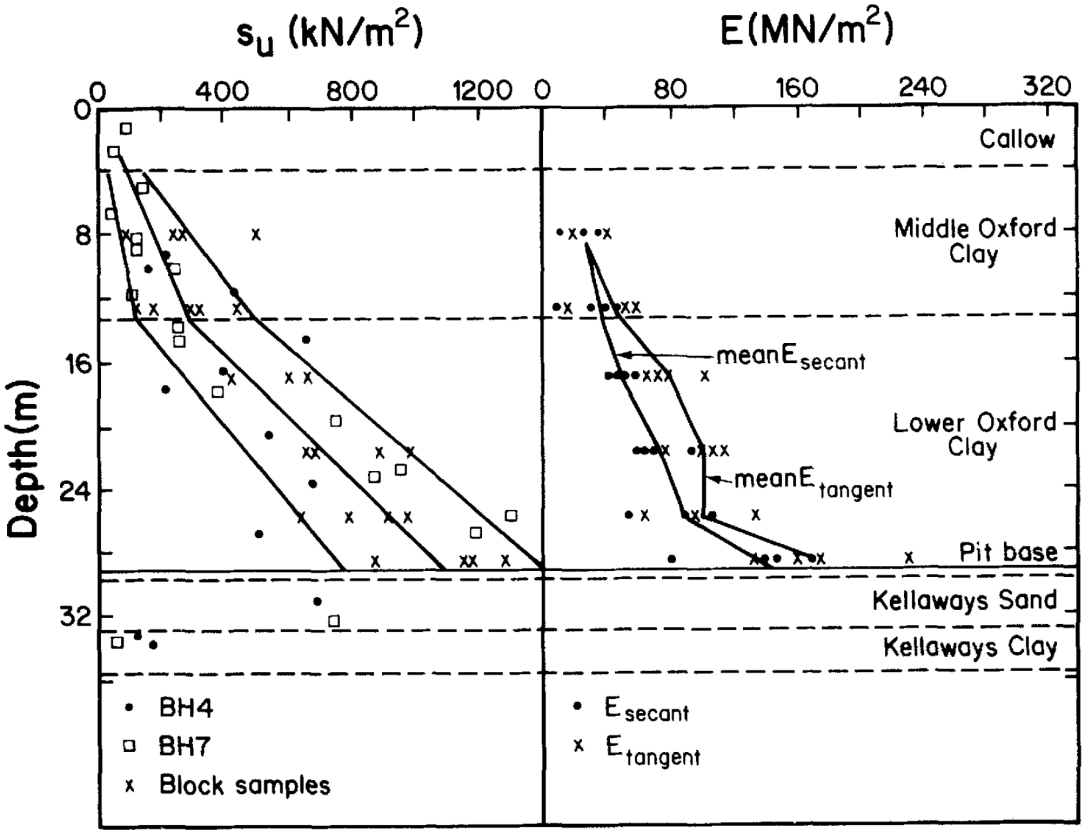

Figure 2.3. Undrained shear strength and modulus of elasticity of Oxford Clay from near Peterborough (Burland et al., 1977)

Cooke and Price (1973) reported on the variation of the modulus of elasticity with depth for distributed clay close to a concrete pile installed in London Clay at Hendon, North London, in which the clay extended from the ground surface to a depth of 30m and the pile was seated to a depth of 3.5 m. The shear modulus varied from 70 MPa at the ground surface to 150 MPa at a depth of 3.5 m, which is comparable with the results obtained from an analysis of settlement records (Hooper, 1973).

Burland et al. (1977) studied the depth variation in the geotechnical properties of Oxford Clay and Kellaways Beds at Saxon pit; the results, obtained from excavation and laboratory tests, showed that the vertical Young's modulus increases with depth, although the variation is not necessarily linear (See Figure 2.3). As we can see from Figure 2.3, the rate of increase in the Young's modulus, E , is higher at greater depths in Oxford Clay and it increases with depth from 10 MPa to 160 MPa.

In order to provide an example of the application of the variation of the modulus of elasticity, a simple linear fit and an exponential fit have been completed for the data provided by Burland et al. (1977):

$$G = \frac{E_{\text{secant}}}{2(1+\nu)} = \frac{E_{\text{secant}}}{3} \tag{2.1}$$

$$G(z) = 3.33e^{0.0879*z} \tag{2.2}$$

$$G(z) = 3.33 + 1.062 * z \tag{2.3}$$

In the above equations, the SI unit of the modulus of elasticity (shear modulus G and secant Young's modulus E_{secant}) is in MPa and the SI unit of z is meters (m). Figure 2.4 shows the variations in the vertical displacement along the z-axis for the fitted linear and exponential variation of shear modulus to the data provided by Burland et al. (1977). The numerical results for these two variations are presented in the following chapters.

Cripps and Taylor (1981) investigated the engineering properties of mudrocks, which have characteristics between soil and rock, with depth, including the shear modulus variation. They compiled the engineering properties and parameters of mudrock from various investigations and studied different factors influencing the results such as lithology, exhumation, type and method of testing and degree of weathering. They showed that the elastic moduli of mudrocks increase with depth; however, this increase is not necessarily linear.

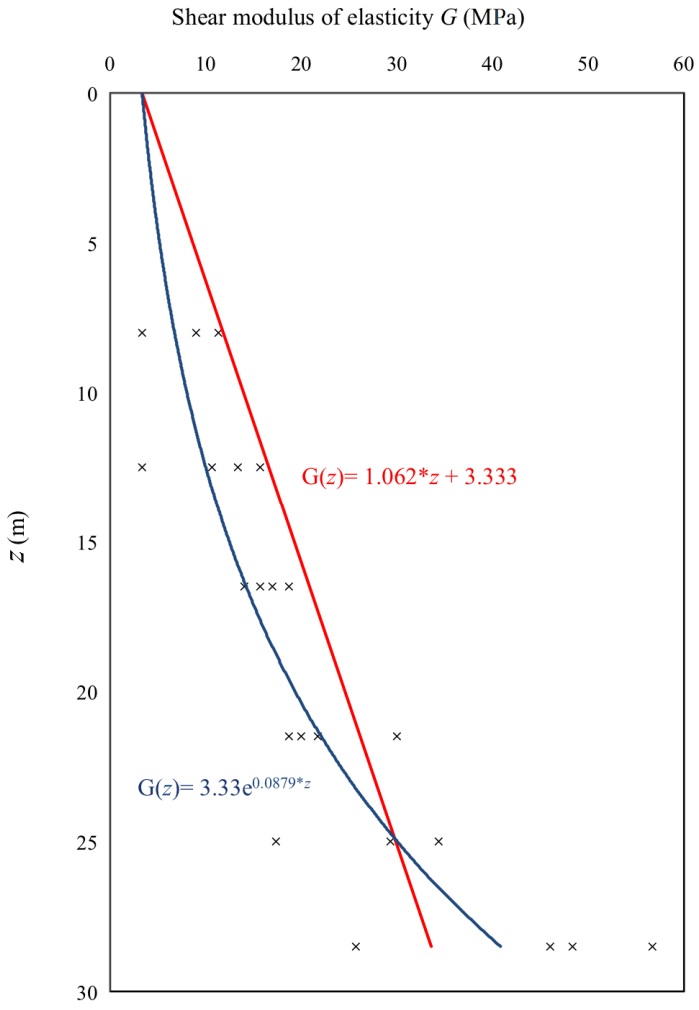

Figure 2.4: Variations of vertical displacement along the z-axis for the fitted linear and exponential variation of shear modulus to the data provided by Burland et al. (1977)

Cripps and Taylor (1986) collected published values of engineering properties of London over-consolidated clay and mudrock for different territories and formations in order to present their ranges and averages for use as references of their typical values. Table 2.1 shows the variation of shear modulus with depth for different territories with compact information about the type of test, type of clay, type of loading and their corresponding references.

Table 2.1: Variation of modulus of elasticity in depth for different territories (Cripps and Taylor, 1986).

Modulus of elasticity of London Clay

Location	Type of clay	Initial or reload	Secant modulus (MN/m^2)	Depth (m)	Type of test	Reference
Ashford Common	blue	I	40—148	10—45	38 mm triaxial	Ward et al., 1965
	blue	I	2.6—115	10—45	150 mm plate	
Hendon	brown	R	18—116	2—11	pressuremeter	Windle and Wroth, 1977
	brown	R	20—62	3—25	38 mm triaxial	Marsland, 1973c
	brown	R	16—60	3—25	98 mm triaxial	
	brown	R	74—107	6—24	865 mm plate	
	brown	I	70—150	0—4	pile test	Cooke and Price, 1973
Chelsea	brown/grey	R	24—80	3—175	38 mm triaxial	Marsland, 1973c
	brown/grey	R	20—62	3—17.5	98 mm triaxial	
	brown/grey	R	90—125	11—16	865 mm plate	
Paddington	blue	I	E_t = 37.5—54	19—43	38 mm triaxial	Skempton and Henkel, 19
Victoria	blue	I	E_t = 25—27	4—14	38 mm triaxial	

Modulus of Elasticity (MN/m^2)

It can be seen from Table 2.1 that the modulus of elasticity generally increases with depth. The values from 38 mm triaxial tests have an average of between 20 MPa close to the ground surface and to 70 MPa at a depth of 25 m. A comparison to 38 mm triaxial test results with the 98 mm diameter sample results show that a lower stiffness for the clay is obtained from the triaxial test with 98mm diameter sample size. This range is higher for plate loading and pressuremeter tests, where the clay displays a higher stiffness.

Gunn et al. (2003) investigated the variation of shear modulus with depth in Oxford clays and Kellaways formations in two different sites at Huntingdon, and South Peterborough, U.K. There is a sequence of overconsolidated clays and

mudstones at both sites. Figure 2.5 shows the sequence of the soil in South Petersborough, which consists of ballast, overconsolidated clay and mudstones from the Oxford Clay. There is about 4.3 m of overconsolidated clays overlying the mudstone beneath the ballast.

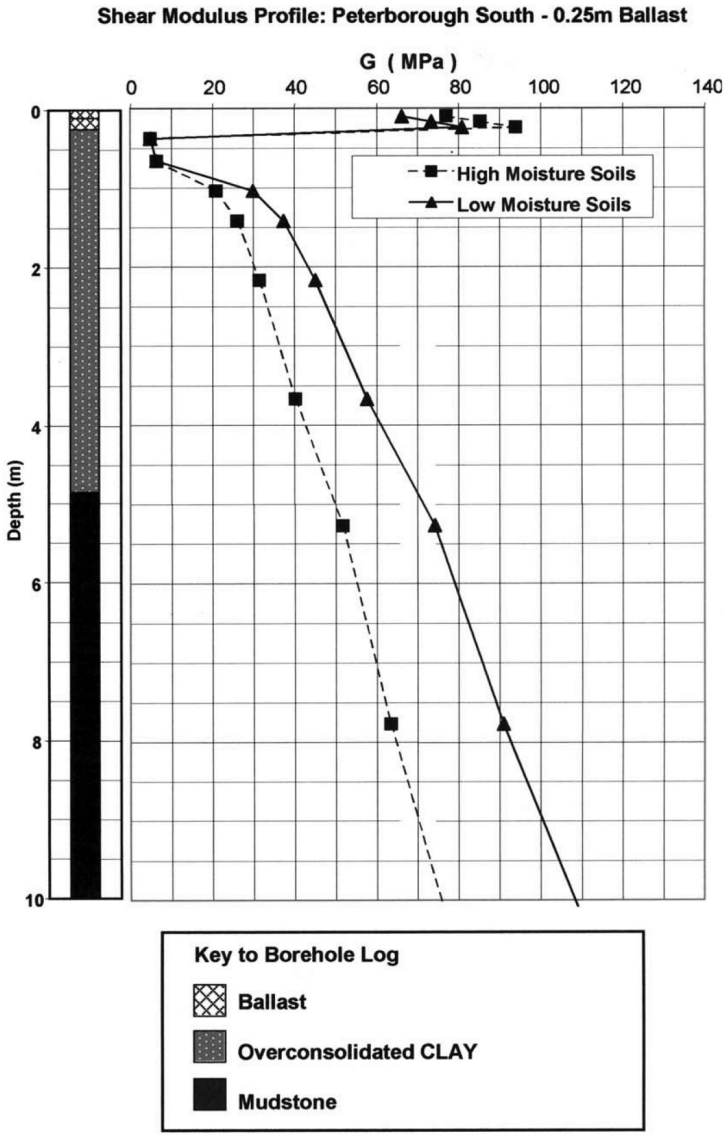

Figure 2.5: Shear modulus variation profile of a sequence south of Peterborough (Gunn et al., 2003)

It can be seen from Figure 2.5 that the shear modulus increases with depth in the overconsolidated clay and mudstone, from 5 MPa for a depth lower than 1 m to 70 MPa and 100 MPa at a depth of 10 m for low moisture soils, and high moisture soils respectively. The rate of increase in the shear modulus is higher at shallower depths. The same pattern was observed for the site south of Huntingdon. The shear modulus in overconsolidated clay at a depth of 4m was 30 MPa and reached 80 MPa and 100 MPa at depth 10 m for low moisture soils and high moisture soils, respectively.

Studies of the variation in the shear modulus with depth are not limited to clays in the UK and clay in general; Shibuya et al. (1992) conducted a series of tests to measure the elastic shear modulus of soft clays using shear wave velocity at 9 different sites. They then introduced an empirical relationship to estimate the maximum shear modulus at depth based on the results of the shear wave velocity tests. The results show that the shear modulus of elasticity increased with depth and the rate of increase was higher at greater depths.

The results of large plate tests at various depths conducted by Abbiss (1979) show that the stiffness of chalk and also its static Young's modulus increases with depth. There have also been a few tests that have measured the modulus of elasticity under drained condition (Atkinson, 1975; Hooper and Wood, 1977). Hooper and Wood (1977) reported that the effective vertical modulus of elasticity increased from approximately 7.5 MN/m^2 at the ground surface to 20 MN/m^2 at a depth of 18m.

2.4 Summary

All the investigations mentioned above show that the modulus of elasticity in soils generally increases with depth, although the variation is not necessarily linear or exponential. However, it was observed that the rate of increase in the shear modulus is usually higher at shallower depths. Comparisons between the in-situ and laboratory tests indicate that the testing method significantly affects the results. By comparing the results with settlement records, it was concluded, in

numerous references, that the results determined from plate loading test give more reliable results compared to the laboratory tests. Laboratory tests, such as the triaxial test, give considerably lower elastic moduli than the plate loading test, and these results were variable and hard to interpret.

CHAPTER 3

GOVERNING EQUATIONS

3. 1 General

There are several approaches to the formulation of the elastostatic problem related to a non-homogeneous medium. The development of the partial differential equations governing the elastic non-homogeneity problem is relatively straightforward and only the essential steps are presented here for completeness. Accounts of the developments are given in several references (e.g. Korenev, 1957, Gibson, 1967; Popov, 1973). The elastic material is assumed to be inhomogeneous such that the elastic constants $G(r,z)$ and $\nu(r,z)$ have variations of the forms

$$G(r,z) = G(z);\ \ z \in (0,\infty), \tag{3.1}$$

$$\nu(r,z) = \nu = \text{Constant};\ \ z \in (0,\infty) \tag{3.2}$$

In this thesis two variations for shear modulus are considered; the non-homogeneity either has an exponential variation over the entire depth of the half-space or over a finite depth, beyond which it is constant.

The exponential variation of the shear modulus is given by

$$G(z) = G_0 e^{\lambda z}, \tag{3.3}$$

and the segmental variation would be

$$G_1(z) = G_0 e^{\lambda z}, \quad z \le d \; ; \; G_2(z) = G_0 e^{\lambda d}, \quad z \ge d \tag{3.4}$$

We now introduce the non-dimensional parameter $\tilde{\lambda}$ for characterizing the non-homogeneity, such that $\lambda = \tilde{\lambda} / a$.

We consider the class of axisymmetric problems in the theory of elasticity, referred to the cylindrical polar coordinate system (r, θ, z), where the displacement vector is

$$\mathbf{u} = \{u_r(r,z), 0, u_z(r,z)\} \tag{3.5}$$

and the strain tensor $\boldsymbol{\varepsilon}$ is defined by

$$\boldsymbol{\varepsilon} = \begin{pmatrix} \dfrac{\partial u_r}{\partial r} & 0 & \dfrac{1}{2}\left(\dfrac{\partial u_r}{\partial z} + \dfrac{\partial u_z}{\partial r} \right) \\ 0 & \dfrac{u_r}{r} & 0 \\ \dfrac{1}{2}\left(\dfrac{\partial u_r}{\partial z} + \dfrac{\partial u_z}{\partial r} \right) & 0 & \dfrac{\partial u_z}{\partial z} \end{pmatrix} \tag{3.6}$$

For axial symmetry, the non-zero components of the Cauchy stress tensor $\boldsymbol{\sigma}$ are

$$\boldsymbol{\sigma} = \begin{pmatrix} \sigma_{rr} & 0 & \sigma_{rz} \\ 0 & \sigma_{\theta\theta} & 0 \\ \sigma_{rz} & 0 & \sigma_{zz} \end{pmatrix} \tag{3.7}$$

and the constitutive relationship for a non-homogeneous elastic material in which the linear elastic shear modulus varies with the coordinate direction z, takes the form

$$\boldsymbol{\sigma} = 2G(z)[\alpha e\mathbf{I} + \boldsymbol{\varepsilon}] \tag{3.8}$$

where $G(z)$ is the linear elastic shear modulus, $\mathbf{I}$ is the unit matrix and

$$e = \mathrm{tr}(\boldsymbol{\varepsilon}) \quad ; \quad \alpha = \frac{\nu}{(1-2\nu)} \tag{3.9}$$

and ν is Poisson's ratio, which is assumed to be a constant. We specifically restrict attention to incompressible elastic materials for which isochoric deformations give

$$\mathrm{tr}(\boldsymbol{\varepsilon}) = 0 \quad ; \quad \nu = 1/2 \tag{3.10}$$

The constraints (3.10) imply that the constitutive equations (3.8) are indeterminate to within an isotropic stress state $f(r,z)$ (e.g. Spencer, 1970, 1980; Selvadurai and Spencer, 1972); this needs to be determined from the solution of the equations of equilibrium, which, in the absence of body forces and for axial symmetry, reduce to

$$\nabla.\boldsymbol{\sigma} = 0 \tag{3.11}$$

which gives

$$\frac{\partial \sigma_{rr}}{\partial r} + \frac{\partial \sigma_{rz}}{\partial z} + \frac{\sigma_{rr} - \sigma_{\theta\theta}}{r} = 0 \tag{3.12}$$

$$\frac{\partial \sigma_{rz}}{\partial r} + \frac{\partial \sigma_{zz}}{\partial z} + \frac{\sigma_{rz}}{r} = 0 \tag{3.13}$$

Using constitutive equations applicable to an incompressible elastic material with a spatial variation in the linear elastic shear modulus as defined by (3.8), the equations of equilibrium (3.12) and (3.13) can be expressed in terms of the displacements as follows:

$$\nabla^2 u_r + \frac{\partial f}{\partial r} - \frac{u_r}{r^2} + \frac{1}{G}\frac{dG}{dz}\left(\frac{\partial u_z}{\partial r} + \frac{\partial u_r}{\partial z}\right) = 0 \tag{3.14}$$

$$\nabla^2 u_z + \frac{\partial f}{\partial z} + \frac{1}{G}\frac{dG}{dz}\left(f + 2\frac{\partial u_z}{\partial z}\right) = 0 \tag{3.15}$$

where ∇^2 is the axisymmetric form of Laplace's operator given by

$$\nabla^2 = \frac{\partial^2}{\partial r^2} + \frac{1}{r}\frac{\partial}{\partial r} + \frac{\partial^2}{\partial z^2} \tag{3.16}$$

Eliminating the function $f(r,z)$ between (3.14) and (3.15) and based on the assumption that the differentiations commute, we obtain,

$$\begin{aligned} g(z)\nabla^2 u_r + \nabla^2 \frac{\partial u_r}{\partial z} - \frac{\partial}{\partial r}(\nabla^2 u_z) + g(z)\left(\frac{\partial^2 u_r}{\partial z^2} - \frac{u_r}{r^2} - \frac{\partial^2 u_z}{\partial r \partial z}\right) - \frac{1}{r^2}\frac{\partial u_r}{\partial z} \\ + \left[g^2(z) + \frac{dg(z)}{dz}\right]\left(\frac{\partial u_z}{\partial r} + \frac{\partial u_r}{\partial z}\right) = 0 \end{aligned} \tag{3.17}$$

where

$$g(z) = \frac{1}{G}\frac{dG}{dz} \tag{3.18}$$

3. 2 Exponential variation of shear modulus

By restricting attention to the exponential variation of the elastic shear modulus of equation (3.3), the equation (3.17) can be reduced to

$$\begin{aligned} \lambda\nabla^2 u_r + \nabla^2 \frac{\partial u_r}{\partial z} - \frac{\partial}{\partial r}(\nabla^2 u_z) + \lambda\left(\frac{\partial^2 u_r}{\partial z^2} - \frac{u_r}{r^2} - \frac{\partial^2 u_z}{\partial r \partial z}\right) \\ - \frac{1}{r^2}\frac{\partial u_r}{\partial z} + [\lambda^2]\left(\frac{\partial u_z}{\partial r} + \frac{\partial u_r}{\partial z}\right) = 0 \end{aligned} \tag{3.19}$$

The results (3.19) together with the incompressibility condition

$$\frac{\partial u_r}{\partial r} + \frac{u_r}{r} + \frac{\partial u_z}{\partial z} = 0 \tag{3.20}$$

constitute the set of coupled partial differential equations governing the displacement field.

In order to solve equations (3.19) and (3.20) we introduce Hankel transform representations (Sneddon, 1951; Selvadurai, 2000a) of the following form

$$u_r(r,z) = \int_0^\infty \xi U_r(\xi,z) J_1(\xi r) d\xi \tag{3.21}$$

$$u_z(r,z) = \int_0^\infty \xi U_z(\xi,z) J_0(\xi r) d\xi \tag{3.22}$$

where ξ is the Hankel transform parameter and J_n is the n^{th}-order Bessel function of the first kind. Substituting (3.21) and (3.22) into (3.19) and (3.20) gives rise to the following:

$$\frac{dU_z}{dz} + \xi U_r = 0 \tag{3.23}$$

$$\frac{d^3U_r}{dz^3} + 2\lambda\frac{d^2U_r}{dz^2} + \xi\frac{d^2U_z}{dz^2} + (\lambda^2 - \xi^2)\frac{dU_r}{dz} + \xi\lambda\frac{dU_z}{dz} - \lambda\xi^2 U_r - \xi(\xi^2+\lambda^2)U_z = 0 \tag{3.24}$$

Substituting of (3.23) in (3.24) we obtain

$$\frac{d^4U_z}{dz^4} + 2\lambda\frac{d^3U_z}{dz^3} + (\lambda^2 - 2\xi^2)\frac{d^2U_z}{dz^2} - 2\lambda\xi^2\frac{dU_z}{dz} + \xi^2(\xi^2+\lambda^2)U_z = 0 \tag{3.25}$$

which is the partial differential equation governing the axial displacement field.

Considering the expressions for the stress-strain relationships (3.8), the strain-displacement relations (3.6) and the integral expressions (3.21) and (3.22) for the displacement components, the transformed expressions for the stress components $\sigma_{zz}(r,z)$ and $\sigma_{rz}(r,z)$ can be written as

$$\tilde{\sigma}^0_{zz}(\xi,z) = G(z)[F + 2\frac{dU_z}{dz}] \tag{3.26}$$

$$\tilde{\sigma}_{rz}^{1} = G(z)[-\xi U_z + \frac{dU_r}{dz}] \tag{3.27}$$

where F is the Hankel transform of f defined by

$$F(\xi, z) = \int_0^\infty r f(r, z) J_0(\xi r) dr \tag{3.28}$$

The inverse of these stress components are given by

$$\sigma_{zz}(r, z) = G(z) \int_0^\infty \xi [F + 2\frac{dU_z}{dz}] J_0(\xi r) d\xi \tag{3.29}$$

$$\sigma_{rz}(r, z) = G(z) \int_0^\infty \xi [-\xi U_z + \frac{dU_r}{dz}] J_1(\xi r) d\xi \tag{3.30}$$

3. 3 Segmental variation of shear modulus

The same procedure is adopted for the segmental variation of the shear modulus. By restricting attention to a segmental variation in the elastic shear modulus of equation (3.4), the equation (3.17) applicable to the separate domains, takes the form

$$\begin{aligned} &\lambda \nabla^2 u_r + \nabla^2 \frac{\partial u_r}{\partial z} - \frac{\partial}{\partial r}(\nabla^2 u_z) + \lambda(\frac{\partial^2 u_r}{\partial z^2} - \frac{u_r}{r^2} - \frac{\partial^2 u_z}{\partial r \partial z}) \\ &\quad - \frac{1}{r^2}\frac{\partial u_r}{\partial z} + [\lambda^2](\frac{\partial u_z}{\partial r} + \frac{\partial u_r}{\partial z}) = 0, \ \ z \le d \end{aligned} \tag{3.31a}$$

$$\nabla^2 \frac{\partial u_r}{\partial z} - \frac{\partial}{\partial r}(\nabla^2 u_z) - \frac{1}{r^2}\frac{\partial u_r}{\partial z} = 0, \ \ z \ge d \tag{3.31b}$$

The results (3.31) together with the incompressibility condition of equation (3.20) will form the set of coupled partial differential equations governing the displacement field. By using Hankel transform representations (3.21) and (3.22), the equations (3.31) can be written in the following form

$$\frac{dU_z}{dz} + \xi U_r = 0 \tag{3.32}$$

$$\frac{d^3U_r}{dz^3}+2\lambda\frac{d^2U_r}{dz^2}+\xi\frac{d^2U_z}{dz^2}+(\lambda^2-\xi^2)\frac{dU_r}{dz}+\xi\lambda\frac{dU_z}{dz}-\lambda\xi^2U_r-\xi(\xi^2+\lambda^2)U_z=0 \tag{3.33a}$$

$$\frac{d^4U_z}{dz^4}-2\xi^2\frac{d^2U_z}{dz^2}+\xi^4U_z=0,\ \ z\geq d \tag{3.33b}$$

By substituting the equation (3.32) into equations (3.33) we have

$$\frac{d^4U_z}{dz^4}+2\lambda\frac{d^3U_z}{dz^3}+(\lambda^2-2\xi^2)\frac{d^2U_z}{dz^2}-2\lambda\xi^2\frac{dU_z}{dz}+\xi^2(\xi^2+\lambda^2)U_z=0,\ \ z\leq d \tag{3.34a}$$

$$\frac{d^4U_z}{dz^4}-2\xi^2\frac{d^2U_z}{dz^2}+\xi^4U_z=0,\ \ z\geq d \tag{3.34b}$$

CHAPTER 4

TRACTION BOUNDARY VALUE PROBLEMS

4.1 Introduction

This chapter deals with the traction boundary value problems of an inhomogeneous elastic halfspace. The axisymmetric problem of the interior loading of an inhomogeneous isotropic incompressible elastic halfspace by a uniform circular load of finite radius is considered. The problem is an approximation for the loading induced by an embedded foundation, such as an end bearing pile (Poulos and Davis, 1975), an anchor plate (Selvadurai, 1989, 1993, 1994; Rajapakse and Selvadurai, 1991) or a test device such as a screw plate (Selvadurai et al., 1980). The interior loading of an isotropic homogeneous elastic halfspace was first examined by Mindlin (1936); here the study is extended to include the influence of elastic non-homogeneity. The problem of the interior loading of a non-homogeneous medium with a linear variation in the shear modulus was examined by Rajapakse (1990a) and Rajapakse and Selvadurai (1991) who extended the analysis to include circular footings and anchor plates in non-homogeneous elastic media. Two types of elastic non-homogeneity in the

shear modulus are considered in this thesis: (i) exponential variation with depth over the entire halfspace region and (ii) exponential variation with depth over a finite depth, beyond which the elastic shear modulus is assumed to be constant. The solution of these problems is accomplished using an integral transform formulation of the resulting equations of elasticity. The adaptive numerical quadrature technique is used to evaluate the integrals obtained from the integral transform technique. Numerical results are presented in order to show the influence of non-homogeneity on the responses of an incompressible elastic halfspace. The numerical results are then used to establish the accuracy of finite element results for the analogous problems.

In the case of the discrete variation in the elastic non-homogeneity, the demarcation point between the variations is assumed to be the point of application of the interior circular loads. The procedure can, however, be extended to include the case where the demarcation point is located at an arbitrary position in relation to the plane of application of the axisymmetric interior loading. The numerical results for the surface displacement of the halfspace region are used to compare the influences of the bounded and unbounded values in the linear elastic shear modulus. The results derived from these two types of variation are also compared with equivalent results for the problem of the undrained interior loading of a halfspace with a linear variation in the elastic shear modulus (Rajapakse, 1990a).

In section 4.3, the results are extended to the case where the medium is a layer of finite depth d and of infinite lateral extent and the layer is loaded on its surface by a vertical pressure p_0. The elastic layer is assumed to be incompressible and its shear modulus increases exponentially with depth. The same problem was considered by Gibson et al. (1971) where the Poisson's ratio was 0.5 and the shear modulus varied linearly with depth. Gibson and Brown (1979) also examined the surface settlement at the corner of a rectangular area of uniform loading, when the material had a constant Poisson's ratios of 1/2, 1/3, and 0 and the shear modulus varied linearly with depth.

In the last section of this chapter the results for the axisymmetric distributed radial loading of an incompressible elastic halfspace is considered, when the elastic shear modulus varies with depth in an exponential manner. The developments in this section will be used in the next chapter to calculate the bonded contact of a rigid disc with a halfspace. The same procedure has been used to formulate the traction boundary values and numerical results are presented to show how non-homogeneity influences the results.

4.2 The axisymmetric internal loading of an incompressible elastic halfspace with an exponential variation in the linear elastic shear modulus

In this section we examine the problem of the axisymmetric interior loading of incompressible elastic halfspace in which the elastic shear modulus varies exponentially over the entire depth. The governing equations as well as the boundary conditions of the problem are presented and the influence of non-homogeneity on the response of halfspace is investigated.

4.2.1 Governing equations

The problem is that of an incompressible non-homogeneous elastic halfspace, which is loaded internally by an axially directed circular load of radius a with stress intensity p_0 and situated at a depth $z = d$ from the traction free surface of the halfspace (Figure 4.1).

The most convenient approach for formulating boundary value problems of this type (Selvadurai, 1993, 2000a,b; Rajapakse, 1990a) is to consider that the original halfspace regions are composed of (i) a layer region (superscript $^{(1)}$) occupying the domain $r \in (0,\infty)$ and $z \in (0,d)$ and (ii) a halfspace region (superscript $^{(2)}$) occupying the domain $r \in (0,\infty)$ and $z \in (d,\infty)$.

The elastic layer region and the elastic halfspace region are subjected to the following boundary, interface and regularity conditions:

$$\sigma_{zz}^{(1)}(r,0) = 0; \quad \sigma_{rz}^{(1)}(r,0) = 0 \tag{4.1}$$

$$u_r^{(1)}(r,d) = u_r^{(2)}(r,d);\ u_z^{(1)}(r,d) = u_z^{(2)}(r,d) \tag{4.2}$$

$$\sigma_{zz}^{(1)}(r,d) - \sigma_{zz}^{(2)}(r,d) = \begin{cases} p(r), & r \le a \\ 0, & r > a \end{cases} \tag{4.3}$$

$$\sigma_{rz}^{(1)}(r,d) = \sigma_{rz}^{(2)}(r,d) \tag{4.4}$$

In equation (4.3), $p(r)$ represents the intensity of the internally applied pressure over the circular area. In addition to these boundary and continuity conditions, it is assumed that the displacements and stresses should satisfy the appropriate regularity conditions in the layer and halfspace regions as $r, z \to \infty$.

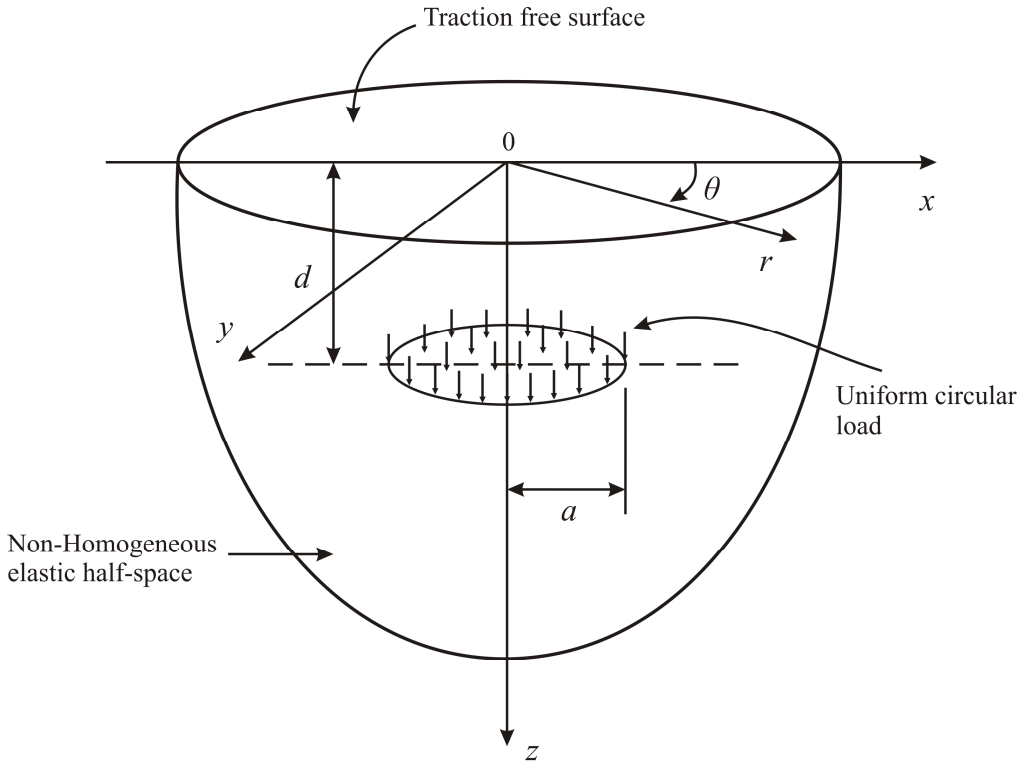

Figure 4.1: Axisymmetric Mindlin loads acting at the interior of an incompressible non-homogeneous elastic halfspace

Consistent with the regularity condition at infinity, the general solutions of equation (3.25) can be written as

$$U_z(\xi,z)=\begin{cases}A_1e^{-k_1z}+B_1e^{-k_2z}+C_1e^{k_3z}+D_1e^{k_4z} & ; \quad z<d\\ A_2e^{-k_1z}+B_2e^{-k_2z} & ; \quad z>d\end{cases} \tag{4.5}$$

where

$$k_1=\frac{1}{2}[\lambda+\sqrt{\lambda^2+4i\lambda\xi+4\xi}]$$

$$k_2=\frac{1}{2}[\lambda+\sqrt{\lambda^2-4i\lambda\xi+4\xi^2}]$$

$$k_3=\frac{1}{2}[-\lambda+\sqrt{\lambda^2+4i\lambda\xi+4\xi^2}]$$

$$k_4=\frac{1}{2}[-\lambda+\sqrt{\lambda^2-4i\lambda\xi+4\xi^2}] \tag{4.6}$$

From equations (3.23) and (4.5), the general solution of $U_r(\xi,z)$ can be expressed as

$$U_r(\xi,z)=\begin{cases}\frac{A_1k_1}{\xi}e^{-k_1z}+\frac{B_1k_2}{\xi}e^{-k_2z}-\frac{C_1k_3}{\xi}e^{k_3z}-\frac{D_1k_4}{\xi}e^{k_4z}, & z<d\\ \frac{A_2k_1}{\xi}e^{-k_1z}+\frac{B_2k_2}{\xi}e^{-k_2z}, & z>d\end{cases} \tag{4.7}$$

where A,B,C and D in equations (4.5) and (4.7) are arbitrary functions of ξ to be determined from appropriate boundary and continuity conditions. The equation (3.14) can be reduced to

$$\frac{d^2U_r}{dz^2}-\xi^2U_r-\xi F+\lambda(\frac{dU_r}{dz}-\xi U_z)=0 \tag{4.8}$$

The substitution of (4.5) and (4.7) into (4.8) results in

$$F(z)=\begin{cases}A_1q_1e^{-k_1z}+B_1q_2e^{-k_2z}+C_1q_3e^{k_3z}+D_1q_4e^{k_4z}, & z<d\\ A_2q_1e^{-k_1z}+B_2q_2e^{-k_2z}, & z>d\end{cases} \tag{4.9}$$

where

$$q_i = \frac{k_i^3}{\xi^2} - k_i - \frac{\lambda k_i^2}{\xi^2} - \lambda \qquad i = 1,2$$

$$q_{i+2} = -\frac{k_{i+2}^3}{\xi} + k_{i+2} - \frac{\lambda k_{i+2}^2}{\xi^2} - \lambda \qquad i = 1,2 \tag{4.10}$$

Substituting equations (4.5), (4.7) and (4.9) into the boundary and continuity equations defined by (4.1) to (4.4) results in a system of linear simultaneous equations for the arbitrary functions $A_1(\xi), A_2(\xi), B_1(\xi), B_2(\xi)$, …, etc., as follows:

$$A_1\theta_1 + B_1\theta_2 + C_1\theta_3 + D_1\theta_4 = 0 \tag{4.11}$$

$$A_1\eta_1 + B_1\eta_2 + C_1\eta_3 + D_1\eta_4 = 0 \tag{4.12}$$

$$[A_1 - A_2]\beta_1 e^{-k_1 d} + [B_1 - B_2]\beta_2 e^{-k_2 d} - C\beta_3 e^{k_3 d} - D\beta_4 e^{k_4 d} = 0 \tag{4.13}$$

$$[A_1 - A_2]e^{-k_1 d} + [B_1 - B_2]e^{-k_2 d} + C_1 e^{k_3 d} + D_1 e^{k_4 d} = 0 \tag{4.14}$$

$$[A_1 - A_2]\eta_1 e^{-k_1 d} + [B_1 - B_2]\eta_2 e^{-k_2 d} + C_1\eta_3 e^{k_3 d} + D_1\eta_4 e^{k_4 d} = 0 \tag{4.15}$$

$$[A_1 - A_2]\theta_1 e^{-k_1 d} + [B_1 - B_2]\theta_2 e^{-k_2 d} + C_1\theta_3 e^{k_3 d} + D_1\theta_4 e^{k_4 d} = \frac{\tilde{p}(\xi)}{G(d)} \tag{4.16}$$

where

$$\beta_i = \frac{k_i}{\xi}; \quad \eta_i = \xi + \frac{k_i^2}{\xi} \quad ; \quad i = 1,2,3,4$$
$$\theta_i = q_i - 2k_i \quad ; \quad \theta_{i+2} = q_{i+2} + 2k_{i+2}; \quad i = 1,2 \tag{4.17}$$

$$G(d) = G_0 e^{\lambda d} \tag{4.18}$$

$$\tilde{p}(\xi) = \int_0^\infty r p(r) J_0(\xi r) dr \tag{4.19}$$

The substitution of the explicit results for the arbitrary functions A_1, B_1, C_1, D_1, A_2 and B_2 in equations (4.5), (4.7), (3.29) and (3.30) results in explicit solutions for the displacements and stresses at an arbitrary point within the domain of the non-homogeneous elastic halfspace. The expressions for stresses and displacements involve infinite integrals with integrands decaying exponentially with increasing values of the Hankel transform parameter ξ. This completes the formal analysis of the axisymmetric internal loading of an incompressible elastic halfspace region with an exponential variation of the linear elastic shear modulus with depth.

4.2.2 Numerical results from analytical solutions and computational estimates

The procedure outlined in the previous section leads to explicit infinite integral expressions for the displacement and stress fields within the non-homogeneous but isotropic elastic halfspace region subjected to an axisymmetric circular load of constant stress intensity p_0. The integrands of these integrals cannot be expressed in explicit forms. Consequently, results of interest for practical applications can only be developed through a numerical integration of the infinite integrals. Eason et al. (1955) developed a special numerical procedure to evaluate such infinite integrals and further applications are investigated by Selvadurai and Rajapakse (1985) and Oliveira et al. (2012). Due to the singular nature of these integrands, an adaptive numerical procedure is used to enhance the accuracy of the numerical results; examples of such an application are given by Rahimian et al. (2007) and Katebi et al. (2010). For numerical evaluation of the integrals, the upper limit of integration is replaced by a finite value ξ_0; this limit is increased until a convergent result is obtained.

The approach outlined in this section was applied to evaluate the influence of the non-homogeneity on the displacements of a non-homogeneous elastic halfspace under uniform internal loading over a circular area. It should be pointed out that all numerical results are presented in non-dimensional forms.

Figure 4.2 shows the surface displacement of a non-homogeneous incompressible elastic halfspace for different $\tilde{\lambda}$, which is directly related to the shear modulus by $G=G_0e^{\lambda z}$ and $\lambda=\tilde{\lambda}/a$. The value of $\tilde{\lambda}=0$ represents the case of a homogeneous halfspace in which $G=G_0$ for the entire depth.

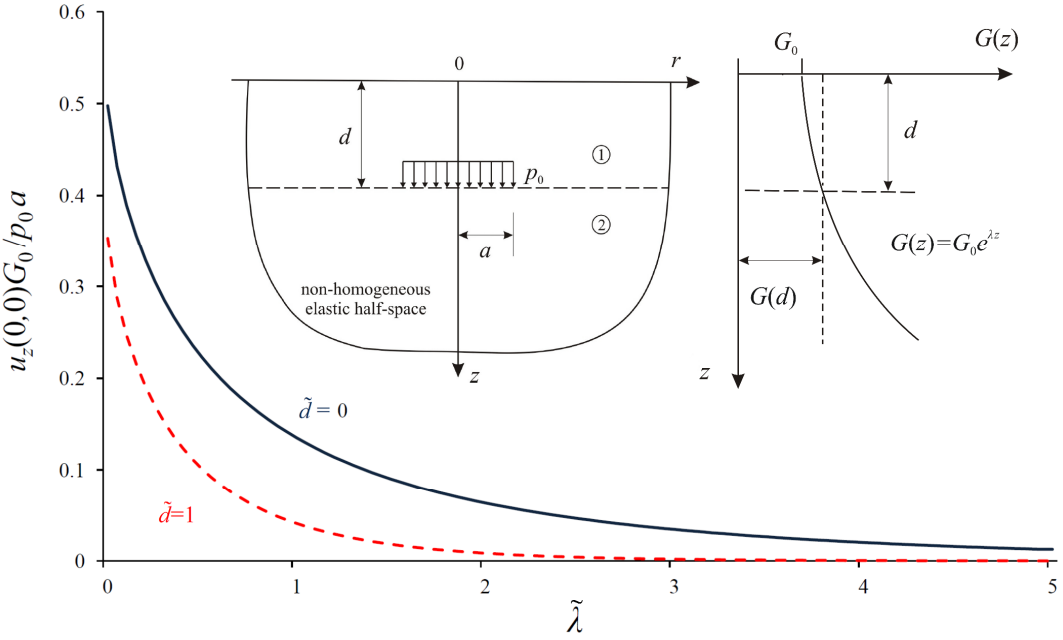

Figure 4.2: Variation of the vertical displacement for different $\tilde{\lambda}$

The variations in vertical displacement for different locations of the loading $\tilde{d}(\tilde{d}=d/a)$ are shown in Figure 4.3. It is evident that the presence of non-homogeneous conditions has a significant effect on the maximum surface displacement of the halfspace.

To provide a better estimate of the relative influence of the elastic non-homogeneity on the displacements of the medium, the ratio of the displacement in a non-homogeneous medium to a homogeneous medium for different values of $\tilde{\lambda}$ is illustrated in Figure 4.4.

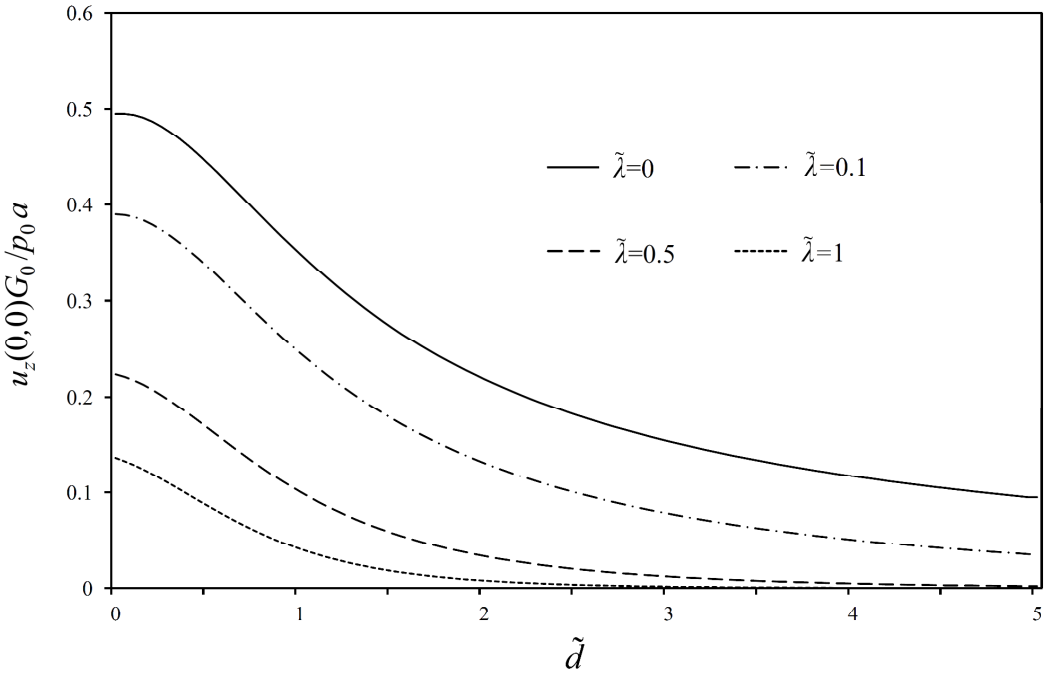

Figure 4.3: Variation of the vertical displacement for different depths of loading ($\tilde{d}$)

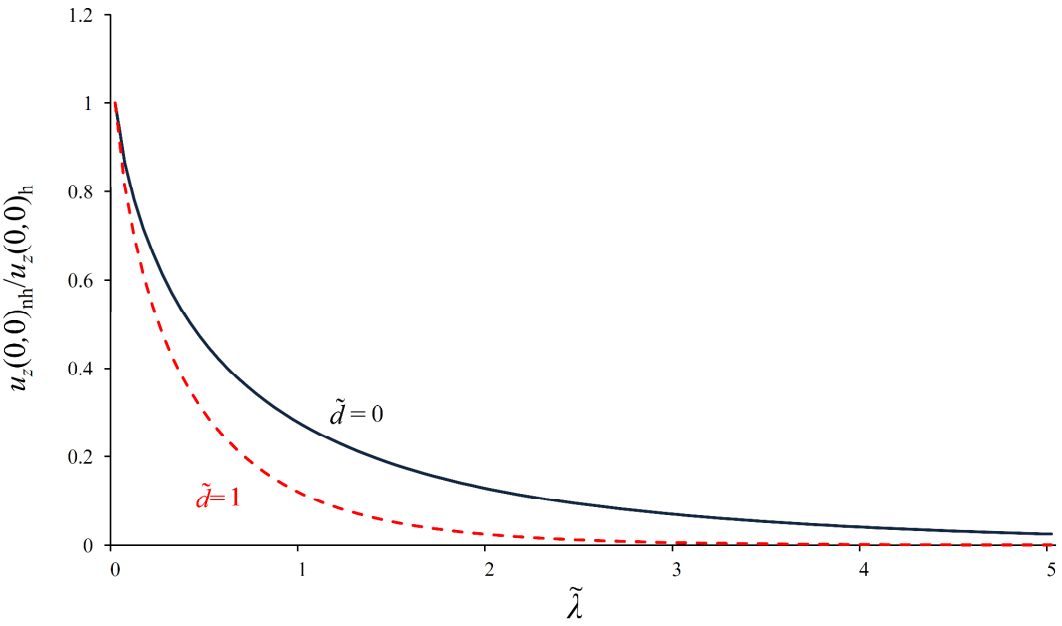

Figure 4.4: Ratio of displacement in a non-homogeneous medium to a homogeneous medium for different $\tilde{\lambda}$

Figure 4.5 shows the variation of the vertical displacement of a non-homogeneous incompressible halfspace in the z-direction for different shear moduli at depths $\tilde{d}=0$ and $\tilde{d}=1$respectively.

The computational results are also indicated by the symbols □, ○, ∆, etc. in Figures 4.5, 4.6 and 4.7. By comparing the computational results with analytical results, it can be seen that there is an excellent correlation between the analytical results derived for the exponential variations in the shear modulus, and the computational results (accurate to within 0.3 %). This almost negligible difference could have arisen because the halfspace region was idealized as a finite domain. The discrepancies are considered to be well within the range acceptable for engineering application of the results.

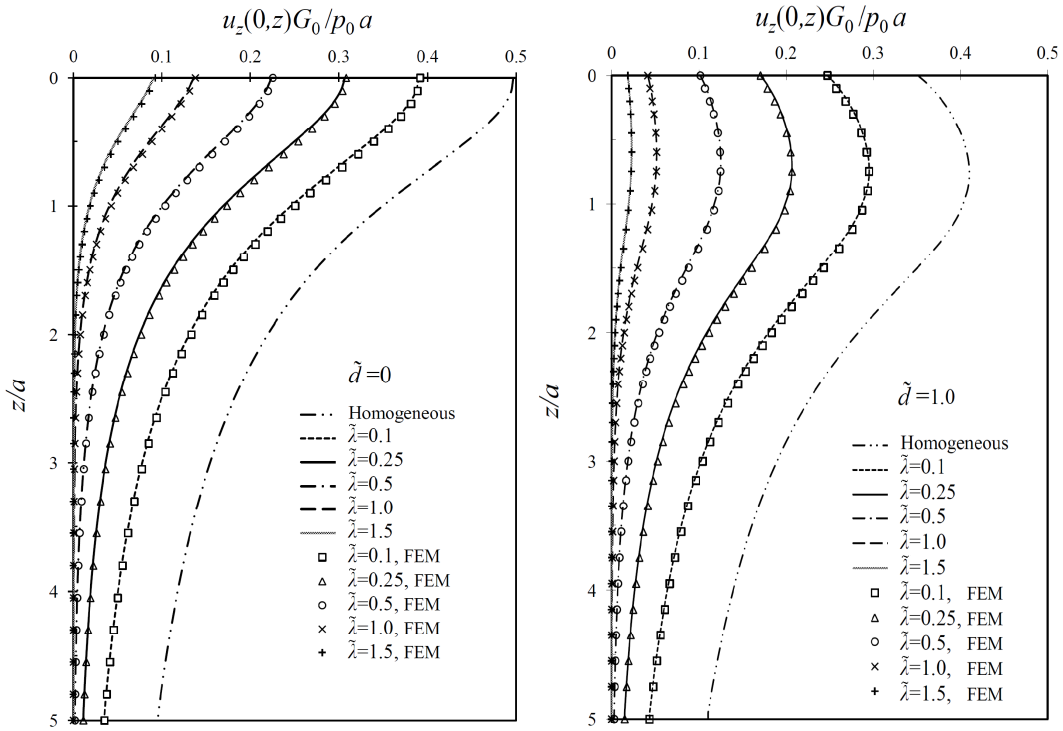

Figure 4.5: Variation of the vertical displacement along the z-axis for different $\tilde{\lambda}$ at depths $\tilde{d}=0$ and $\tilde{d}=1$

Furthermore, the variations in the vertical displacement of a non-homogeneous incompressible halfspace along the *r*-axis for different $\tilde{\lambda}$ at depths $\tilde{d}=0$ and $\tilde{d}=1$ are shown in Figure 4.6. This figure illustrate that the response of the medium is influenced by the degree of non-homogeneity. As would be expected, the vertical displacement decreases as the shear modulus increases, if all other parameters are kept constant. (i.e. as G increases, the stiffness of the halfspace also increases).

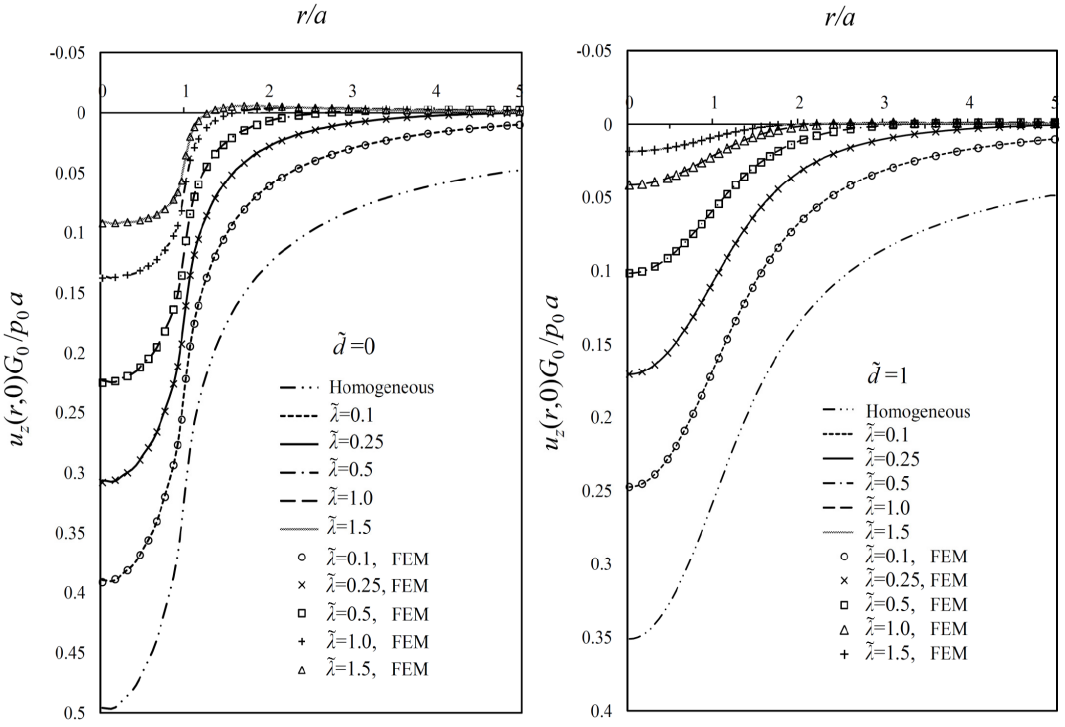

Figure 4.6: Variation of the vertical displacement along the *r*-axis for different $\tilde{\lambda}$ at depths $\tilde{d}=0$ and $\tilde{d}=1$

The numerical results for the linear and exponential fit mentioned in chapter 2 are shown in Figure 4.7a. For a better understanding of how the degree of non-homogeneity influences the response, the variation of vertical displacements along the *z*-axis for the fitted data has been plotted in Figure 4.7b for different depths and diameter of the loading.

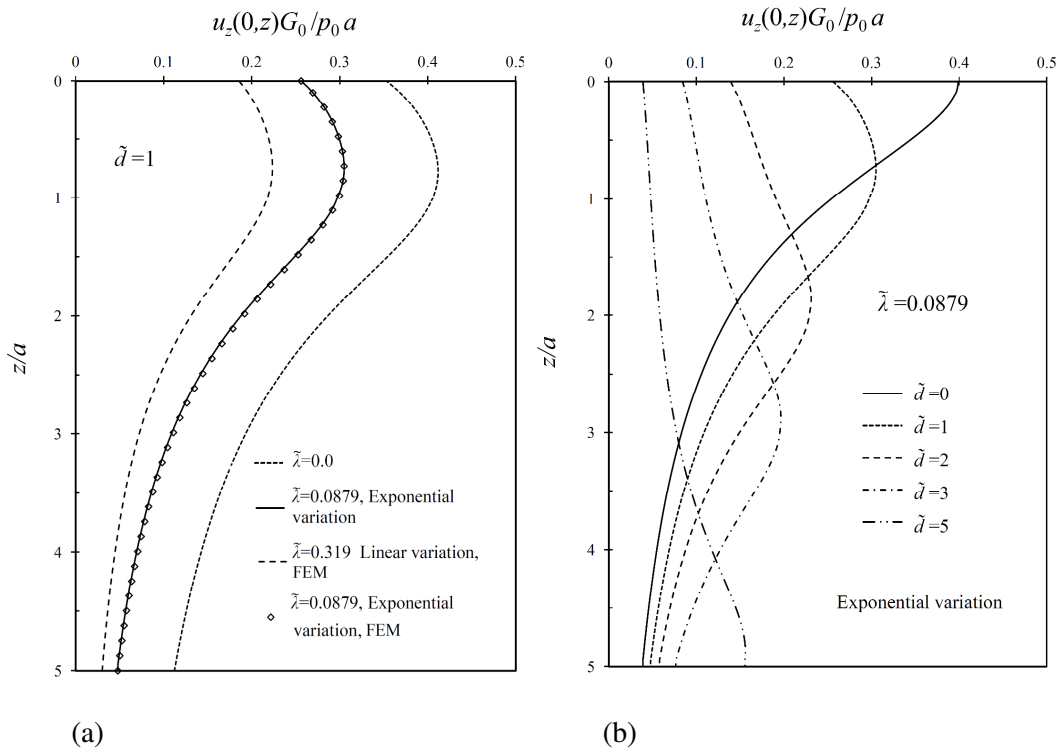

Figure 4.7: Variations of vertical displacement along the z-axis for (a) the fitted linear and exponential variation of shear modulus to the data provided by Burland et al. (1977), (b) the fitted exponential variation of shear modulus to the data provided by Burland et al. (1977)

4.3 The axisymmetric internal loading of an incompressible elastic halfspace with segmental variation in the linear elastic shear modulus

This section examines the problem of the axisymmetric interior loading of an incompressible isotropic elastic halfspace where the linear elastic shear modulus has an exponential variation over a finite depth, beyond which it is constant. The equations of elasticity governing this type of non-homogeneity and the numerical results are presented. Numerical results are used to compare the influence of the bounded and unbounded values of the shear modulus and to verify the accuracy of the finite element results.

4.3.1 Governing equations

Referring to Figure 4.1, the physical domain of interest is exactly the same as in the previous section and is taken to be an incompressible, non-homogeneous elastic halfspace subjected to an axially directed circular load of radius a with stress intensity p_0 situated at a depth $z = d$ from the traction free surface of the halfspace. The shear modulus $G(z)$ has an exponential variation over a finite depth beyond which it is constant according to equation (3.4).

The elastic layer region and the elastic halfspace region are subjected to the following boundary and interface conditions:

$$\sigma_{zz}^{(1)}(r,0) = 0;\ \sigma_{rz}^{(1)}(r,0) = 0 \tag{4.20}$$

$$u_r^{(1)}(r,d) = u_r^{(2)}(r,d);\ u_z^{(1)}(r,d) = u_z^{(2)}(r,d) \tag{4.21}$$

$$\sigma_{zz}^{(1)}(r,d) - \sigma_{zz}^{(2)}(r,d) = \begin{cases} p(r), & r \le a \\ 0, & r > a \end{cases} \tag{4.22}$$

$$\sigma_{rz}^{(1)}(r,d) = \sigma_{rz}^{(2)}(r,d) \tag{4.23}$$

In equation (4.22), $p(r)$ represents the intensity of the internally applied pressure over the circular area. In addition, the displacement and stress fields should satisfy the regularity conditions applicable to the layer and halfspace regions as $r, z \to \infty$. Consistent with the regularity conditions at infinity, the transformed solution for the displacement components $u_r(r,z)$ and $u_z(r,z)$ can be written as

$$u_z(r,z) = \int_0^\infty [A_1 e^{-k_1 z} + B_1 e^{-k_2 z} + C_1 e^{k_3 z} + D_1 e^{k_4 z}]\xi J_0(\xi r) d\xi \ ; \qquad z < d \tag{4.24a}$$

$$u_z(r,z) = \int_0^\infty [A_2 e^{-\xi z} + B_2 z e^{-\xi z}]\xi J_0(\xi r) d\xi, \qquad ; \quad z > d \tag{4.24b}$$

And

$$u_r(r,z) = \int_0^\infty [\frac{A_1 k_1}{\xi} e^{-k_1 z} + \frac{B_1 k_2}{\xi} e^{-k_2 z} - \frac{C_1 k_3}{\xi} e^{k_3 z} - \frac{D_1 k_4}{\xi} e^{k_4 z}]\xi J_1(\xi r) d\xi; \qquad z < d \tag{4.25a}$$

$$u_r(r,z) = \int_0^\infty [A_2 e^{-\xi z} + B_2 (z - \frac{1}{\xi}) e^{-\xi z}] \, \xi J_1(\xi r) d\xi \; ; \qquad z > d \qquad (4.25b)$$

where k_1, k_2, k_3, k_4 are defined by equation (4.6) and A, B, C and D are arbitrary functions of ξ to be determined from appropriate boundary and continuity conditions.

Using (4.24), (4.25) and (3.15), $f(r,z)$ takes the following form

$$f(r,z) = \int_0^\infty [A_1 q_1 e^{-k_1 z} + B_1 q_2 e^{-k_2 z} + C_1 q_3 e^{k_3 z} + D_1 q_4 e^{k_4 z}] \xi J_0(\xi r) d\xi \; ; \quad z < d \qquad (4.26a)$$

$$f(r,z) = \int_0^\infty [-2B_2 e^{-\xi z}] \xi J_0(\xi r) d\xi \; ; \qquad z > d \qquad (4.26b)$$

where q_1, q_2, q_3, q_4 are defined by equation (4.10). Substituting equations (4.24), (4.25) and (4.26) into the boundary and continuity equations defined by (4.20) - (4.23) gives a system of linear simultaneous equations for the arbitrary functions $A_1(\xi), A_2(\xi), B_1(\xi), B_2(\xi)$, …, etc.,. The substitution of the explicit results for arbitrary functions A_1, B_1, C_1, D_1, A_2 and B_2 in equations (3.29), (3.30), (4.24) and (4.25) results in explicit solutions for the displacements and stresses at an arbitrary point within the domain of the non-homogeneous elastic halfspace. The expressions for stresses and displacements involve infinite integrals with integrands decaying exponentially with increasing values of the Hankel transform parameter ξ. This completes the formal analysis of the axisymmetric internal loading of an incompressible elastic halfspace region with an exponential variation of the linear elastic shear modulus with depth.

4.3.2 Numerical results: the influence of variations in the elastic shear modulus with depth

The same numerical procedure used in section 4.2.2 was applied to evaluate the explicit infinite integral expressions for the displacement and stress fields within the non-homogeneous elastic halfspace under a buried circular load.

In the following, numerical results are presented to illustrate the influence of segmental non-homogeneity on results of engineering interest. Furthermore, in order to have a better understanding of the influence of non-homogeneity on displacements and stresses, a comparison has been made between these results and those obtained from section 4.2 and Rajapakse (1990a).

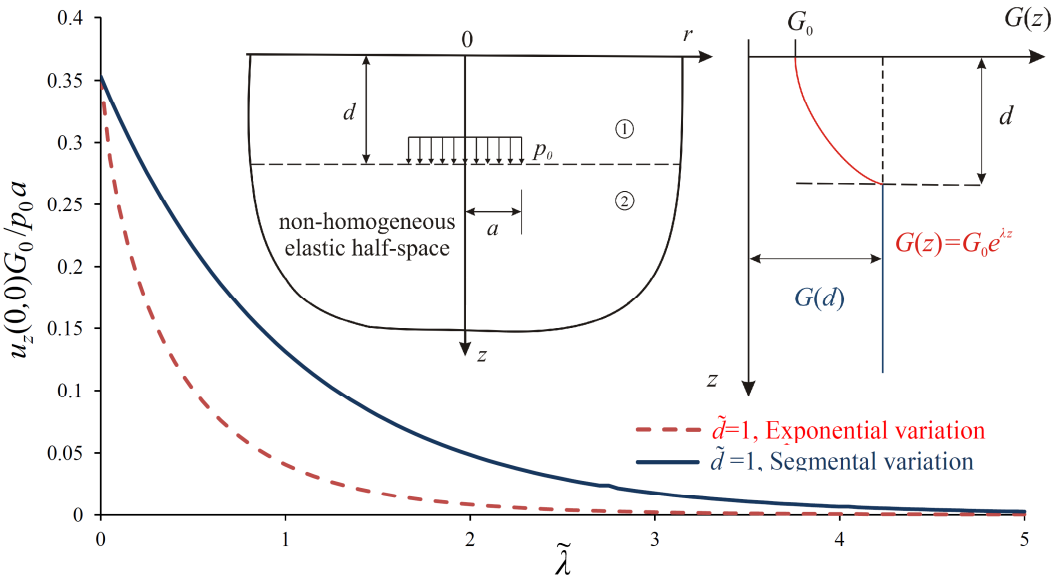

Figure 4.8. Variation of the vertical displacement for different $\tilde{\lambda}$ ($\tilde{\lambda}$ is directly related to the shear modulus obtained from Eq. 3.4)

In previous section the problem with an exponential variation of the shear modulus was considered, while Rajapakse (1990a) considered a linear variation in the shear modulus. Exponential, segmental and linear variations are given by equations (3.3), (3.4) and (4.27) respectively.

$$G(z) = G_0 + mz, \qquad m \geq 0 \tag{4.27}$$

Since we have different variations of the shear modulus, we need to be able to relate these variations to each other in order to make comparisons. These can be related thorough the following equation:

$$\left[\frac{dG_{\text{Exp}}(z)}{dz}\right]_{z=0} = \left[\frac{dG_{\text{Linear}}(z)}{dz}\right]_{z=0} \tag{4.28}$$

Equation (4.28) along with equations (3.3) and (4.27) yields

$$\lambda = \frac{m}{G_0} \tag{4.29}$$

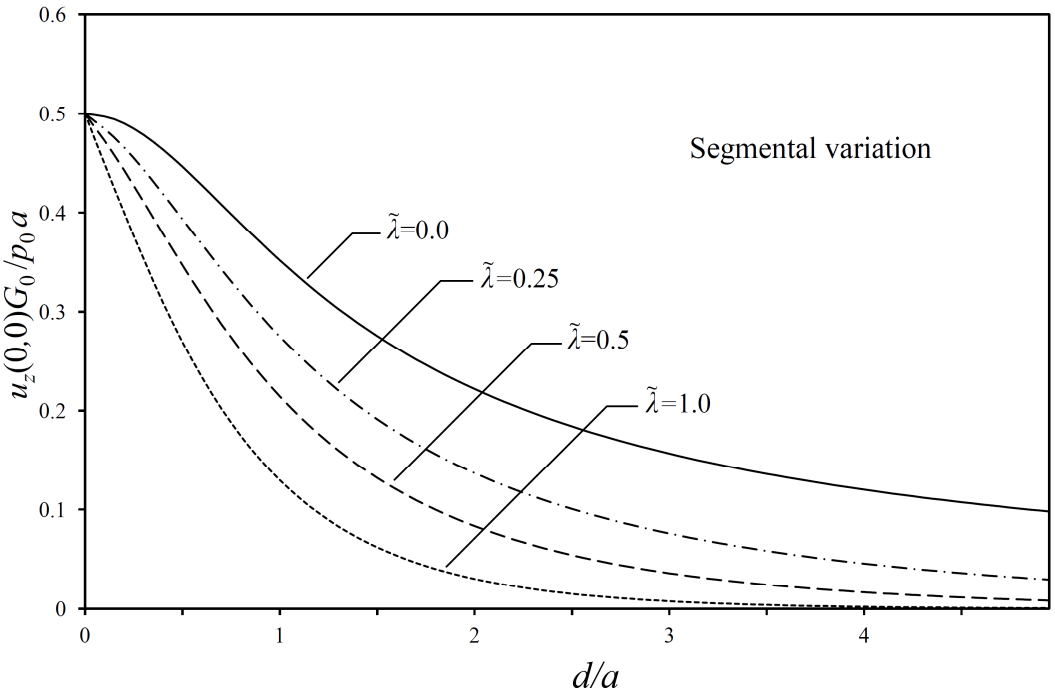

Figure 4.9. Vertical surface displacement for different depths and diameters of the loading

Figure 4.8 shows the surface displacement of a non-homogeneous incompressible elastic halfspace for different $\tilde{\lambda}$, which is directly related to the shear modulus. A comparison between exponential and segmental variations can also be seen in Figure 4.8. The x-axis shows the variation of $\tilde{\lambda}$ in which $\tilde{\lambda}=0$ represents the homogeneous case.

The vertical surface displacement for different depths and diameters of the loading $\tilde{d}(\tilde{d}=d/a)$ are shown in Figure 4.9 while the variations of vertical

displacement along the z-axis for different depths of the loading $\tilde{d}(\tilde{d}=d/a)$ are shown in Figure 4.10. It is evident that the presence of non-homogeneity has a significant effect on the maximum displacement of the halfspace.

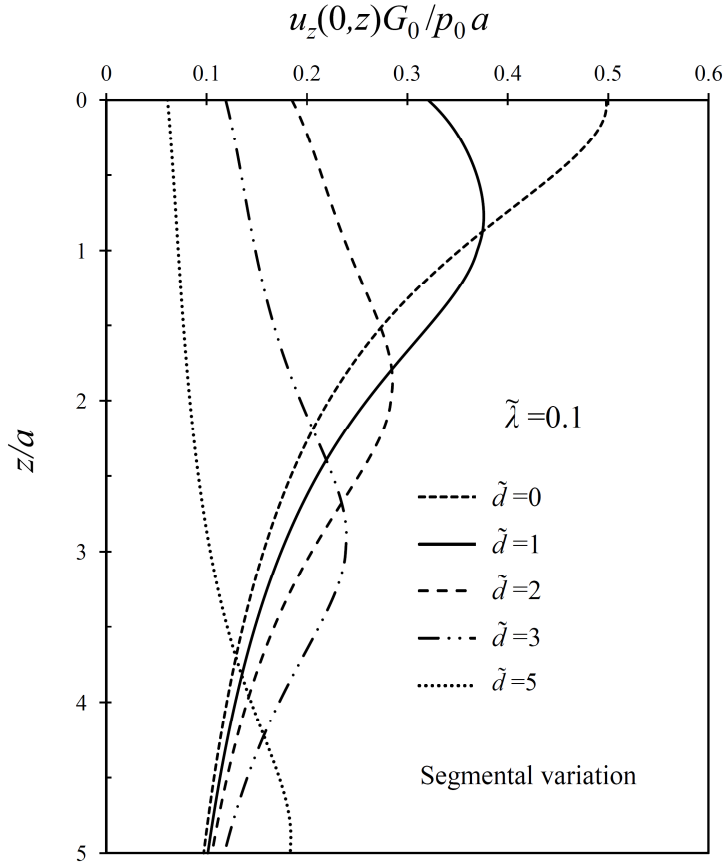

Figure 4.10: Variations of vertical displacement along the z-axis for different depths of the loading

To provide a better estimate of the relative influence of the elastic non-homogeneity on the displacements of the medium, the ratio of the displacement in a non-homogeneous medium to that in a homogeneous medium has been evaluated for different values of $\tilde{\lambda}$ and are presented in Figure 4.11 for both exponential and segmental variations.

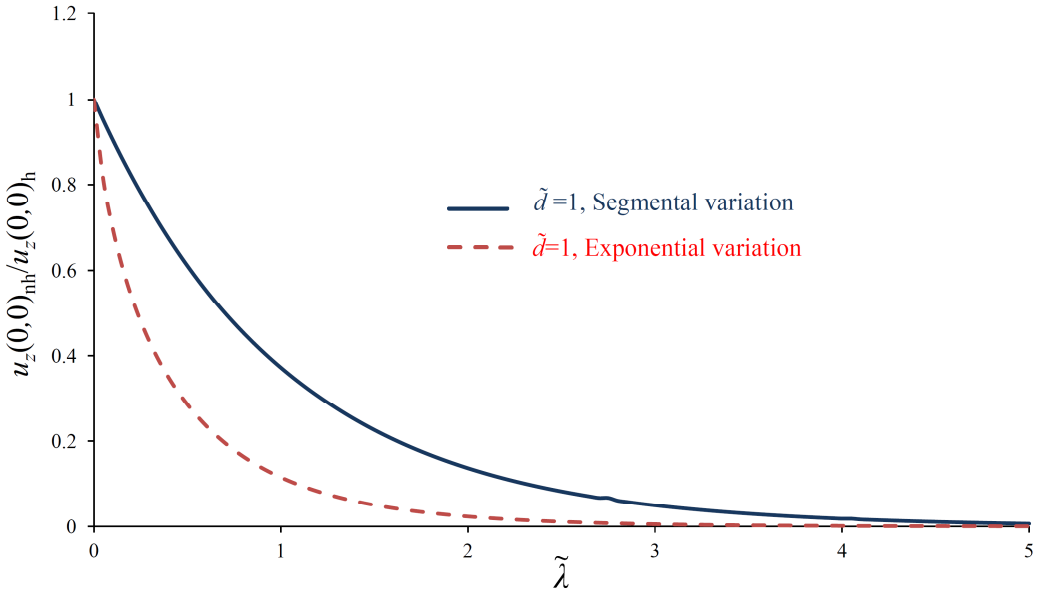

Figure 4.11: Ratio of displacement in a non-homogeneous medium to a homogeneous medium for different $\tilde{\lambda}$

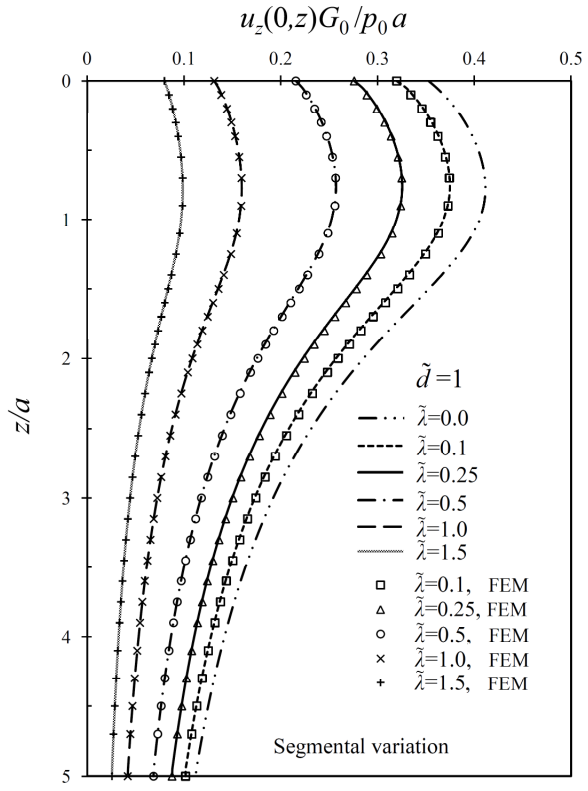

Figures 4.12: Variation of the vertical displacement along the z-axis for different $\tilde{\lambda}$ at a depth $\tilde{d}$ =1

Figure 4.12 shows the variation of the vertical displacement of a non-homogeneous incompressible halfspace with segmental variation of the shear modulus in the z-direction for different $\tilde{\lambda}$ at a depth $\tilde{d}=1$. The comparison of the vertical displacement along the z-direction for different shear modulus is shown in Figure 4.13. As would be expected, the vertical displacement is much lower for the exponential variation compared to the linear or segmental variation of the shear modulus.

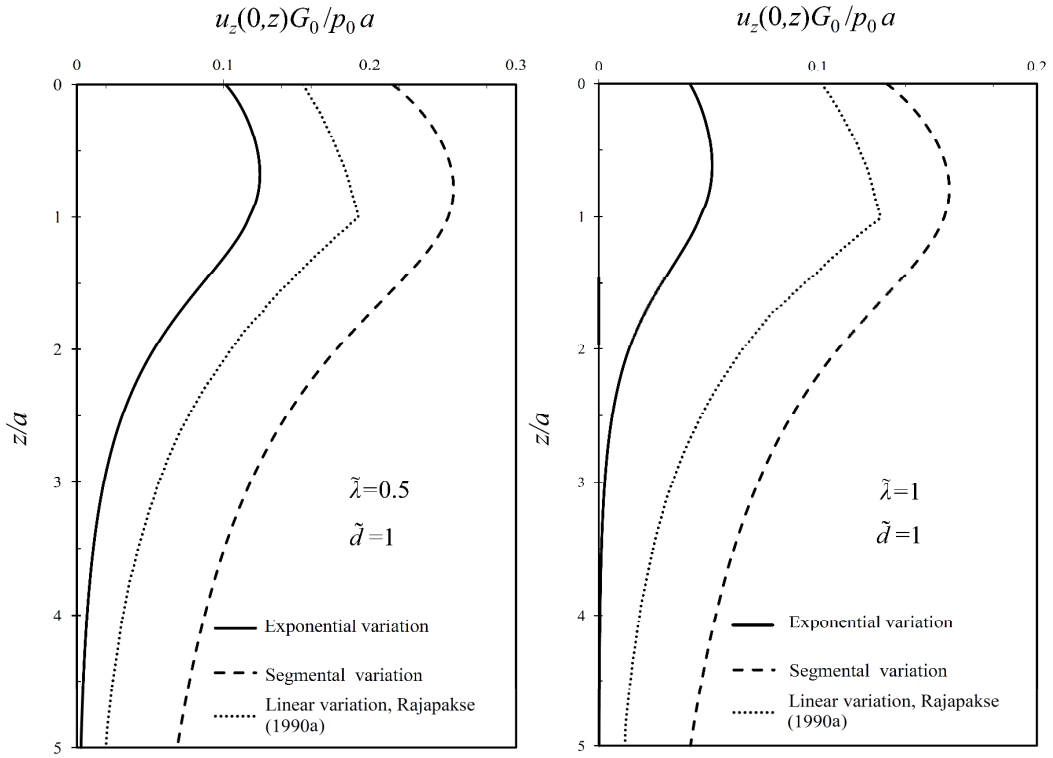

Figure 4.13: Comparison of vertical displacement along the z-axis for $\tilde{\lambda}=0.5$ and $\tilde{\lambda}=1$

Furthermore, the variation of vertical displacement of a non-homogeneous incompressible halfspace with segmental variation along the r-axis at depth $\tilde{d}=1$ is shown in Figure 4.14. Figure 4.15 compares of the vertical displacement along the r-axis for exponential, segmental, and linear variations of the shear modulus. As can be seen in the results presented in Figure 4.15, the slope of the curve should be zero on $r=0$; however, this is not correctly addressed by the results of Rajapakse (1990a).

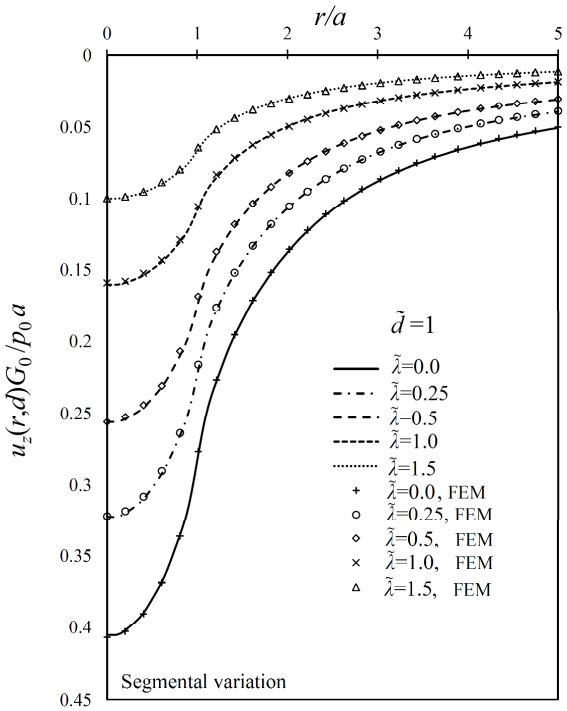

Figures 4.14: Variation of the vertical displacement along the *r*-axis for different $\tilde{\lambda}$ at a depth $\tilde{d}=1$

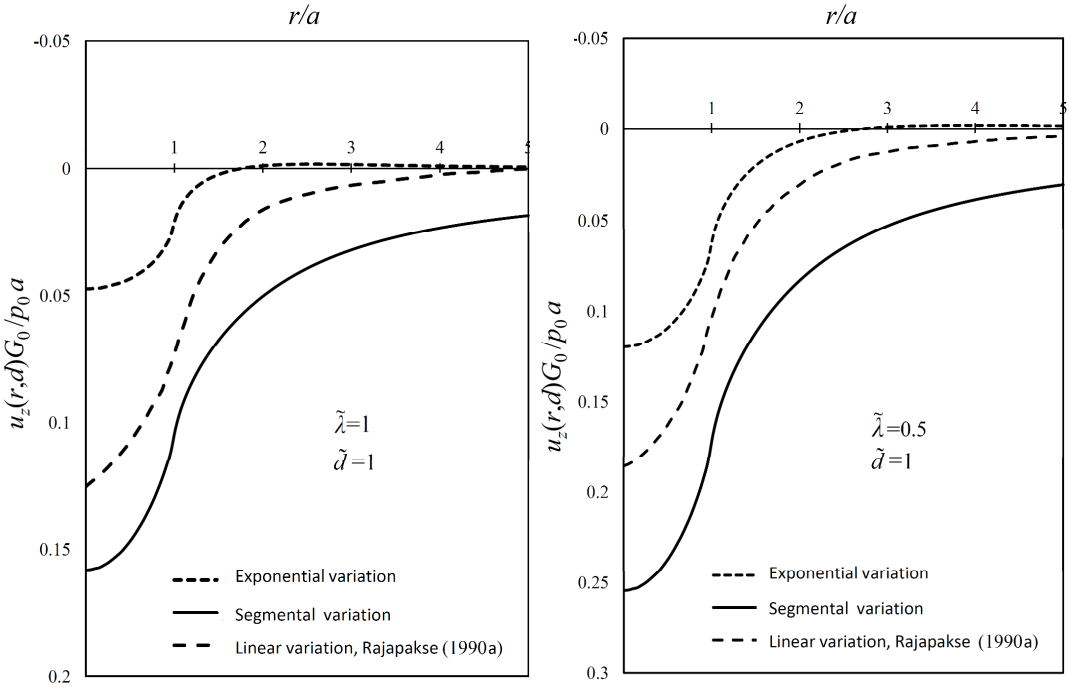

Figure 4.15: Comparison of vertical displacement along the *r*-axis for $\tilde{\lambda}=0.5$ and $\tilde{\lambda}=1$

The figures presented illustrate that the response of the medium is influenced by the degree of non-homogeneity. As would be expected, the vertical displacement decreases as the shear modulus increases, if all other parameters are kept constant (i.e. as G increases, the stiffness of the halfspace also increases).

Figure 4.16 shows the variation of non-dimensionalized vertical stress along the z-direction for segmental non-homogeneity at a depth $\tilde{d}=2$. As is evident from this Figure, σ_{zz} sustains a discontinuity at $\tilde{d}=2$ due to the effect of an externally applied load. It can be observed that σ_{zz} decreases with the increase in the shear modulus but, unlike the displacement, the influence of non-homogeneity is moderate and limited to the vicinity of the applied load.

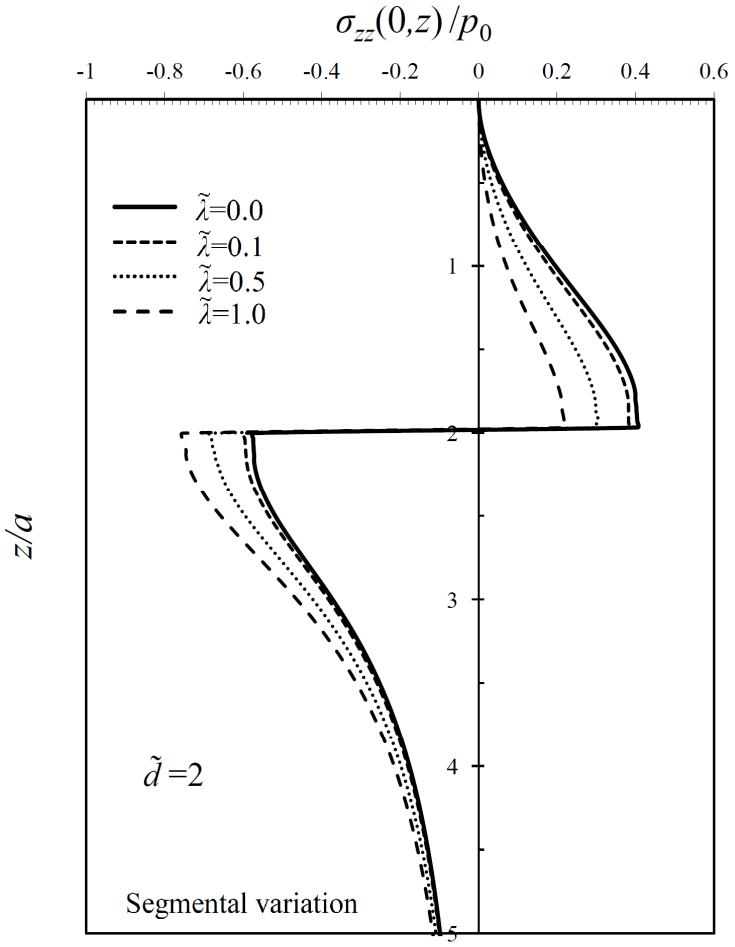

Figure 4.16: Normal stress along the z-axis

4.4 Settlement of a uniform circular load on an incompressible elastic finite layer whose shear modulus varies exponentially with depth

In the previous chapter, the influence of non-homogeneities on the stresses and displacements of a loaded incompressible isotropic elastic halfspace was considered. The loading was a uniform circular load in the interior of a halfspace. In the section 4.2, the shear modulus was considered to vary exponentially with depth over the entire halfspace region while in section 4.3, it was assumed to vary exponentially with depth over a finite depth, beyond which the elastic shear modulus was constant.

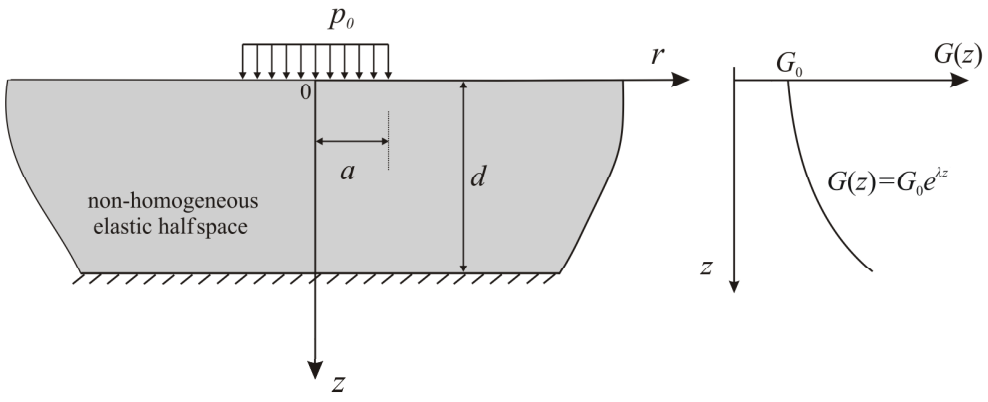

Figure 4.17: Uniform circular load on the surface of an undrained non-homogeneous elastic layer with a depth d

The present section extends these results for the case where the medium is a layer of finite depth d and of infinite lateral extent. The layer is loaded on its surface $z = 0$ by a vertical pressure p_0 uniformly distributed over a circular area of radius a while the base $z = d$ is considered to be the underlying rigid medium (Figure 4.17). The elastic layer is assumed to be incompressible with a shear modulus that increases exponentially with depth. The analytical formulation of the problem is presented as Bessel integrals with the aid of Hankel transforms.

Numerical results are presented to show how non-homogeneity influences the displacements and stresses.

4.4.1 Governing equations

We consider the problem of an incompressible non-homogeneous elastic layer of depth *d* subjected to a circular surface load of radius a with a stress intensity p_0 (Fig. 4.17). The boundary and interface conditions of the problem are:

$$\sigma_{rz}^{(1)}(r,0) = 0 \tag{4.30}$$

$$\sigma_{zz}(r,0) = \begin{cases} p(r), & r \le a \\ 0, & r > a \end{cases} \tag{4.31}$$

$$u_r(r,d) = 0;\ u_z(r,d) = 0 \tag{4.32}$$

In equation (4.31), $p(r)$ represents the intensity of the internally applied pressure over the circular area. With the aid of equations (3.21), (3.22) and (3.25) the transformed solution for the displacement components $u_r(r,z)$ and $u_z(r,z)$ can be written as

$$u_z(r,z) = \int_0^\infty [A_1 e^{-k_1 z} + B_1 e^{-k_2 z} + C_1 e^{k_3 z} + D_1 e^{k_4 z}]\xi J_0(\xi r) d\xi\ ; \qquad 0 < z < d \tag{4.33}$$

$$u_r(r,z) = \int_0^\infty [\frac{A_1 k_1}{\xi} e^{-k_1 z} + \frac{B_1 k_2}{\xi} e^{-k_2 z} - \frac{C_1 k_3}{\xi} e^{k_3 z} - \frac{D_1 k_4}{\xi} e^{k_4 z}]\xi J_1(\xi r) d\xi; \quad 0 < z < d \tag{4.34}$$

where k_1, k_2, k_3, k_4 are defined in equation (4.6) and A, B, C and D are arbitrary functions of ξ to be determined from the appropriate boundary conditions. Using the above equation along with equations (3.15) and (3.28) we have

$$f(r,z) = \int_0^\infty [A_1 q_1 e^{-k_1 z} + B_1 q_2 e^{-k_2 z} + C_1 q_3 e^{k_3 z} + D_1 q_4 e^{k_4 z}]\xi J_0(\xi r) d\xi\ ;\ 0 < z < d \tag{4.35}$$

where q_1, q_2, q_3, q_4 are defined by equation (4.10). Substitution of the equations (4.33), (4.34) and (4.35) into the boundary and continuity equations defined by

(4.30) to (4.32) results in a system of linear simultaneous equations for the arbitrary functions $A_1(\xi), B_1(\xi), C_1(\xi), D_1(\xi)$, …., etc., as follows :

$$A_1\eta_1 + B_1\eta_2 + C_1\eta_3 + D_1\eta_4 = 0 \tag{4.36}$$

$$A_1\theta_1 + B_1\theta_2 + C_1\theta_3 + D_1\theta_4 = \frac{\tilde{p}(\xi)}{G_0} \tag{4.37}$$

$$A_1\beta_1 e^{-k_1 d} + B_1\beta_2 e^{-k_2 d} - C\beta_3 e^{k_3 d} - D\beta_4 e^{k_4 d} = 0 \tag{4.38}$$

$$A_1 e^{-k_1 d} + B_1 e^{-k_2 d} + C_1 e^{k_3 d} + D_1 e^{k_4 d} = 0 \tag{4.39}$$

where $\beta_i, \theta_i, \eta_i$ $(i = 1, 2, 3, 4)$ is defined by equation (4.17) and $\tilde{p}(\xi)$ by equation (4.19). Substitution of the explicit solution for arbitrary functions A_1, B_1 C_1, and D_1 in equations (4.33) and (4.34) results in explicit solutions for the displacements and stresses at an arbitrary point within the domain of the elastic halfspace. The expressions for stresses and displacements involve infinite integrals with integrands decaying exponentially with increasing values of the Hankel transform parameter ξ, which will be solved in the next section.

4.4.2 Numerical results

In the preceding sections, the solutions for displacements and stresses in a non-homogeneous elastic layer region under uniform axial stress p_0 applied at the surface within a circular area *a*, were have been developed in terms of infinite integrals. These integrals have particularly complicated integrands and cannot be evaluated in exact closed form. Consequently, it is necessary to evaluate them numerically. The same numerical procedure as adopted in section 4.2 was applied to evaluate the explicit infinite integral expressions for the displacement and stress fields within the non-homogeneous elastic halfspace under a buried circular load. In the ensuing we present numerical results that illustrate how exponential inhomogeneity can influence the results of engineering interest. It should be pointed out that all numerical results are presented in a non-dimensional form.

Figure 4.18 shows the surface displacement of a non-homogeneous incompressible elastic layer region with a depth $\tilde{d} = 300$, which resembles the halfspace results, for different $\tilde{\lambda}$ which is directly related to the shear modulus by equation (3.3). These results are compared to results presented in previous sections in order to check the accuracy of the results.

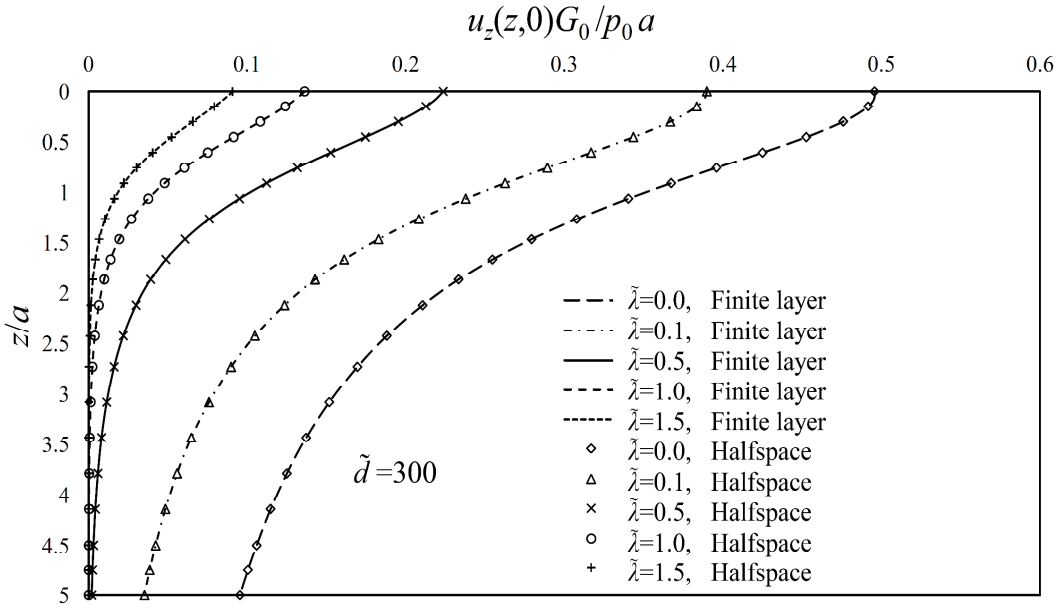

Figure 4.18: Variation of the vertical displacement along the *z*-axis for different $\tilde{\lambda}$ ($\tilde{\lambda}$ is directly related to the shear modulus obtained from by Eq. 3.3) for $\tilde{d} = 300$

Figures 4.19 and 4.20 show the variation of the vertical displacement along the *z*-axis for different $\tilde{\lambda}$ for a depth of the layer region $\tilde{\lambda} = 10$ and 15, respectively. It is evident that the presence of non-homogeneous conditions has a significant effect on the maximum surface displacement of the halfspace. By comparing Figures 4.18, 4.19 and 4.20, it can also be seen that the depth of the layer region has a significant effect on the results but this effect is not uniform for different $\tilde{\lambda}$; this will be discussed further in following paragraphs.

It should be mentioned that the computational results are indicated by the symbols □, ○, Δ, etc. in Figures 4.19 to 4.21.

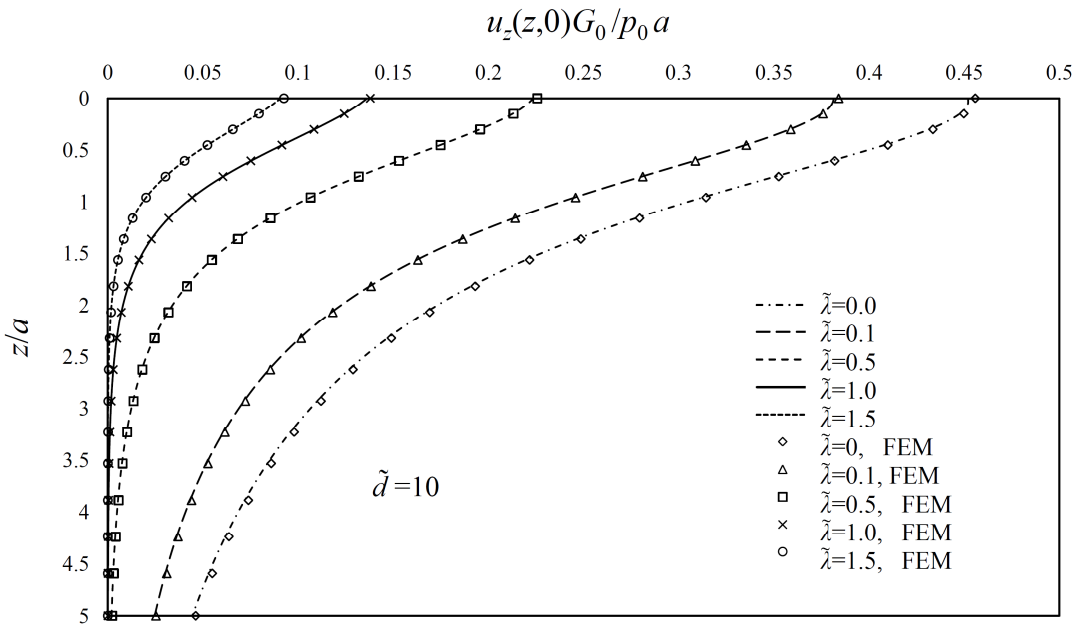

Figure 4.19: Variation of the vertical displacement along the z-axis for different $\tilde{\lambda}$ for $\tilde{d}=10$

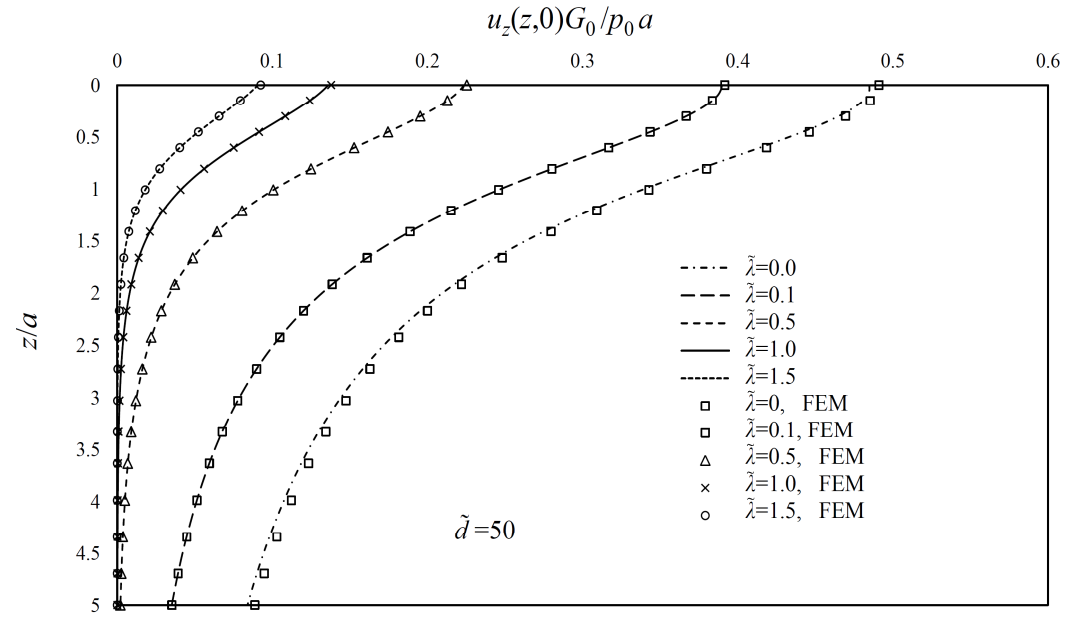

Figure 4.20: Variation of the vertical displacement along the z-axis for different $\tilde{\lambda}$ for $\tilde{d}=50$

When comparing the computational results with the analytical results, there is an excellent correlation between the analytical results derived for the exponential variations in the shear modulus, and the computational results.

Figure 4.21 shows the variation of the vertical displacement along the *r*-axis for different $\tilde{\lambda}$ for two depths of loading, $\tilde{d}=10$ and $\tilde{d}=50$. In order to provide a better estimate of the relative influence of the depth of the layer region on the displacements of the medium and also the influence of non-homogeneity for the different depths, the surface displacement has been evaluated for different $\tilde{d}$.

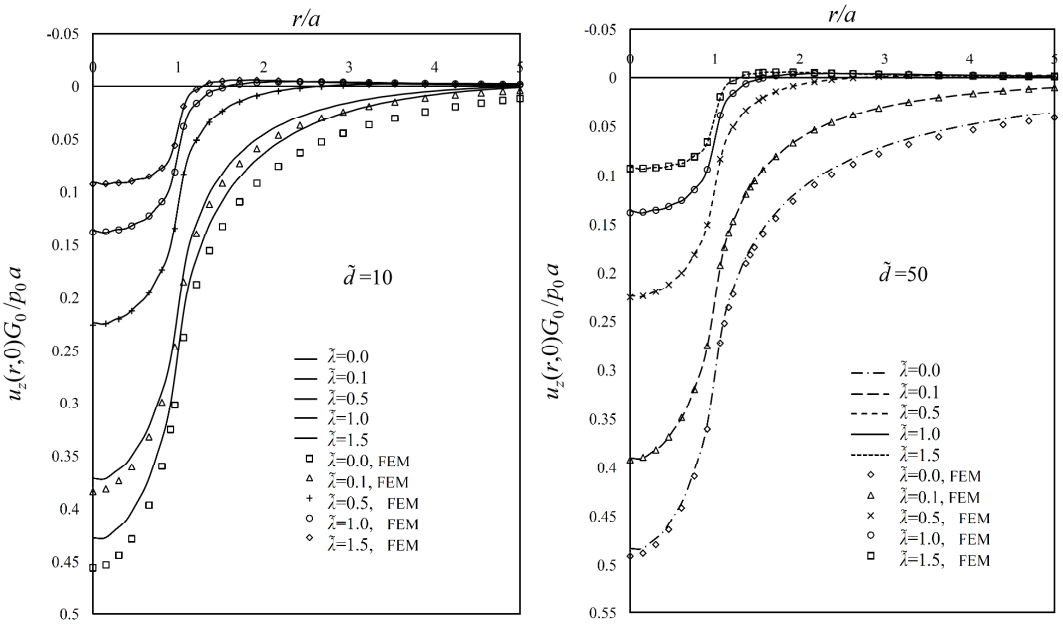

Figure 4.21: Variation of the vertical displacement along the *r*-axis for different $\tilde{\lambda}$ for (a) $\tilde{d}=50$ (b) $\tilde{d}=100$

Figure 4.22 shows the vertical surface displacement for different depths of the layer region for different values of $\tilde{\lambda}$. It can be seen from these figures that the depth of loading has a significant effect on the displacement but this affect decreases as the non-homogeneity increases. This could have been anticipated since the stiffness of the medium increases as *G* increases. It can also be seen in Figure 4.22 that the depth when the finite region resembles the halfspace

decreases as the non-homogeneity increases and, at $\tilde{\lambda}=1.5$, the finite layer resembles halfspace when the depth of the finite layer reaches almost 8 times the radius of loading.

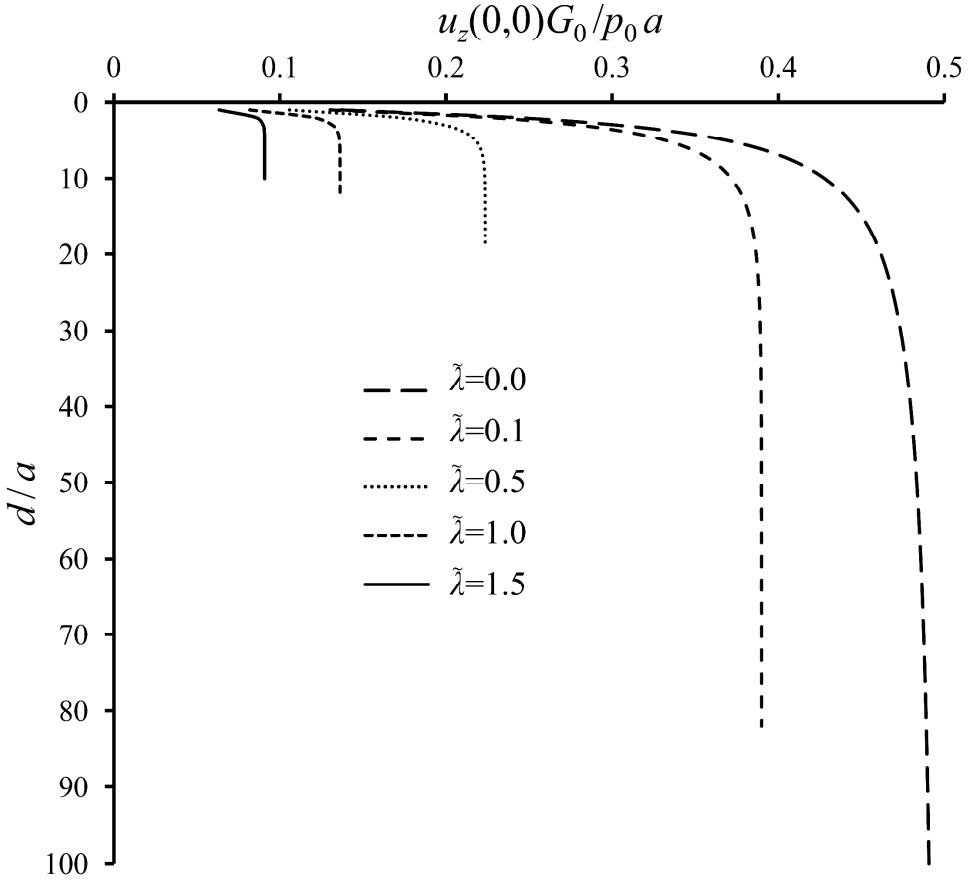

Figure 4.22: Vertical surface displacement for different depths of the layer region for $\tilde{\lambda}=0.0, 0.1, 0.5, 1.0, 1.5$

4.5 Axisymmetric distributed radial loading on a surface of an incompressible elastic halfspace with an exponential variation in the linear elastic shear modulus

In this section we develop the results for the axisymmetric distributed radial loading of an incompressible elastic halfspace where the elastic shear modulus varies with depth in an exponential manner. The development of this section will

be used in the following chapter in order to calculate the bonded contact of a rigid disc with a halfspace. The same procedure was used to formulate the traction boundary value and the numerical results are presented to show the influence of non-homogeneity on the results.

4.5.1 Governing equations

We consider the problem of an incompressible non-homogeneous halfspace subjected to a surface distributed radial load of radius a with stress intensity τ_0 (Figure 4.23). The boundary and interface conditions of the problem are as follows:

$$\sigma_{zz}^{(1)}(r,0) = 0 \tag{4.40}$$

$$\sigma_{rz}^{(1)}(r,0) = \begin{cases} \tau(r), & r \le a \\ 0, & r > a \end{cases} \tag{4.41}$$

In equation (4.41), $\tau(r)$ represents the intensity of the lateral load over the circular area.

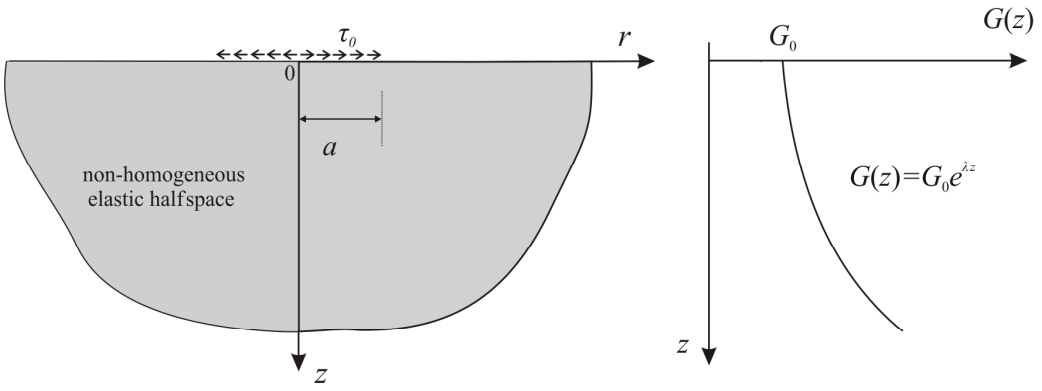

Figure 4.23: Uniform lateral circular load on the surface of an undrained non-homogeneous elastic halfspace

With the aid of equations (4.7), (4.9) and (4.11) along with regularity conditions at infinity, the transformed solution for the displacement components $u_r(r,z)$, $u_z(r,z)$, and $f(r,z)$ can be written as

$$u_z(r,z)=\int_0^\infty [Ae^{-k_1 z}+Be^{-k_2 z}]\xi J_0(\xi r)d\xi \ ; \qquad 0<z<d \tag{4.42}$$

$$u_r(r,z)=\int_0^\infty [\frac{Ak_1}{\xi}e^{-k_1 z}+\frac{Bk_2}{\xi}e^{-k_2 z}]\xi J_1(\xi r)d\xi ; \qquad 0<z<d \tag{4.43}$$

$$f(r,z)=\int_0^\infty [Aq_1 e^{-k_1 z}+Bq_2 e^{-k_2 z}]\xi J_0(\xi r)d\xi \ ; \ 0<z<d \tag{4.44}$$

where k_1, k_2 are defined by equation (4.6) and q_1, q_2 are defined by equation (4.10). *A* and *B* are arbitrary functions of ξ to be determined from the appropriate boundary conditions.

Substituting equations (4.42), (4.43) and (4.44) into the boundary and continuity equations defined by (4.40) and (4.41) results in:

$$A=\frac{\tilde{\tau}(\xi)}{G_0}\frac{(2k_2-q_2)\xi}{(q_2-2k_2)(k_1^2+\xi^2)+(2k_1-q_1)(k_2^2+\xi^2)} \tag{4.45}$$

$$B=\frac{\tilde{\tau}(\xi)}{G_0}\frac{(q_1-2k_1)\xi}{(q_2-2k_2)(k_1^2+\xi^2)+(2k_1-q_1)(k_2^2+\xi^2)} \tag{4.46}$$

where $\tilde{\tau}(\xi)$ is defined as

$$\tilde{\tau}(\xi)=\int_0^\infty r\tau(r)J_1(\xi r)dr \tag{4.47}$$

4.5.2 Numerical results

The same numerical procedure presented in the previous sections is used to evaluate the integral equations (4.42), (4.43) and (4.44). All the results presented here are dimensionless.

Figure 4.24 shows the radial surface displacement of a non-homogeneous incompressible elastic halfspace for different λ along the *r*-axis subjected to a radial distributed load. The value of $\tilde{\lambda}=0$ represents the case of the homogeneous halfspace in which $G=G_0$ for the entire depth. The computational results are also indicated by the symbols □, ○.

As it can be seen from Figure 4.24, the radial displacement decreases as the non-homogeneity increases.

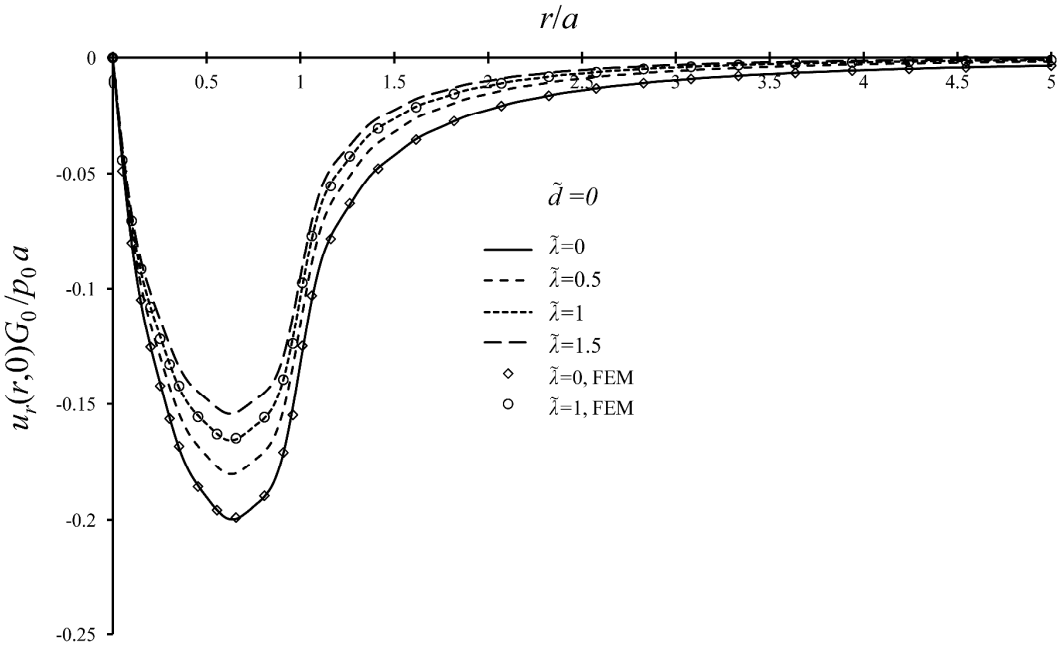

Figure 4.24 Radial surface displacement of a non-homogeneous incompressible elastic halfspace for different $\tilde{\lambda}$ along the *r*-axis

4.6 Finite element model, calibrating with the known analytical results

To provide a comparison with the analytical solutions, a finite element analysis of the incompressible non-homogeneous elastic halfspace problem was performed using the COMSOL Multiphysics^{TM} software. The domain of interest in the problems developed in this thesis is an incompressible halfspace, which extends

to infinity in both the *r*- and *z*-directions. In the finite element model in this thesis, the axisymmetric halfspace region is represented as a finite domain where the outer boundaries extend to 1000 times the radius of the loaded area in both the *r*- and *z*-directions. In order to obtain this ratio $(l/a = 1000)$, a calibration was performed between computational results with different (l/a) ratios and known analytical solutions for the classical contact problem (Selvadurai, 1979a; Gladwell, 1980). A mixed $U-P$ formulation was employed in the COMSOL Multiphysics™ software in order to model an incompressible material.

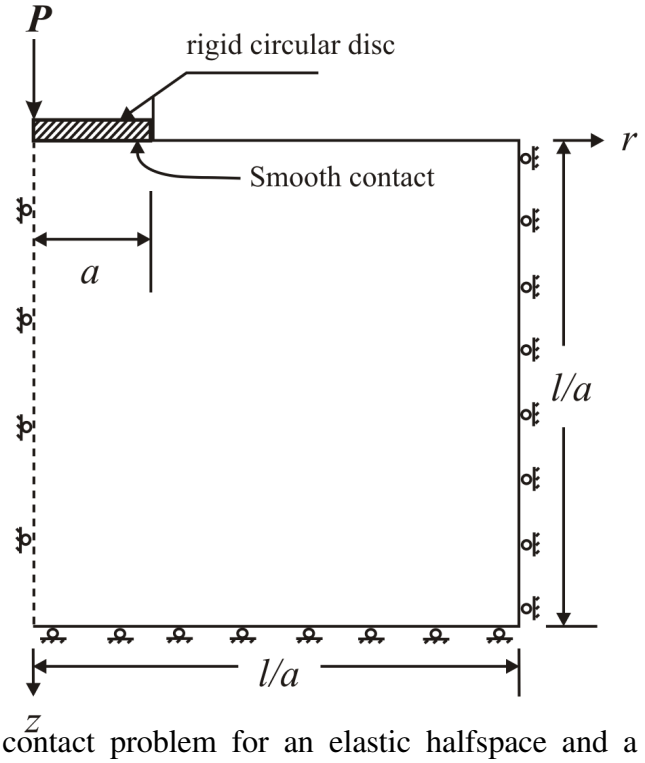

Figure 4.25 The contact problem for an elastic halfspace and a rigid circular indentor modeled by a finite domain

Figure 4.25 shows the finite element representation of the classical problem of the indentation of the surface of a homogeneous halfspace by a rigid circular disc of radius *a*, subjected to an axial load P. As can be seen from Figure 4.26, the analytical and computational results are virtually identical beyond $l/a = 1000$. The same (l/a) ratio was used to develop computational results for the non-homogeneous case.

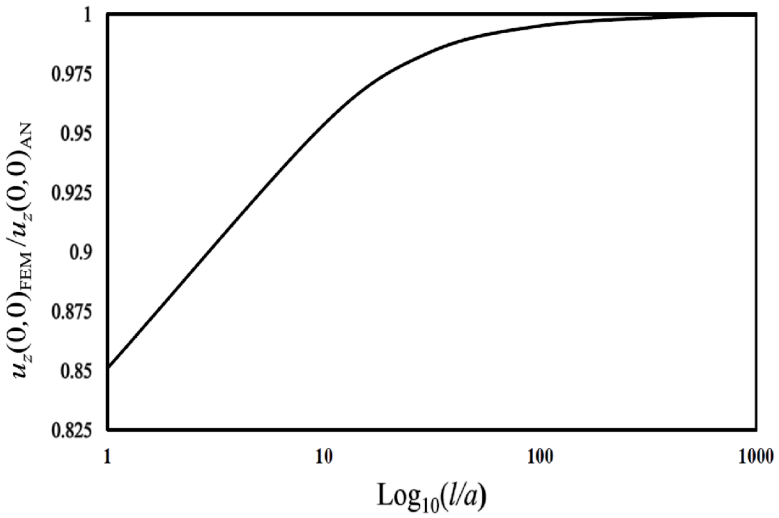

Figure 4.26 Vertical displacement for different l / a

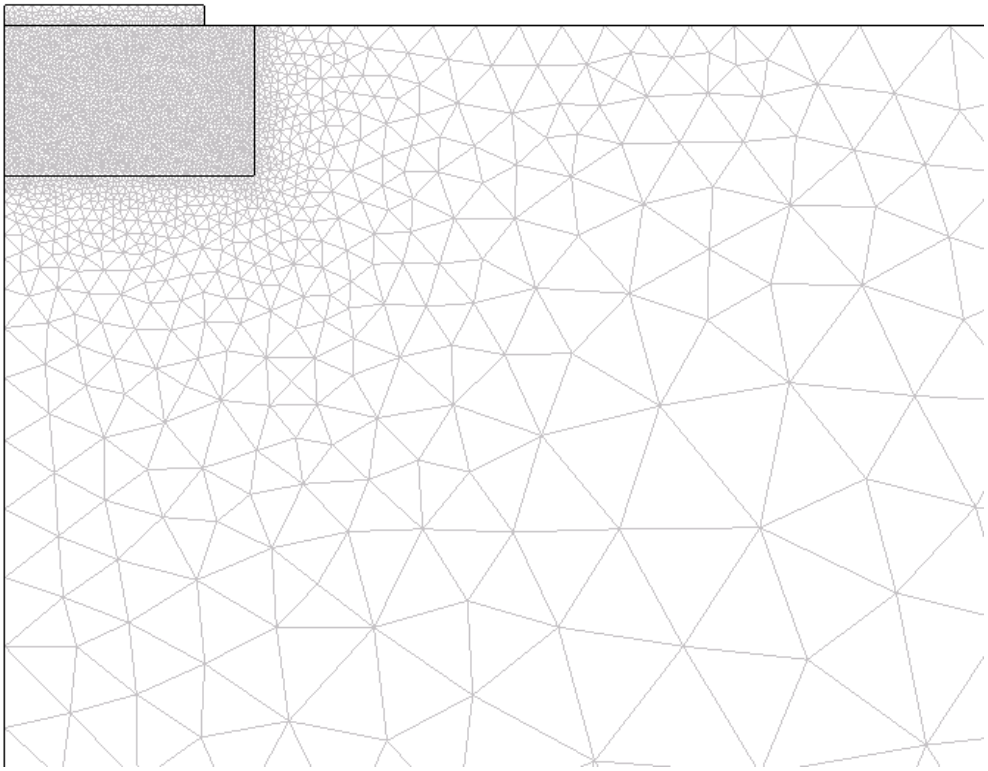

Figure 4.27 Finite element representation of the classic problem of the indentation of the surface of an incompressible halfspace by rigid circular disc.

The analytical results developed in this thesis are compared with the FE results for a non-homogeneous incompressible halfspace with either exponential or segmental variation of the shear modulus (the computational results are indicated by the symbols □, ○, Δ, etc. in the associated Figures).

Figure 4.27 shows, as an example, the FE model of the indentation problem between an incompressible non-homogeneous elastic halfspace and a rigid circular disc subjected to uniform pressure p_0 . As it can be seen the mesh size is finer around the rigid indenter. The model shown in Figure 4.27 consists of 9498 elements and 43299 degree of freedom.

CHAPTER 5

CONTACT PROBLEMS – MIXED BOUNDARY VALUE PROBLEMS

5.1 Introduction

The topic of contact mechanics occupies an important position in the mechanics of solids where the results derived for the interaction of a rigid indenter and a halfspace form the basic problem. The classical elasticity solutions to the mechanics of contact commences with the solutions by Hertz (1882) and Boussinesq (1885) and developments in this area are documented in several texts and review articles by Korenev (1960), Galin (1961), Sneddon (1951, 1965), Ufliand (1956), Goodman (1974), de Pater and Kalker (1975), Selvadurai (1979a, 2000b, 2007), Gladwell (1980), Johnson (1985), Aleynikov (2011) and Barber (2010). The great majority of the classical studies in this area focus on the contact problem where the halfspace region is homogeneous and the indenter is both rigid and axisymmetric. Departures to this model are documented by Gorbunov-Posadov (1940), Selvadurai (1979 b,c; 1980, 1981, 1984a), Gladwell (1980), Rajapakse and Selvadurai (1986), Selvadurai and Dumont (2011), and Aleynikov

(2011) who examine the cases where the contacting element possesses flexural stiffness.

In this chapter we examine the problem of adhesive contact between a rigid circular punch and an incompressible elastic halfspace region where the shear modulus of the elastic material varies exponentially with depth. Also, unless otherwise stated, the rigid circular indenter is assumed to have a flat base, which makes the class of problems examined in the paper purely axisymmetric. In particular, attention is focused on estimating the influence of the elastic inhomogeneity on the adhesive elastic stiffness of the rigid circular indenter. The solution of the adhesive contact problem is achieved using a numerical scheme where the fundamental solutions for the axisymmetric loading of the non-homogeneous halfspace region due to normal and shear loads applied over discrete regions of the surface of the halfspace are combined to determine the axial and radial displacements over the region of the indenter. The distribution of the discrete values of the contact stresses are determined by considering the displacement constraints imposed on the contact region and the overall equilibrium of the indenter. This approach to the analysis of the adhesive contact problem related to the indentation of the inhomogeneous halfspace region is an extension to similar procedures that have been successfully used in discretized approaches for solving soil-structure interaction problems (Selvadurai, 1979a).

We also examine the contact problem between a flexible circular plate and an incompressible non-homogeneous isotropic elastic halfspace is examined using the energy method. The shear modulus is assumed to vary exponentially with depth. The variational approach proposed by Selvadurai (1979c, 1980) was used to analyse the flexural behaviour of a finite plate resting on an elastic halfspace. In this approach, the deflected shape of the plate in represented by a power series in terms of the radial coordinate r, which satisfies the kinematic constraints of the plate formation. The total potential energy functional is then developed for the plastic-elastic halfspace region which is defined in terms of four undetermined constants characterizing the deflected shape of the plate. Invoking the Kirchhoff

boundary conditions applicable to the free edge of the plate can eliminate two constants in the series and two remaining constants are evaluated by the minimization of the total potential energy functional of the system.

5.2 Adhesive contact problem for a non-homogenous incompressible elastic halfspace

In this section we examine the axisymmetric adhesive contact problem for a rigid circular plate and an incompressible elastic halfspace, where the linear elastic shear modulus varies exponentially with depth. The analytical solution of the mixed boundary value problem entails a set of coupled integral equations that cannot be solved easily through the use of techniques proposed in the literature. In this thesis a computational scheme is adopted where the contact normal and contact shear stress distributions are approximated by their discretized equivalents. The consideration of compatibility of deformations due to indentation by a rigid disc in adhesive contact yields a set of algebraic equations that give the discretized equivalents of the contacts stresses and the axial stiffness of the elastic halfspace.

5.2.1 Theoretical developments

Prior to developing a numerical approach to the solution of the adhesive contact problem, it is instructive to record salient results applicable to the indentation of the *homogeneous elastic halfspace* region. To provide some generality, we consider the indentation of the *homogeneous elastic halfspace* problem with no restriction on Poisson's ratio. We consider an axisymmetric formulation of the contact problem where the displacement and stress fields referred to the cylindrical polar coordinate system are given by

$$\mathbf{u}(r,z) = \{u_r(r,z),\, u_z(r,z)\} \tag{5.1}$$

and

$$\boldsymbol{\sigma}(r,z)=\begin{pmatrix}\sigma_{rr} & 0 & \sigma_{rz}\\ 0 & \sigma_{\theta\theta} & 0\\ \sigma_{rz} & 0 & \sigma_{zz}\end{pmatrix} \tag{5.2}$$

The mixed boundary value problem governing the adhesive indentation of the homogeneous elastic halfspace is given by

$$\begin{aligned} &u_z(r,0)=\Delta \quad ; \quad 0\le r\le a\\ &u_r(r,0)=0 \quad ; \quad 0\le r\le a\\ &\sigma_{zz}(r,0)=0 \; ; \quad a<r<\infty\\ &\sigma_{rz}(r,0)=0 \; ; \quad a<r<\infty \end{aligned} \tag{5.3}$$

In addition, the displacement and stress fields should reduce to zero as $r,z\to\infty$. The solution to the indentation problem was presented in a general fashion by Mossakovskii (1954) and Ufliand (1956) where the axial displacement distribution was defined by $w(r)$ and the radial displacement was defined by $u(r)$. $u(r)$. The *contact normal stress* $\sigma_{zz}(r)$ normalized with respect to the shear modulus and (Δ/a) is expressed as $\sigma_{zz}(r)=-\{G\Delta/a(1-\nu)\}\tilde{\sigma}(\tilde{\xi})$ and the *contact shear stress* $\sigma_{rz}(r)$ in the adhesive zone, normalized with respect to the shear modulus and (Δ/a) is expressed as $\sigma_{rz}(r)=-\{G\Delta/a(1-\nu)\}\tilde{\tau}(\tilde{\xi})$. The normalized stresses $\sigma(\tilde{\xi})$ and $\tau(\tilde{\xi})$ are governed by a pair of coupled integral equations of the form

$$\int_{\tilde{\xi}}^{1}\frac{t\tilde{\sigma}(t)dt}{\sqrt{t^2-\tilde{\xi}^2}}-\gamma\left\{\int_0^1\tilde{\tau}(t)dt-\tilde{\xi}\int_0^{\tilde{\xi}}\frac{\tilde{\tau}(t)dt}{\sqrt{\tilde{\xi}^2-t^2}}\right\}=\frac{d}{d\tilde{\xi}}\int_0^{\tilde{\xi}}\frac{t\tilde{w}(t)dt}{\sqrt{\tilde{\xi}^2-t^2}}=\tilde{w}^*(\tilde{\xi}) \tag{5.4}$$

$$\tilde{\xi}\int_{\tilde{\xi}}^{1}\frac{\tilde{\tau}(t)dt}{\sqrt{t^2-\tilde{\xi}^2}}-\gamma\int_0^{\tilde{\xi}}\frac{t\tilde{\sigma}(t)dt}{\sqrt{\tilde{\xi}^2-t^2}}=\int_0^{\tilde{\xi}}\frac{d}{dt}\left[t\tilde{u}(t)\right]\frac{dt}{\sqrt{\tilde{\xi}^2-t^2}}=\tilde{u}^*(\tilde{\xi}) \tag{5.5}$$

where $\tilde{\xi}=r/a$, $u_z(r)=\Delta\tilde{w}(\tilde{\xi})$, $u_r(r)=\Delta\tilde{u}(\tilde{\xi})$ and Δ is the axial indentation. Also, $\tilde{w}^*(\tilde{\xi})$ and $\tilde{u}^*(\tilde{\xi})$ are non-dimensional displacements that are prescribed in

the contact zone and γ=(1-2ν)/(2-2ν) . For example, in the case of a rigid circular indenter in adhesive contact with an elastic halfspace region, $\tilde{w}(\tilde{\xi}) = 1$ and $\tilde{u}(\tilde{\xi}) = 0$. Using a Wiener-Hopf/Hilbert transform technique (Gladwell, 1980) for the solution of the mixed boundary value problem, these authors (Mossakovskii, 1954; Ufliand, 1956) were able to develop explicit expressions for the distribution of contact stresses at the base of the indenter and use the results to obtain a relationship between the force P necessary to induce the induced displacement Δ; i.e.

$$\frac{P}{8\Delta a\mu} = \frac{\log_e(3-4\nu)}{2(1-2\nu)} \tag{5.6}$$

An alternative to the development of an exact solution was first proposed by Selvadurai (1984b, 2000c, 2003, and 2009) and was applied by Selvadurai and Au (1986) to investigate the mechanics of anchors embedded at bimaterial interface regions. Selvadurai's bounding procedure involves the introduction of either inextensibility constraints or frictionless conditions at the interface between the bimaterial regions. The same approach can be adopted to "bound" the axial stiffness of the bonded rigid indenter. The mixed boundary value problem defined by (5.3) is replaced by reduced boundary value problems that impose either an inextensibility constraint over the entire surface of the halfspace or a frictionless constraint over the entire surface of the halfspace. The relevant sets of boundary conditions are, respectively,

$$u_z(r,0) = \Delta \quad ; \quad 0 \le r \le a$$

$$u_r(r,0) = 0 \quad ; \quad 0 \le r < \infty$$

$$\sigma_{zz}(r,0) = 0 \; ; \quad a < r < \infty \tag{5.7}$$

and

$$u_z(r,0) = \Delta \quad ; \quad 0 \le r \le a$$

$$\sigma_{rz}(r,0) = 0 \ ; \quad 0 \le r < \infty$$

$$\sigma_{zz}(r,0) = 0 \ ; \quad a < r < \infty \tag{5.8}$$

The solution of the mixed boundary value problems defined by Eqs. (5.7) and (5.8) is elementary (Sneddon, 1951, 1965; Selvadurai, 1979a, 2000b; Gladwell, 1980) and, using these results, the bounds for the elastic stiffness of the bonded rigid disc can be expressed in the form

$$\frac{1}{2(1-\nu)} \le \frac{P}{8\Delta a\mu} \le \frac{2(1-\nu)}{(3-4\nu)} \tag{5.9}$$

In the limit when $\nu = 0$, the exact solution Eq. (5.6) gives

$$\frac{P}{8\Delta a\mu} = \frac{\log_e 3}{2} \approx 0.55 \tag{5.10}$$

and the bounds (5.9) give

$$0.50 \le \frac{P}{8\Delta a\mu} \le 0.67 \tag{5.11}$$

In the limit when $\nu = 1/2$, the bounds Eq. (5.9) converge and yield the same result as the exact solution (Eq. (5.6)). The influence of material incompressibility on the behaviour of the contact problem is clearly evident and, in the case of the isotropic homogeneous elasticity problem applicable to an incompressible elastic material, the absence of radial displacement on the surface of the halfspace due to Boussinesq's fundamental result for the normal loading of the halfspace region (Bousssinesq, 1885; Michell, 1900; Love, 1927; Westergaard, 1952; Timoshenko and Goodier, 1970; Selvadurai, 2000d, 2001a,b; Barber, 2010) pre-empts the need to consider the constraints imposed by bonding in the solution of the contact problem. This observation is strictly applicable to the case of a *homogeneous elastic halfspace* problem and does not generally apply in situations where the incompressible elastic halfspace region is non-homogeneous.

5.2.3 The adhesive indentation of a non-homogeneous isotropic elastic halfspace

We now consider the problem of the indentation of an incompressible non-homogeneous isotropic elastic halfspace region by a rigid circular indenter of radius a with a flat base, which is bonded to the surface of the halfspace (Figure, 5.1). The non-homogeneity considered in this section assumes that the shear modulus of the elastic medium varies exponentially according to Eq. (3.3).

The objective of the study is to establish the influence of both the adhesive contact and the exponential variation in the shear modulus on the elastic stiffness of the rigid indenter. To the authors' knowledge, this problem has not been investigated in the literature on contact problems. In particular, the method of solution is based on the discretization of the contact normal stresses and contact shear stresses in the bonded region, which yields a set of algebraic equations that can be solved to develop results of engineering interest.

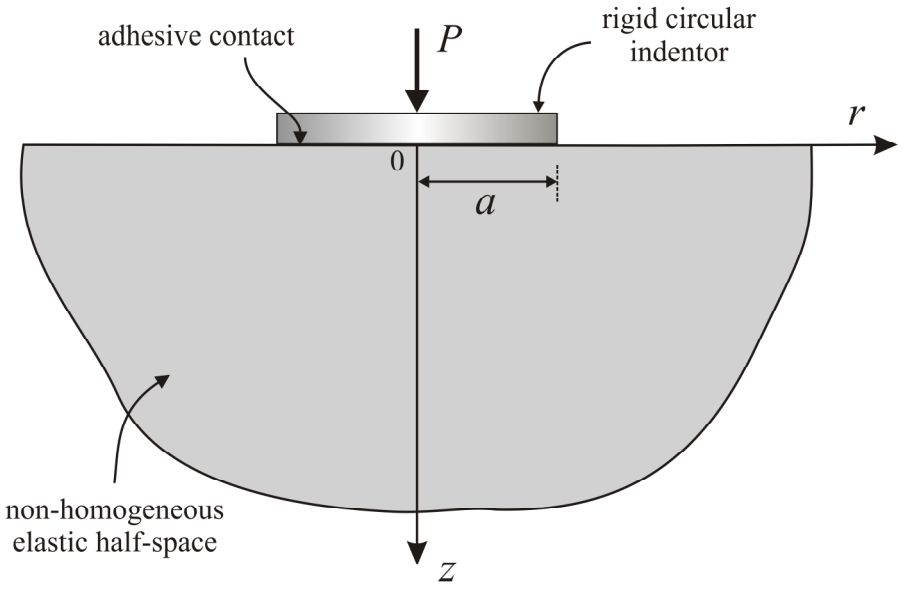

Figure 5.1: Indentation of an incompressible non-homogeneous elastic halfspace

Prior to the application of the computational approach it is instructive to illustrate the basic concepts of the adhesive contact problem related to the non-

homogeneous elastic halfspace. Consider the problem where the surface of the non-homogeneous elastic halfspace region is subjected, separately, to (i) a normal ring load of intensity N (units of force/unit length) applied at the location $r = \rho$ and (ii) a radially directed ring load of intensity T (units of force/unit length) applied at the location $r = \rho$ (Figure, 5.2).

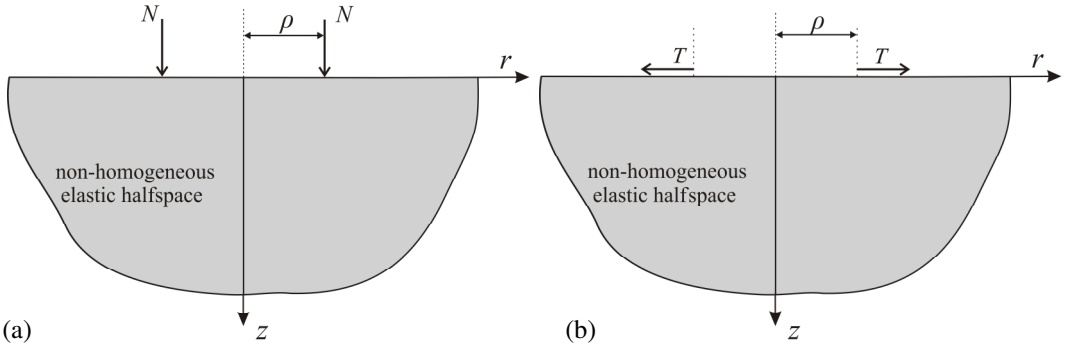

Figure 5.2: (a) Normal ring load of intensity N (units of force/unit length) applied at the location $r = \rho$; (b) A radially directed ring load of intensity T (units of force/unit length) applied at the location $r = \rho$

The choice of these special forms of the fundamental results for N and T pre-supposes that the application of the discretization technique is restricted to axisymmetric contact problems related to an incompressible non-homogeneous elastic halfspace. The method of solution of the traction boundary value problems relevant to these basic loading configurations was outlined in previous chapter. It can be shown that the axial and radial displacements at the surface of the halfspace region due to the normal ring loading N can be expressed in the general forms

$$u_z^N(r,0) = \frac{N}{G_0} I_{zz}^N(r,\rho); \quad 0 \le r < \infty$$

$$u_r^N(r,0) = \frac{N}{G_0} I_{rz}^N(r,\rho); \quad 0 \le r < \infty \tag{5.12}$$

where the integrals $I_{zz}^N(r,\rho)$ and $I_{rz}^N(r,\rho)$ are given by

$$I_{zz}^{N}(r,\rho)=\int_0^{\infty}\left(\frac{(k_1^2-k_2^2)}{(2k_1-q_1)(\xi^2+k_2^2)+(q_2-2k_2)(\xi^2+k_1^2)}\right)\rho\xi J_0(\xi r)J_0(\xi\rho)\,d\xi$$

$$I_{rz}^{N}(r,\rho)=\int_0^{\infty}\left(\frac{k_2(\xi^2+k_1^2)-k_1(\xi^2+k_2^2)}{(2k_1-q_1)(\xi^2+k_2^2)+(q_2-2k_2)(\xi^2+k_1^2)}\right)\rho J_1(\xi r)J_0(\xi\rho)\,d\xi \tag{5.13}$$

with

$$k_1=\frac{1}{2}[\lambda+\sqrt{\lambda^2+4i\lambda\xi+4\xi^2}]\quad ;\quad k_2=\frac{1}{2}[\lambda+\sqrt{\lambda^2-4i\lambda\xi+4\xi^2}] \tag{5.14}$$

and

$$q_i=\frac{k_i^3}{\xi^2}-k_i-\frac{\lambda k_i^2}{\xi^2}-\lambda;\quad i=1,2 \tag{5.15}$$

Similarly, the axial and radial displacements on the surface of the halfspace region due to the radial ring loading T can be expressed in the general forms

$$u_z^T(r,0)=\frac{T}{G_0}\,I_{zr}^T(r,\rho);\quad 0\le r<\infty$$

$$u_r^T(r,0)=\frac{T}{G_0}\,I_{rr}^T(r,\rho);\quad 0\le r<\infty \tag{5.16}$$

where the integrals $I_{rr}^T(r,\rho)$ and $I_{zr}^T(r,\rho)$ are given by

$$I_{zr}^{T}(r,\rho)=\int_0^{\infty}\left(\frac{(q_1-2k_1)+(2k_2-q_2)}{(2k_1-q_1)(\xi^2+k_2^2)+(q_2-2k_2)(\xi^2+k_1^2)}\right)\rho\xi^2 J_0(\xi r)J_1(\xi\rho)d\xi$$

$$I_{rr}^{T}(r,\rho)=\int_0^{\infty}\left(\frac{k_2q_1-k_1q_2}{(2k_1-q_1)(\xi^2+k_2^2)+(q_2-2k_2)(\xi^2+k_1^2)}\right)\rho\xi J_1(\xi r)J_1(\xi\rho)d\xi \tag{5.17}$$

The displacement fields given by Eqs. (5.12) and (5.16) will satisfy the regularity conditions required for the displacement field to vanish as $r\to\infty$ and the traction boundary conditions applicable to the ring loads. For the *normal ring load*

$$\sigma_{zz}(r,0) = N\,\delta(r-\rho)\;;\quad 0 \le r < \infty$$

$$\sigma_{rz}(r,0) = 0;\qquad\qquad 0 \le r < \infty \tag{5.18}$$

where $\delta(r-\rho)$ is the Dirac delta function. Similarly, for the *radial ring load*

$$\sigma_{zz}(r,0) = 0;\qquad\qquad 0 \le r < \infty$$

$$\sigma_{rz}(r,0) = T\,\delta(r-\rho)\;;\quad 0 \le r < \infty \tag{5.19}$$

The formal expressions for the axial and radial displacement fields generated by the contact normal stress $\sigma(r)$ and the contact shear stress $\tau(r)$ in the adhesive contact region of the rigid indenter can be written as

$$u_z(r,0) = \int_0^a \frac{\sigma(\rho)}{G_0}\, I_{zz}^N(r,\rho)d\rho + \int_0^a \frac{\tau(\rho)}{G_0}\, I_{zr}^T(r,\rho)d\rho;\quad 0 \le r < \infty \tag{5.20}$$

$$u_r(r,0) = \int_0^a \frac{\tau(\rho)}{G_0}\, I_{rr}^T(r,\rho)d\rho + \int_0^a \frac{\sigma(\rho)}{G_0}\, I_{rz}^N(r,\rho)d\rho;\quad 0 \le r < \infty \tag{5.21}$$

The boundary conditions applicable to the adhesive contact problem are

$$u_z(r,0) = \Delta\;;\quad 0 \le r \le a$$

$$u_r(r,0) = 0\;;\quad 0 \le r \le a \tag{5.22}$$

An inspection of the integral expressions for the influence functions $I_{zz}^N(r,\rho)$, $I_{rz}^N(r,\rho)$, etc., and the governing integral expressions indicates that the integral equations (5.20) and (5.21) are unlikely to be solved in a direct fashion to generate compact results of the type (5.6) for the elastic stiffness of the rigid circular indenter in adhesive contact with a non-homogeneous elastic halfspace. Therefore recourse must be made to a computational approach that essentially discretizes the contact stress distributions.

5.2.4 The computational approach for the solution of the adhesive contact problem

We now focus on the development of a computational approach for the solution of the axisymmetric problem of the loading of a rigid circular indenter of radius a subjected to an axisymmetric load P and in adhesive contact with a non-homogeneous elastic halfspace where the elastic modulus varies exponentially with depth. The basic objective is to represent the contact stress distributions $\sigma(r)$ and $\tau(r)$ as discrete regions of uniform stress acting over annular regions. This approach to the solution of contact problems was employed by a number of investigators and a comprehensive review of the approach is presented in Selvadurai (1979a). Representation of the contact stress distributions as discrete values of finite magnitude does not allow the accommodation of the singularities that will be present at the boundary of the rigid indenter. In the case of bonded contact with a homogeneous elastic medium, the normal and shear stresses can exhibit oscillatory forms of the stress singularity that arise in the solution of Wiener-Hopf/Hilbert type problems. The oscillatory stress singularities are, however, integrable and contribute to the finite strain energy in the halfspace region and regular results for the axial stiffness of the bonded indenter. While consideration of the exact stress state is important to the assessment of fracture generation at the boundary of the bonded region, its influence on the estimation of the elastic stiffness is relatively small. Selvadurai (1989) has shown that, in the case of a homogeneous elastic halfspace problem related to a bonded circular indenter, the incorporation of the oscillatory form of the stress singularity does not significantly influence the axial stiffness of the bonded rigid indenter. When the stress singularity at the boundary of the bonded rigid indenter of radius a is represented by a regular singularity of the form $1/(a^2 - r^2)^{1/2}$ the problem can be reduced to the solution of a Fredholm integral equation of the second-kind and a comparison of the results obtained from the exact solution and the above approximation indicates that the difference is less than 0.5% when $\nu = 0$ and the solutions coincide when $\nu = 1/2$. We further note that in the case of an incompressible non-homogeneous elastic halfspace, the local stress field at the

boundary of the contact region will not be oscillatory in order to provide a continuous transition to the analogous problem for the adhesive contact problem associated with a homogeneous incompressible elastic halfspace. In keeping with this observation, we proceed to represent the contact stress distributions by their discrete equivalent distributions and the geometry of the discrete regions is altered to account for sharp stress gradients that could be present at the boundary regions of the contact zone.

5.2.5 Smooth contact problem for a rigid circular indenter

First we consider the indentation of a non-homogeneous incompressible elastic halfspace by a rigid circular indenter of radius a with smooth contact subjected to an axial load P. The method of solution assumes that the plan area of the indenter is discretized into equal annular areas and the contact stress within each annular area is uniform. It is considered that the annular normal load of stress intensity $\sigma_1, \sigma_2, ..., \sigma_n$ acting within the annular region of internal radius $0, r_1, r_2, ..., r_{n-1}$ and external radius $r_1, r_2, ..., r_n$ respectively. Figure 5.3 shows this distribution for $n = 15$. The surface displacement $w_1, w_2, w_3, ..., w_n$ at the mid section of the annular region due to normal surface tractions can be obtained by superposition of the Eqs. (5.23) and (5.24), which are a simplified version of the results developed in the previous chapter,

$$u_z(r,0) = \frac{p_0 a}{G_0} \int_0^\infty \left(\frac{(k_1^2 - k_2^2)}{(2k_1 - q_1)(\xi^2 + k_2^2) + (q_2 - 2k_2)(\xi^2 + k_1^2)} \right) J_0(\xi r) J_1(\xi a) d\xi \quad (5.23)$$

$$u_r(r,0) = \frac{p_0 a}{G_0} \int_0^\infty \left(\frac{k_2(\xi^2 + k_1^2) - k_1(\xi^2 + k_2^2)}{\xi(2k_1 - q_1)(\xi^2 + k_2^2) + \xi(q_2 - 2k_2)(\xi^2 + k_1^2)} \right) J_1(\xi r) J_1(\xi a) d\xi \quad (5.24)$$

where k_1, k_2, q_1 and q_2 are defined by Eqs. (5.14) and (5.15).

The compatibility between the settlement of the non-homogenous incompressible halfspace and settlement of the indenter, Δ, is then established at the mid location of each annular region. The physical domain of interest is taken to be a non-

homogeneous incompressible ($v = 1/2$) elastic halfspace in which the shear modulus has an exponential variation over the entire depth of the halfspace. In order to assign equal annular areas, the dimensions of r_i take the following form

$$r_i = (\frac{i}{n})^{\frac{1}{2}} a; \quad i = 1, 2, 3, ..., n \tag{5.25}$$

Similarly for the mid points,

$$r_{m1} = 0, \; r_{mi} = (\frac{r_{i-1} + r_i}{2}); \; i = 2, 3, ..., n \tag{5.26}$$

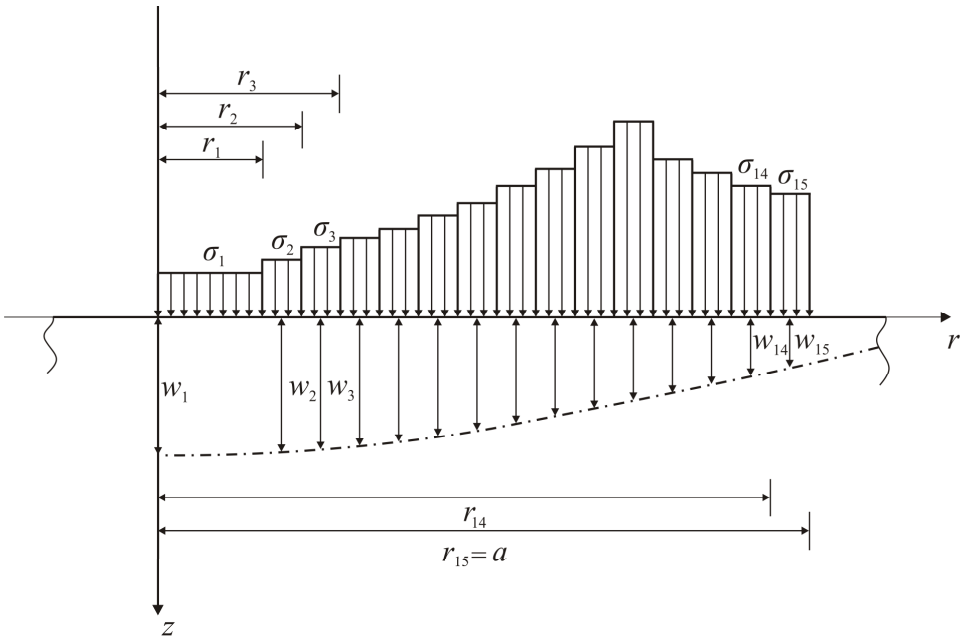

Figure 5.3 Elastic incompressible non-homogeneous halfspace subjected to concentric distributions of annular loads

We further assume that the uniform normal stress elements σ_i can be presented as multiples of the average pressure p_0 that is applied externally to the rigid indenter

$$\sigma_i = \tilde{\sigma}_i p_0 \quad \text{where } i = 1, 2, 3, ..., n \tag{5.27}$$

where

$$p_0 = \frac{P}{\pi a^2} \tag{5.28}$$

Using the above reductions, it is possible to express the surface displacements w_i due to normal contact stresses $\tilde{\sigma}_i$ in the form of the matrix relation

$$\{\mathbf{w}\} = \frac{p_0 a}{G_0}[\mathbf{C}]\{\tilde{\boldsymbol{\sigma}}\} \tag{5.29}$$

where $\{\mathbf{w}\}$ and $\{\tilde{\boldsymbol{\sigma}}\}$ are column vectors and the coefficients of the square matrix $[\mathbf{C}]$ are as follows.

$$[\mathbf{C}] = \begin{bmatrix} w_{11} & w_{12} & w_{13} & \cdots & w_{1j} \\ w_{21} & w_{22} & w_{23} & \cdots & w_{2j} \\ w_{31} & w_{32} & w_{33} & \cdots & w_{3j} \\ \vdots & \vdots & \vdots & \ddots & \vdots \\ w_{i1} & w_{i2} & w_{i2} & \cdots & w_{ij} \end{bmatrix} \tag{5.30}$$

where w_{ij} is the surface displacement at the annuli mid point location i due to the normal contact stress σ_j $(i = j)$.

The results in the form presented here are applicable to the calculation of surface displacements involving any arbitrary distributed loading with an axisymmetric profile, which can be useful for geotechnical engineering studies in general.

We shall now focus attention on the rigid indenter problem. For compatibility at the soil-indenter interface, w_i will have the same value as the rigid displacement of the indenter Δ; this constitutes an additional unknown of the problem. The remaining equation required for the solution of Eq. (5.29) is furnished by the equilibrium equation for the entire indenter, i.e.

$$\sum_{i=1}^{n} \tilde{\sigma}_i = n \tag{5.31}$$

The matrix formed by combining Eqs. (5.29) and (5.31) can be inverted to determine the non-dimensional contact stresses $\tilde{\sigma}_i$ and the non-dimensional indenter displacement

$$\Delta^* = \frac{G_0 \Delta}{p_0 a} \tag{5.32}$$

The accuracy of this discretized solution can be verified by comparing the computational estimates with the exact closed form results given by the classical result of Boussinesq (1885).

Here, the rigid indenter is discretized into 5, 10, 15 and 20 equal annular areas (i.e. $n = 5,10,15,20$). Table 5.1 presents the comparison between the Boussinesq (1885) and the discretized solution for $n = 5,10,15,20$ respectively. The accuracy of solution depends on the number of annular regions. However, the number of annular regions cannot be increased indefinitely; such a procedure usually results in an ill-conditioned set of equations due to the singular nature of the contact stress at $r = a$. It can be seen from Table 5.1 that the accuracy of the results increases by increasing the discretized areas from 5 to 15 but the accuracy is reduced by increasing the number of discretized areas from 15 to 20 due to the singularity effect at the indenter boundary.

Table 5.1: Comparison of analytical and numerical solutions

n	5	10	15	20	Boussinesq (1885)
Δ^*	0.400676	0.395437	0.394525	0.378847	0.392699

Ideally, both the contact stresses and the indentation should be predicted with equal accuracy in a discretization approach. Due to the simplification of representing a singular stress field as a finite value over an annular region, the

discretized contact stresses will exhibit a departure from the theoretical Boussinesq (1885) profile as n is increased. Furthermore, a direct comparison of the stress values obtained at the mid-points of the annular regions from the discretization scheme with the stress values computed at the corresponding points applicable to the analytical solution for the compressive contact stress will not capture the overall effect of the stress gradients associated with Boussinesq's result for the contact stress at the base of a smooth rigid indenter, given by

$$\sigma_{zz}(r,0) = \frac{P}{2\pi a\sqrt{a^2 - r^2}} \tag{5.33}$$

where P is the total load applied to the indenter and a is the radius of the indenter. For this reason, it is necessary to calculate the average stress within either the central element or an intermediate element, which is calculated using Boussinesq's distribution. Consider the case where the contact region is discretized into n equi-areal regions with a circular central region and $(n-1)$ annular exterior regions. Consider an annular region bounded by $r \in (\tilde{\rho}_i a, \tilde{\rho}_e a)$, where $\tilde{\rho}_i a$ is the interior radius of the annulus and $\tilde{\rho}_e a$ is the external radius. The relationship between the radii $\tilde{\rho}_i$ and $\tilde{\rho}_e$ is given by

$$\tilde{\rho}_e = \left(\tilde{\rho}_i^2 + \frac{1}{n} \right)^{1/2} \tag{5.34}$$

The total force acting over the interval $r \in (\tilde{\rho}_i a, \tilde{\rho}_e a)$ due to the Boussinesq distribution is given by

$$P^* = \int_{\tilde{\rho}_i a}^{\tilde{\rho}_e a} \int_0^{2\pi} \frac{P\, r\, dr\, d\theta}{2\pi a\sqrt{a^2 - r^2}} = \frac{P}{a} \int_{\tilde{\rho}_i a}^{\tilde{\rho}_e a} \frac{r\, dr}{\sqrt{a^2 - r^2}} \tag{5.35}$$

The average stress in the annular region $r \in (\tilde{\rho}_i a, \tilde{\rho}_e a)$ due to the Boussinesq distribution is

$$\sigma_i = \frac{nP}{\pi a^2} \left(\sqrt{1 - \tilde{\rho}_i^2} - \sqrt{1 - \tilde{\rho}_e^2} \right) \tag{5.36}$$

The average stress within the annulus normalized with respect to the average stress over the entire contact region, $P/\pi a^2$, is given by

$$\tilde{\sigma}_i = n\left[\sqrt{1-\tilde{\rho}_i^2} - \sqrt{1-\tilde{\rho}_e^2}\right] \tag{5.37}$$

Table 5.2 compares the contact stress between the techniques proposed in this paper and those determined using Eq. (5.37) from Boussinesq's results.

Table 5.2: Comparison of contact stress between Boussinesq`s results and the current study

	center		outermost annular boundary region	
n	10	15	10	15
$\tilde{\sigma}_i$ (Boussinesq (1885)	0.5132	0.5086	3.1622	3.8729
$\tilde{\sigma}_i$ (current study $\tilde{\lambda}=0$)	0.5157	0.5098	2.9832	3.8463

In these computations, (i) when $n=10$, the discrepancy in the displacement is - 0.7%, the discrepancy in the contact stresses at the center of the indenter is - 0.48% and the discrepancy in the contact stress at the annular boundary region is - 5.66%., and (ii) when $n=15$, the discrepancy in the displacement is - 0.465%, the discrepancy in the contact stresses at the center of the indenter is - 0.24% and the discrepancy in the contact stress at the annular boundary region is - 0.68% . In the discretized analysis of the adhesive contact problem for the inhomogeneous incompressible elastic halfspace, the discretizations are selected as $n=10$ and $n=15$. It should also be noted that any computational estimates for the contact problem, based on either finite element or boundary element approaches, will display similar manifestations, unless special provisions are made to include singularity elements at the boundary point of the indenting region and infinite elements are used to capture the semi-infinite domain.

Figure 5.4 shows the ratio of the displacement of the rigid indenter on a non-homogeneous medium using the numerical discretized solution to the

homogeneous medium based on analytical results given by Boussinesq (1885) for different shear modulus. Figure 5.4 shows that the response is influenced by the degree of non-homogeneity. As would be expected, the vertical displacement decreases as the shear modulus increases. It is evident that the non-homogeneous condition has a significant effect on the response of the indenter.

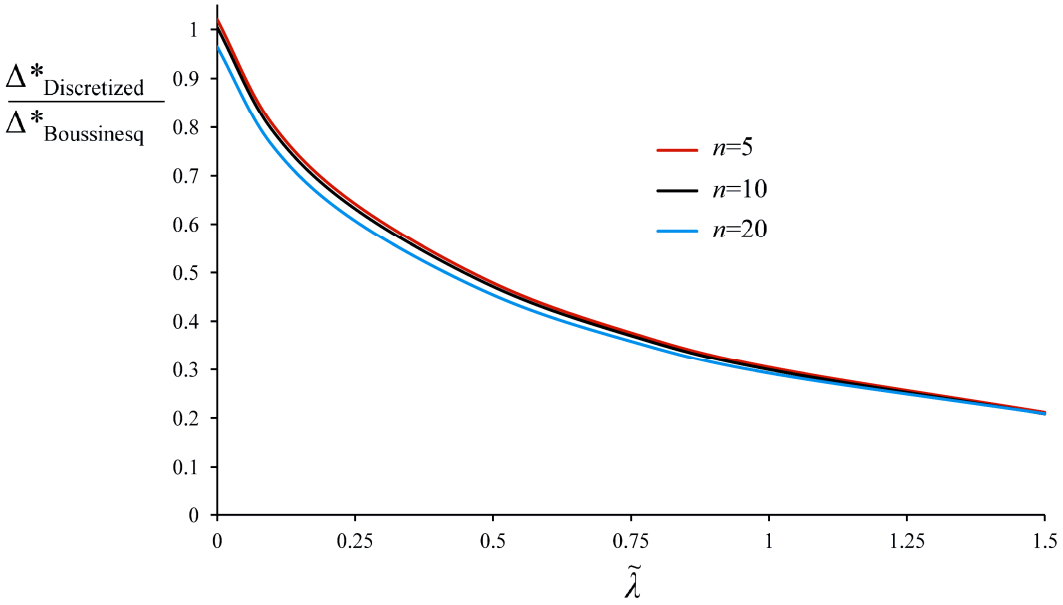

Figure 5.4: Ratio of displacement of the rigid indenter on a non-homogeneous medium (numerical discretized solution) to homogeneous medium (Boussinesq, 1885) for different $\tilde{\lambda}$, for $n = 5,10,20$

Figure 5.5 shows the contact stress distribution beneath a rigid indenter resting on a non-homogeneous elastic halfspace, for different shear modulus, with $n = 10$. A comparison has also been made between the current results for the contact stress distribution $\tilde{\sigma}_i$ at mid point locations r_{mi} and those determined from the exact result given by Boussinesq (1885). Similar results are presented in Figure 5.6 for the contact pressure distributions obtained for a numerical procedure where $n = 15$.

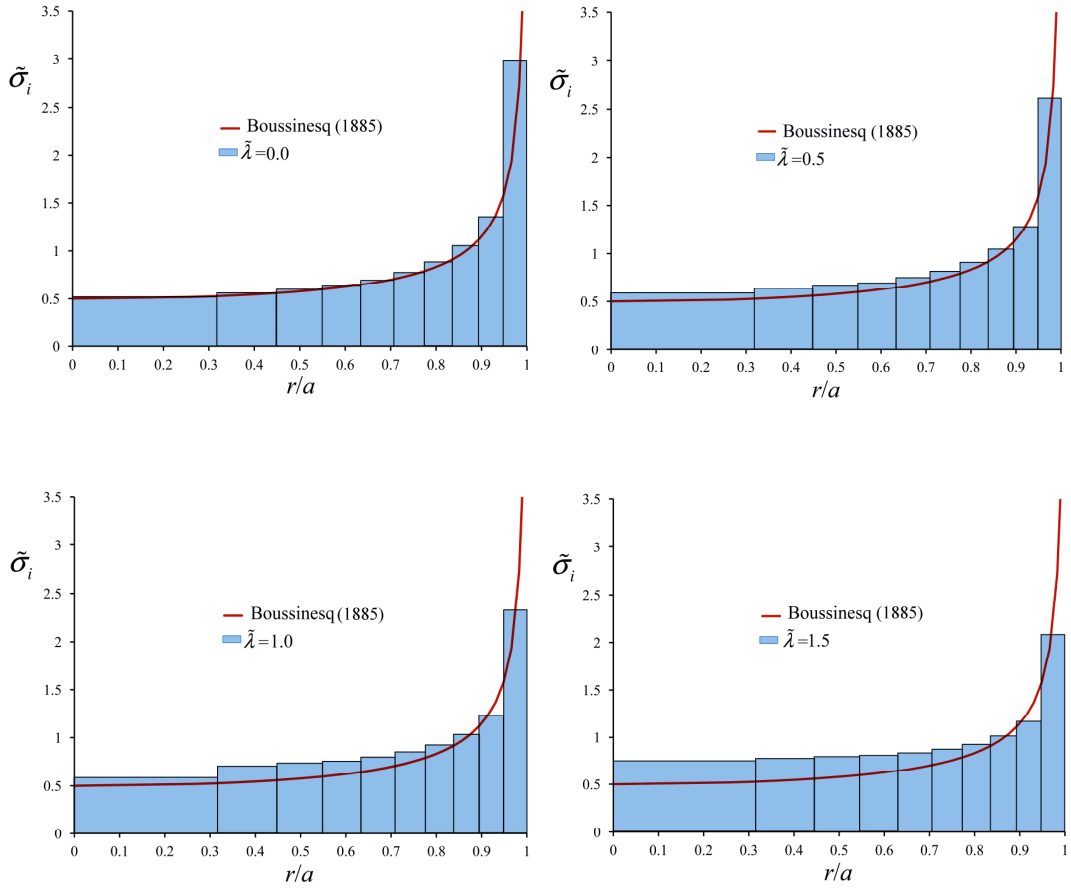

Figure 5.5: Comparison of contact stress distribution ($\tilde{\sigma}_i$) of the rigid indenter between the current results and these given by Boussinesq (1885) (n =10)

As evident from Figures 5.5 and 5.6, there is good correlation between the results obtained from the discretization method and the analytical results given by Boussinesq (1885), when $\tilde{\lambda}=0$. It should also be noted that for the incompressible homogeneous elastic halfspace, the normal contact stresses within the indented area are independent of the elasticity parameters of the halfspace and invariant of the adhesion constraint; i.e. when $\nu=1/2$, $\gamma\to 0$ and (5.4) gives rise to the conventional Abel integral equation for the normal contact stress $\sigma(r)$, which yields Boussinesq's result for the indentation problem (Sneddon, 1951,1965). It can be inferred that the discrepancies between the results for the

indentation of the incompressible non-homogeneous elastic halfspace and Boussinesq's result are likely to be due to the elastic non-homogeneity.

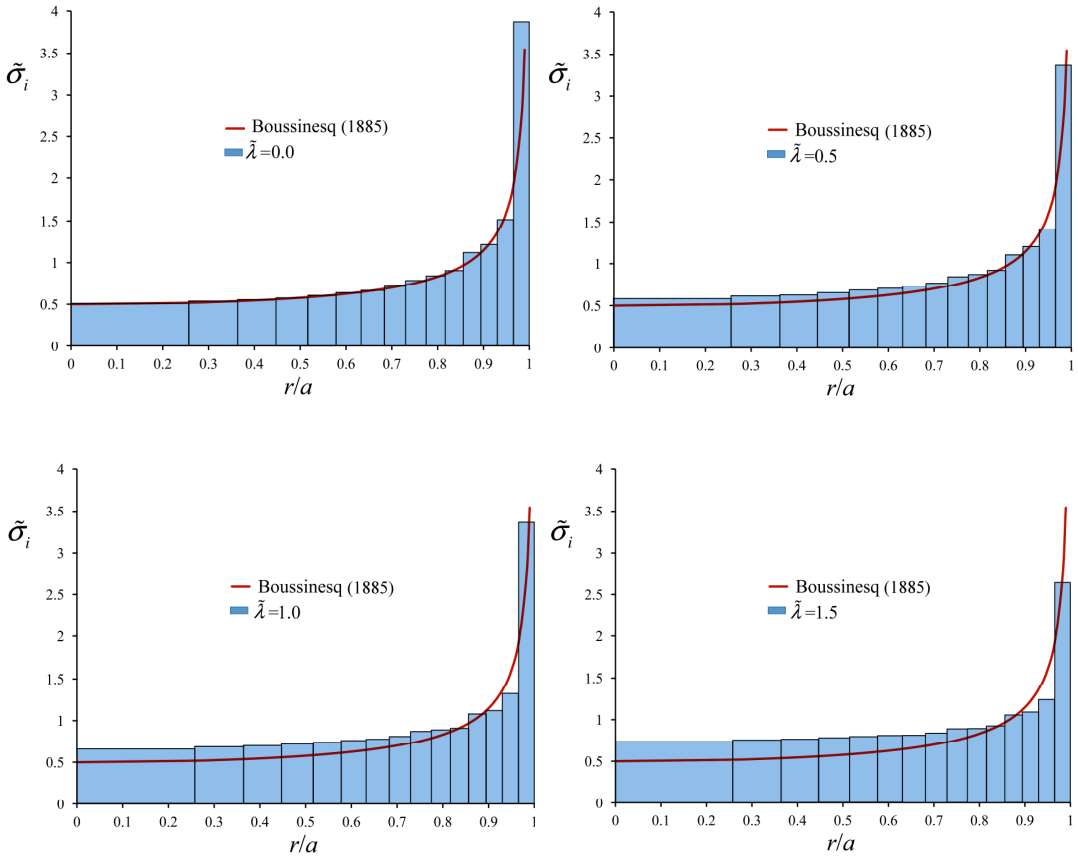

Figure 5.6: Comparison of contact stress distribution ($\tilde{\sigma}_i$) of the rigid indenter between the current results and results given and Boussinesq (1885) (n =15)

5.2.6 Adhesive contact problem for a rigid circular indenter

Attention is now focused on the adhesive contact problem. Here we consider the adhesive contact of a rigid circular indenter of radius a, subjected to an axial load P, with a non-homogeneous incompressible elastic halfspace in which the shear modulus varies exponentially with depth. The boundary conditions applicable to the adhesive contact are given in Eq. (5.7).

In order to solve this problem using a numerical approach similar to that described in section 5.2.5, we first assume that a non-homogenous incompressible elastic

halfspace is subjected to uniform normal surface tractions σ_i^b and uniform shear surface tractions τ_i^b at equal annular locations r_i. Then the compatibility between the settlement of the non-homogenous incompressible halfspace due to the combined actions of normal and shear surface tractions and the settlement of the indenter, Δ, is established at the mid location of each annular region.

We further assume that the uniform normal stress elements σ_i^b and uniform shear stress elements τ_i^b can be presented as multiples of the externally applied average pressure p_0 (see Eq.(5.28)) and an average shear traction τ_0 (to be determined), respectively, in the forms

$$\sigma_i^b = \tilde{\sigma}_i^b p_0 \quad \text{where } i = 1, 2, 3, ..., n \tag{5.38}$$

$$\tau_i^b = \tilde{\tau}_i^b \tau_0 \quad \text{where } i = 1, 2, 3, ..., n \tag{5.39}$$

Using the above reductions, it is possible to express the surface vertical and lateral displacements w_i and u_i due to the contact stresses $\tilde{\sigma}_i^b$ and $\tilde{\tau}_i^b$ in the form of the matrix relation

$$\{\mathbf{w}\} = \frac{p_0 a}{G_0}[\mathbf{C}_1]\{\tilde{\boldsymbol{\sigma}}^b\} + \frac{\tau_0 a}{G_0}[\mathbf{C}_2]\{\tilde{\boldsymbol{\tau}}^b\} \tag{5.40}$$

$$\{\mathbf{u}\} = \frac{p_0 a}{G_0}[\mathbf{C}_3]\{\tilde{\boldsymbol{\sigma}}^b\} + \frac{\tau_0 a}{G_0}[\mathbf{C}_4]\{\tilde{\boldsymbol{\tau}}^b\} \tag{5.41}$$

where $\{\mathbf{w}\}$, $\{\mathbf{u}\}$, $\{\tilde{\boldsymbol{\sigma}}^b\}$ and $\{\tilde{\boldsymbol{\tau}}^b\}$ are column vectors and the coefficients of the square matrix $[\mathbf{C}_i]$ are as follows

$$[\mathbf{C}_1] = \begin{bmatrix} w_{11} & w_{12} & w_{13} & \dots & w_{1j} \\ w_{21} & w_{22} & w_{23} & \dots & w_{2j} \\ w_{31} & w_{32} & w_{33} & \dots & w_{3j} \\ \vdots & \vdots & \vdots & \ddots & \vdots \\ w_{i1} & w_{i2} & w_{i2} & \dots & w_{ij} \end{bmatrix}, [\mathbf{C}_2] = \begin{bmatrix} w'_{11} & w'_{12} & w'_{13} & \dots & w'_{1j} \\ w'_{21} & w'_{22} & w'_{23} & \dots & w'_{2j} \\ w'_{31} & w'_{32} & w'_{33} & \dots & w'_{3j} \\ \vdots & \vdots & \vdots & \ddots & \vdots \\ w'_{i1} & w'_{i2} & w'_{i2} & \dots & w'_{ij} \end{bmatrix} \tag{5.42}$$

$$[\mathbf{C}_3]=\begin{bmatrix} u_{11} & u_{12} & u_{13} & \dots & u_{1j} \\ u_{21} & u_{22} & u_{23} & \dots & u_{2j} \\ u_{31} & u_{32} & u_{33} & \dots & u_{3j} \\ \vdots & \vdots & \vdots & \ddots & \vdots \\ u_{i1} & u_{i2} & u_{i2} & \dots & u_{ij} \end{bmatrix}, \quad [\mathbf{C}_4]=\begin{bmatrix} u'_{11} & u'_{12} & u'_{13} & \dots & u'_{1j} \\ u'_{21} & u'_{22} & u'_{23} & \dots & u'_{2j} \\ u'_{31} & u'_{32} & u'_{33} & \dots & u'_{3j} \\ \vdots & \vdots & \vdots & \ddots & \vdots \\ u'_{i1} & u'_{i2} & u'_{i2} & \dots & u'_{ij} \end{bmatrix} \tag{5.43}$$

where u_{ij} and u'_{ij} are radial surface displacements and w_{ij} and w'_{ij} are the axial surface displacements at the annuli mid point locations due to the normal and radial stress traction σ_j^b and τ_j^b respectively.

The displacement of a non-homogeneous incompressible elastic halfspace subjected to a surface distributed radial load of radius a with stress intensity τ_0 can be found by

$$u_z(r,0)=\frac{\tau_0}{G_0}\int_0^\infty\left(\frac{(q_1-2k_1)+(2k_2-q_2)}{(2k_1-q_1)(\xi^2+k_2^2)+(q_2-2k_2)(\xi^2+k_1^2)}\right) \xi^2 J_0(\xi r)\left[\int_0^a rJ_1(\xi r)dr\right]d\xi \tag{5.44}$$

$$u_r(r,0)=\frac{\tau_0}{G_0}\int_0^\infty\left(\frac{k_2q_1-k_1q_2}{(2k_1-q_1)(\xi^2+k_2^2)+(q_2-2k_2)(\xi^2+k_1^2)}\right) \xi J_1(\xi r)\left[\int_0^a rJ_1(\xi r)dr\right]d\xi \tag{5.45}$$

where k_1, k_2, q_1 and q_2 are defined by Eqs. (5.14) and (5.15).

These equations can be solved numerically using the technique explained in the previous chapter. The axial and radial surface displacement due to the normal tractions σ_j^b at the central location can be obtained by a superposition of the results for the axial and radial displacements given in Equations (5.23), (5.24), (5.44) and (5.45).

The axial and radial surface displacement due to the shear stress traction τ_j^b can be generated from Eq. (4.44) and Eq. (4.45) by superposition. The normal and shear surface tractions are related to each other through the constraint given in Eq. (5.7). Using (5.7) along with Eq. (5.41) results in:

$$\frac{p_0 a}{G_0}[\mathbf{C}_3]\{\tilde{\boldsymbol{\sigma}}^b\} + \frac{\tau_0 a}{G_0}[\mathbf{C}_4]\{\tilde{\boldsymbol{\tau}}^b\} = \{\mathbf{0}\} \tag{5.46}$$

and Eq. (5.46) along with the Eqs. (5.38) and (5.39) can be used to determine the shear tractions based on the normal tractions

$$\{\boldsymbol{\tau}^{\mathbf{b}}\} = [\mathbf{B}]\{\boldsymbol{\sigma}^{\mathbf{b}}\} \tag{5.47}$$

By using Eq. (5.47) we can rewrite the Eq. (5.40) as follows:

$$\{\mathbf{w}\} = \frac{p_0 a}{G_0}[\mathbf{H}]\{\tilde{\boldsymbol{\sigma}}^b\} \tag{5.48}$$

in which $[\mathbf{H}]$ was obtained by adding the two matrices $[\mathbf{C}_1]$ and $[\mathbf{C}_2]$, which also incorporates the result Eq. (5.47). The results, in the form presented here, are applicable to settlement calculations involving any distributed loading with an axisymmetric profile.

For compatibility of displacements at the incompressible non-homogeneous elastic halfspace-indenter interface, w_i will have the same value as the rigid displacement of the indenter Δ; this constitutes an additional unknown of the problem. The remaining equation required for the solution of Eq. (5.48) is the equilibrium equation for the entire indenter given in Eq. (5.31). The matrix formed by combining Eqs. (5.31) and (5.48) can be inverted to determine the non-dimensional contact stresses $\tilde{\sigma}_i^b$ and $\tilde{\tau}_i^b$ and the non-dimensional axial displacement of the indenter in bonded contact with the incompressible non-homogeneous elastic halfspace. The contact normal stresses for the indenter, which is adhesively bonded to the incompressible elastic halfspace, are shown in

Figures 5.5 and 5.6, developed ,respectively, by considering discretizations $n = 10$ and $n = 15$.

The Figure 5.7 presents a comparison of the surface displacement of the rigid indenter for smooth contact, adhesive contact, and for the case where the surface is inextensible (in which $u_r = 0$ throughout the surface of the halfspace). Results are provided for different values of the non-homogeneity parameter $\tilde{\lambda}$. These displacements are normalized with the surface displacement given by Boussinesq (1885).

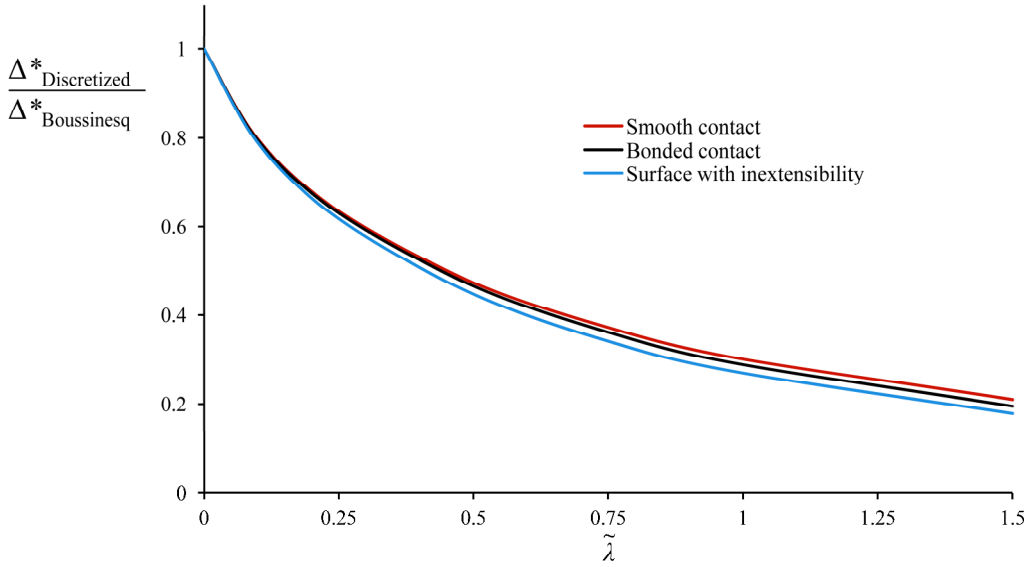

Figure 5.7: Ratio of displacement of the rigid disc on a non-homogeneous medium (numerical discretized solution) to homogeneous medium (Boussinesq, 1885) for different $\tilde{\lambda}$; comparison between smooth, bonded contact and surface with inextensibility

The results show that the stiffness of the indenter in adhesive contact is bounded by the corresponding values for indentation with frictionless contact and the result for the indentational stiffness that incorporated a surface inextensibility constraint (see also Selvadurai, 2009). Figure 5.8 shows the influence of adhesion and the non-homogeneity parameter on the indentational stiffness of the rigid circular indenter. The effect of adhesive contact increases from zero for an incompressible

homogenous halfspace with $\tilde{\lambda} = 0$ to an almost a 10% difference between the settlement of smooth contact and adhesive contact, for a non-homogeneous incompressible halfspace with $\tilde{\lambda} = 2$. However, the change in displacement for $\tilde{\lambda} < 0.25$, which is applicable to a range of variations in the shear modulus with depth observed in saturated clays found in regions of the British Isles, is less than 2%.

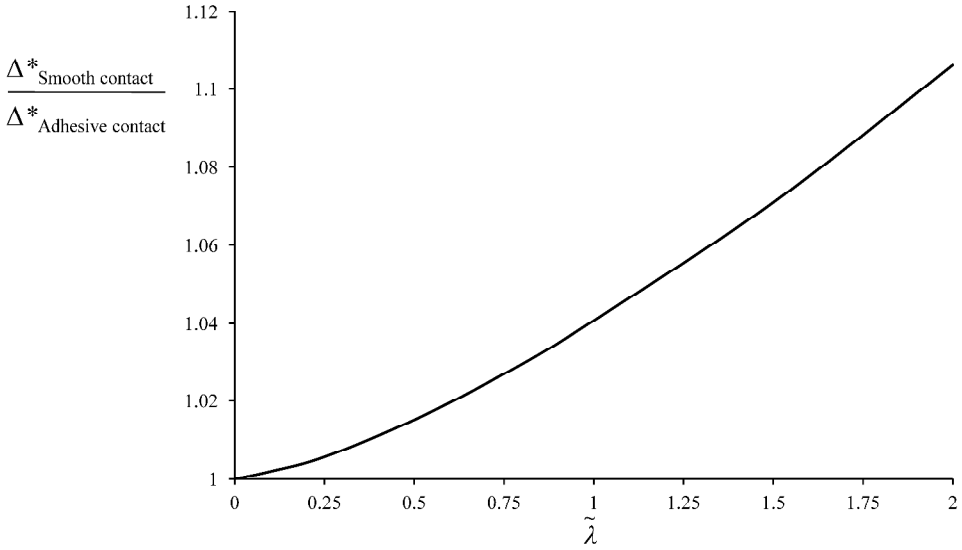

Figure 5.8: Ratio of displacement of the bonded contact rigid indenter to the smooth contact rigid indenter for different values of $\tilde{\lambda}$

5.3 Elastic contact between a flexible circular plate and an incompressible isotropic halfspace with exponential non-homogeneity

The flexural behavior of finite plates resting on the surface of deformable elastic media is of interest to several branches of engineering. The problem has gained significant attention due to its importance in the analysis and design of structural foundations resting on soils and rock media. An extensive review of the topic is given by Selvadurai (1979c). The study of the flexural behavior of a loaded circular plate was investigated by Habel (1937), Zemochkin (1939), and Holmberg (1946) in which the plate was divided into concentric annular regions subjected to uniform annular contact stresses. The classical study by Borowicka

(1936) examined the influence of rigidity of a circular plate, subjected to uniform pressure over the contact surface, resting on an isotropic elastic halfspace by using a power series expansion technique. Ishkova (1951) and Brown (1969) presented a modified solution to the problem in which they considered the effect of near edge singular terms in the approximation of the contact stress distribution. An extensive review on various investigations in this area is given by Selvadurai (1979c), who was the first to employ energy the method to study this problem. In his analysis, the deflected shape of the circular plate is presented in the form of a power series in terms of the radial coordinate *r*. Selvadurai (1979b) investigated the flexural behavior of a circular flexible plate embedded in an elastic medium using the energy method. Following Selvadurai (1979c), Zaman et al. (1988) predicted the flexural behavior of a uniformly loaded flexible circular plate using the energy method approach in which the shape of the plate is approximated by an even power series expansion in terms of the radial coordinates. Selvadurai and Dumont (2011) investigated a contact problem between an isotropic elastic halfpace and a flexible circular plate subjected, simultaneously, to a Mindlin-type axial force. The contact problem was solved using the energy approach.

In this section we examine using an energy method the axisymmetric smooth contact problem for a flexible circular plate and an incompressible non-homogenous elastic halfspace, where the linear elastic shear modulus varies exponentially with depth, using the energy method. The approach adopted approximates the deflected shape of the plate by an even power series expansion, which satisfies the kinematic constraints of the plate deformation and the Kirchhoff boundary condition applicable to a free edge. The remaining coefficients in the power series are evaluated by making use of the principle of minimum potential energy. Using the energy method, the maximum deflection, the relative deflection, and the maximum flexural moment in the circular plate are presented. The results derived from the proposed procedure are compared with equivalent results derived from numerical techniques.

5.3.1 Proposed analytical procedure

With reference to Figure 5.9, we consider the problem of the axisymmetric indentation of an incompressible non-homogeneous elastic halfspace by a flexible circular plate of thickness h and radius a. The plate is subjected to a uniform load of intensity p_0 over its entire surface. The non-homogeneity considered in the paper assumes that the shear modulus of the elastic medium varies exponentially with depth (Eq. 3.3).

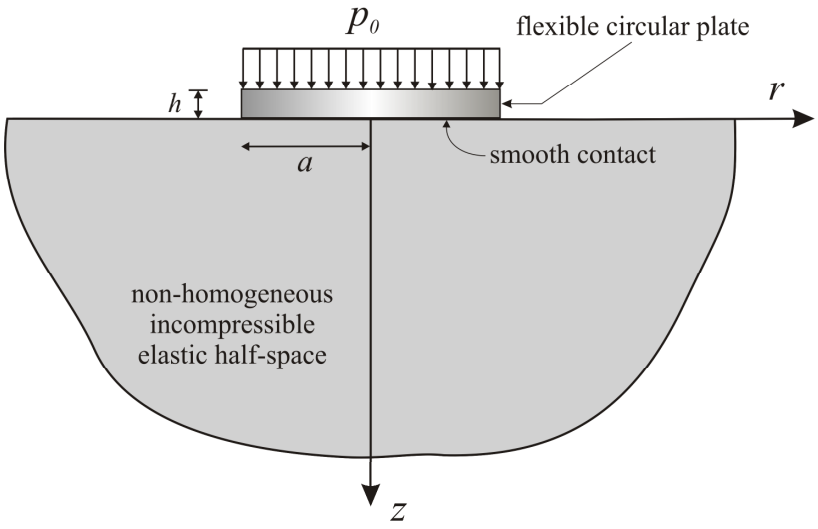

Figure 5.9: Uniformly loaded flexible circular plate on the surface of an incompressible elastic halfspace

It is assumed that there is no loss of contact at the interface. Therefore, the interface displacement can be represented as either the deflected shape of the plate or surface displacement of the halfspace in the z-direction over the contact region $0 \leq r \leq a$. For the analysis of the problem we make use of the variational approach proposed by Selvadurai (1979c). The analysis assumes a prescribed plate deflection $w(r)$, specified to within a set of undetermined constants, in which the deflected shape of the circular plate can be presented in the form of a power seires in terms of the radial coordinate r. The assumed form of $w(r)$ also satisfies the kinematic constraints of the axisymmetric deformation. The energy method of

analysis requires the development of the total potential energy functional for the plastic-elastic halfspace region that consists of (i) the flexural energy of the plate, (ii) the strain energy of the halfspace region, and (iii) the potential energy of the applied loads. The total energy functional developed is defined in terms of the undetermined constants characterizing the deflected shape of the plate. Invoking the Kirchhoff boundary conditions applicable to the free edge of the plate can eliminate two constants in the series and the two remaining constants are evaluated by the minimization of the total potential energy functional of the system.

5.3.2 Variational approach

The proposed formulation is discussed briefly in this section. It is assumed that the deflected shape of the plate can be approximated by the power series expansion:

$$w(r) = a\sum_{i=0}^{3} C_{2i}\left(\frac{r}{a}\right)^{2i} \tag{5.49}$$

in which C_{2i} are arbitrary constants. The assumed form of the plate deflection gives a kinematically admissible plate deflection, rotation and curvature in the plate region. Of the four arbitrary constants, two can be eliminated by invoking the Kirchhoff boundary conditions applicable to the free edge of the circular plate, i.e,

$$M_r(a) = -D\left[\frac{d^2w(r)}{dr^2} + \frac{v_p}{r}\frac{dw(r)}{dr}\right]_{r=a} = 0 \tag{5.50}$$

$$Q_r(a) = -D\left[\frac{d}{dr}\left\{\nabla^2 w(r)\right\}\right]_{r=a} = 0 \tag{5.51}$$

where v_p is the Poisson's ratio of the plate material. The assumed expression for the plate deflection can be reduced to the form

$$w(r) = a\left[C_0 + C_2\left\{\frac{r^2}{a^2} + l_1\frac{r^4}{a^4} + l_2\frac{r^6}{a^6}\right\}\right] \tag{5.52}$$

where

$$l_1 = \frac{-3(1+\nu_p)}{4(2+\nu_p)} \; ; \qquad l_2 = \frac{(1+\nu_p)}{6(2+\nu_p)} \tag{5.53}$$

In following sections, the total potential energy functional for the plastic-elastic halfspace region is developed.

(i) Flexural energy of the plate

First component of the total energy functional corresponds to strain energy of the plate. The flexural behavior of the elastic plate is described by Poisson-Kirchhoff thin plate theory. So the flexural energy of the plate subjected to the axisymmetric deflection $w(r)$ can be given by

$$U_F = \frac{D}{2} \iint_s \left[\{\nabla^2 w(r)\}^2 - \frac{2(1-\nu_p)}{r} \frac{dw(r)}{dr} \frac{d^2 w(r)}{dr^2} \right] r dr d\theta \tag{5.54}$$

where

$$\nabla^2 = \frac{d^2}{dr^2} + \frac{1}{r}\frac{d}{dr}; \qquad D = \frac{G_p h^3}{6(1-\nu_p)} \tag{5.55}$$

and G_p and ν_p are the constant shear modulus and Poisson's ratio of the plate material, respectively, and S represents the plate region.

(ii) Strain energy of the halfspace region

The second component of the total energy functional corresponds to the strain energy of the incompressible non-homogeneous elastic halfspace which is subjected to the displacement field $w(r)$ in the contact region $0 \leq r \leq a$. The elastic strain energy can be developed by computing the work component of the surface tractions that compose the interface contact stresses. Since the interface is assumed to be smooth, only the normal tractions contribute to the strain energy. These normal tractions can be determined by making use of the discretizion method described in section 5.2.5. In order to determine the contact stresses, we

first consider the indentation of a non-homogeneous incompressible elastic halfspace by a circular flexible plate subjected to a load p_0 over its entire surface. The boundary condition of the problem is as follow:

$$u_z(r,0) = w(r) \quad ; \quad 0 \le r \le a$$

$$\sigma_{rz}(r,0) = 0 \; ; \quad 0 \le r < \infty$$

$$\sigma_{zz}(r,0) = 0 \; ; \quad a < r < \infty \tag{5.56}$$

The method of solution assumes that the plan area of the indenter is discretized into fifteen equal annular areas and the contact stress within each annular area is uniform. Considering the annular normal load of stress intensity σ_i (i=1 to 15) acting within the annular region of internal radius r_i and external radius r_{i+1}, the surface displacement w_i at the mid-section of the annular region due to normal surface tractions can be obtained by superposition of the Eqs. (5.23) and (5.24). The compatibility between the settlement of the non-homogenous incompressible halfspace and the settlement of the indenter, $w(r)$, is then established at the mid location of each annular region. For compatibility at the soil-indenter interface, w_i will have the same value as the displacement field $w(r)$. Using Eq. (5.29), the non-dimensional contact stresses $\tilde{\sigma}_i$ and therefore σ_i can be determined in terms of the arbitrary parameter of $w(r)$, i.e, C_0 and C_2.

The strain energy of the halfspace region can be calculated by

$$U_E = \frac{1}{2} f_i w_i; \quad i = 1,2,3,.....,15 \tag{5.57}$$

where f_i is the force in each equal annular area, calculated by multiplying the contact stress σ_i with the area of the annular region (which is equal to $\frac{\pi}{15} a^2$).

(iii) Potential energy of the applied loads

The total potential energy of the uniform external load applied to the plate is given by

$$U_p = -p_0 \iint_S w(r) r dr d\theta \tag{5.58}$$

5.3.3 Total potential energy functional

The total potential energy functional for the plate-elastic medium system is given by

$$U = U_F + U_E + U_p \tag{5.59}$$

By making use of $w(r)$ as defined by (5.49), and using Eqs. (5.54), (5.55) and (5.56), the total potential energy functional (5.57) reduces to the form

$$U = \pi G_0 a^3 \left[C_0^2 \chi_1 + C_0 C_2 \chi_2 + C_2^2 \chi_3 \right] + \pi D C_2^2 \chi_4 - \pi p_0 a^3 \left[C_0 + C_2 \chi_5 \right] \tag{5.60}$$

where the constants $\chi_1, \chi_2, \chi_3, \chi_4$ and χ_5 are given by

$$\chi_1 = \frac{1}{30} \sum_{i=1}^{15} \sum_{j=1}^{15} m_{ij} \tag{5.61}$$

$$\chi_2 = \frac{1}{30} \sum_{i=1}^{15} \sum_{j=1}^{15} \left\{ m_{ij} \left(\frac{r_{mi}^2}{a^2} + l_1 \frac{r_{mi}^4}{a^4} + l_2 \frac{r_{mi}^6}{a^6} \right) + m_{ij} \left(\frac{r_{mj}^2}{a^2} + l_1 \frac{r_{mj}^4}{a^4} + l_2 \frac{r_{mj}^6}{a^6} \right) \right\} \tag{5.62}$$

$$\chi_3 = \frac{1}{30} \sum_{i=1}^{15} \sum_{j=1}^{15} m_{ij} \left(\frac{r_{mi}^2}{a^2} + l_1 \frac{r_{mi}^4}{a^4} + l_2 \frac{r_{mi}^6}{a^6} \right) \left(\frac{r_{mj}^2}{a^2} + l_1 \frac{r_{mj}^4}{a^4} + l_2 \frac{r_{mj}^6}{a^6} \right) \tag{5.63}$$

$$\begin{aligned} \chi_4 = \{ & 8 + 32 l_1 + \frac{144}{3} l_2 + \frac{128}{3} l_1^2 + \frac{648}{5} l_2^2 + 144 l_1 l_2 \\ & - (1 - \nu_p)(4 + 16 l_1 + 24 l_2 + 16 l_1^2 + 36 l_2^2 + 48 l_1 l_2) \} \end{aligned} \tag{5.64}$$

$$\chi_5 = \frac{1}{2} + \frac{l_1}{3} + \frac{l_2}{4} \tag{5.65}$$

The constants C_0 and C_2 can be evaluated from the equations that are generated from the minimization of the total energy functional,

$$\frac{\partial U}{\partial C_0} = 0; \qquad \frac{\partial U}{\partial C_2} = 0 \tag{5.66}$$

The deflected shape of the uniformly loaded circular foundation corresponding to (5.49) is given by

$$w(r)=\frac{\pi a p_0}{4G_0\Omega}\left[\chi_2\chi_5-2\chi_3-R\chi_4+(\chi_2-2\chi_1\chi_5)\left\{\frac{r^2}{a^2}+l_1\frac{r^4}{a^4}+l_2\frac{r^6}{a^6}\right\}\right] \tag{5.67}$$

where

$$\Omega=\chi_2^2-4\chi_1\chi_3-2R\chi_1\chi_4 \tag{5.68}$$

and R is the relative rigidity parameter defined by

$$R=\frac{\pi}{12(1-\nu_p)}\left(\frac{G_p}{G_0}\right)\left(\frac{h}{a}\right)^3=\frac{\pi K_r}{6(1-\nu_p^2)};\qquad K_r=\frac{(1+\nu_p)}{2}\left(\frac{G_p}{G_0}\right)\left(\frac{h}{a}\right)^3 \tag{5.69}$$

and K_r is a similar parameter defined by Brown (1969). The accuracy of the solution for the deflection of the plate approximated by variational approach can be investigated by assigning various limits to the relative rigidity parameter (K_r or R).

5.3.4 Limiting cases

In order to check the accuracy of the results with known analytical problems, two limiting case are considered in this section. In both cases, it is assumed that the non-homogeneous parameter $\tilde{\lambda}\to 0$, which resembles the isotropic homogeneous elastic halfspace.

(i) Rigid circular plate, $R\to\infty$: as the relative rigidity reaches infinity, the indentation problem reduces to Boussinesq's classical result (1885) for the smooth indentation of a rigid circular plate on an isotropic homogeneous halfspace. The corresponding value of the indented displacement for the incompressible material is

$$\lim_{R\to\infty} w(r)=\frac{\pi p_0 a}{8G_0} \tag{5.70}$$

(ii) Flexible circular loading, $R \to 0$: as the relative rigidity reduces to zero, the problem changes to that of the axisymmetric loading of an incompressible elastic halfspace by a uniform circular load of radius a and stress intensity p_0. The two important results of specific interest for geotechnical engineering are the maximum surface deflection and the differential deflection within the loaded area. The equation (5.67) reduces to

$$\lim_{R\to 0} w(r=0) = \frac{p_0 a}{4G_0}\{2.087\} \tag{5.71}$$

The exact result corresponding to the central surface displacement of the uniformly loaded area ($\nu_s = 1/2$) is given by (see, e.g., Timoshenko and Goodier, 1970)

$$w(r=0) = \frac{p_0 a}{4G_0}\{2.00\} \tag{5.72}$$

By comparing the two results (5.71) and (5.72), it can be seen that the energy method estimates the central deflection by 4.35% difference.

The result for the differential deflection obtained from the energy method is

$$\lim_{R\to 0}[w(r=0) - w(r=a)] = \frac{p_0 a}{4G_0}\{0.7327\} \tag{5.73}$$

and corresponding exact solution is

$$[w(r=0) - w(r=a)] = \frac{p_0 a}{4G_0}\{\frac{2\pi - 4}{\pi}\} \tag{5.74}$$

This it shows that the estimate given by energy method overpredicts that from the exact solution by 0.8%.

5.3.5 Maximum flexural moments

The flexural moment in the plate can, in principle, be computed from the expressions

$$M_r = -D\left\{\frac{d^2 w(r)}{dr^2} + \frac{\nu}{r}\frac{dw(r)}{dr}\right\} \tag{5.75}$$

$$M_\theta = -D\left\{\frac{1}{r}\frac{dw(r)}{dr} + \nu_p \frac{d^2w(r)}{dr^2}\right\} \tag{5.76}$$

However, due to the presence of derivatives up to the second order, the flexural moment calculated by Eqs. (5.75) and (5.76) are considerably less accurate compared to the estimation of the plate deflection. A more accurate estimate of the flexural moment in the plate can be obtained by considering the combined action of the external load p_0 and the contact stress distribution (σ_i). A solution for the maximum flexural moment can be computed by superposing the two solutions: (i) a circular plate simply supported along its boundary subjected to a uniform external load p_0, and (ii) a circular plate simply supported along its boundary subjected to the contact stress distribution (σ_i).

(i) From the results given by Timoshenko and Woinowsky-Krienger (1959), (see also Selvadurai (1979a), the maximum flexural moment at the center of an edge-supported plate due to the external load p_0 is given by

$$M^{p}_{\max} = \frac{p_0 a^2 (3+\nu_b)}{16} \tag{5.77}$$

(ii) The maximum flexural moment due to the contact stress (σ_i) acting on an edge-supported plate is given by

$$M^{c}_{\max} = \int_0^a \frac{\xi\sigma(\xi)}{2}\left[\frac{(1-\nu_p)}{2}\left(\frac{a^2-\xi^2}{a^2}\right) - (1-\nu_p)\ln\left(\frac{\xi}{a}\right)\right] d\xi \tag{5.78}$$

where $\sigma(\xi)$ is defined in Eq. (5.27).

5.3.6 Numerical results and discussion

The energy method proposed in the previous section has been used to analyse the indentation problem of a uniformly loaded circular plate resting in smooth contact with an incompressible non-homogeneous halfspace. The main object is to investigate the influence of the elastic non-homogeneity of the incompressible

halfspace and the relative stiffness of the plate-elastic halfspace system on the deflection and flexural moments in the plate. The results are presented for the various relative rigidities from $\log_{10} K_r = 0$ to 3, in which $\log_{10} K_r = 0$ represents a plate with relative flexibility and $\log_{10} K_r = 3$ represents a nearly rigid plate. The Poisson's ratio for the plate is chosen to be $\nu_b = 0.3$. To demonstrate the effect of non-homogeneity on the results, the parameter $\tilde{\lambda}$, which is directly related to the shear modulus by Eq. (3.3), has been used for the range $\tilde{\lambda} = 0$ to 1.5, where $\tilde{\lambda} = 0$ represents an incompressible homogeneous elastic halfspace. In the case of $\tilde{\lambda} = 0$ (homogeneous), the results are compared with the existing numerical results presented by Brown (1969). It should be pointed out that all numerical results are presented in a non-dimensional form.

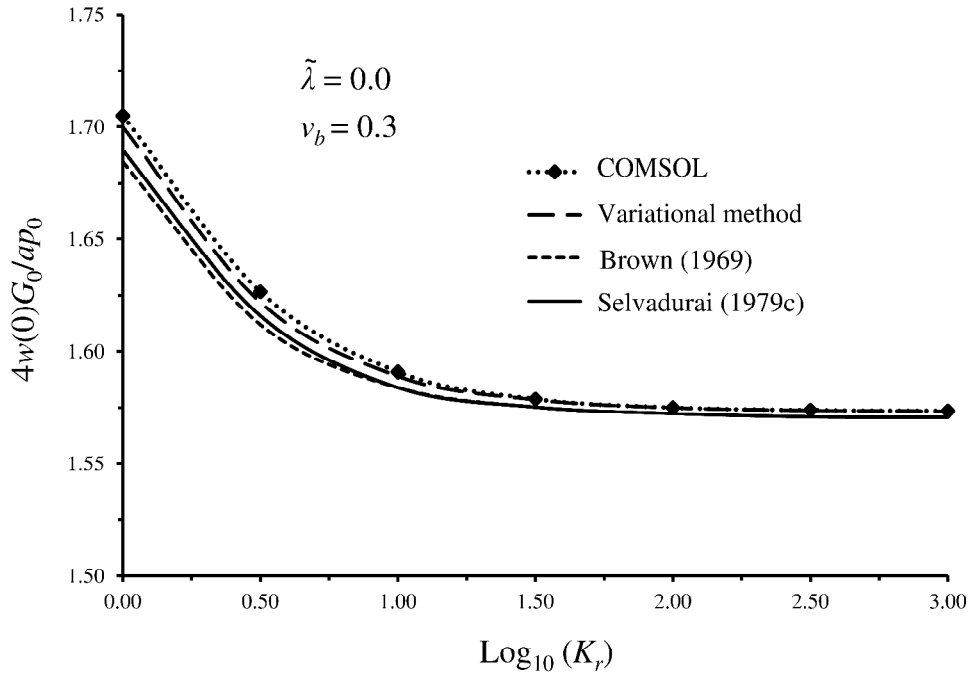

Figure 5.10: Variation of central displacement of the circular plate for different relative rigidities; $\tilde{\lambda} = 0$ (homogeneous)

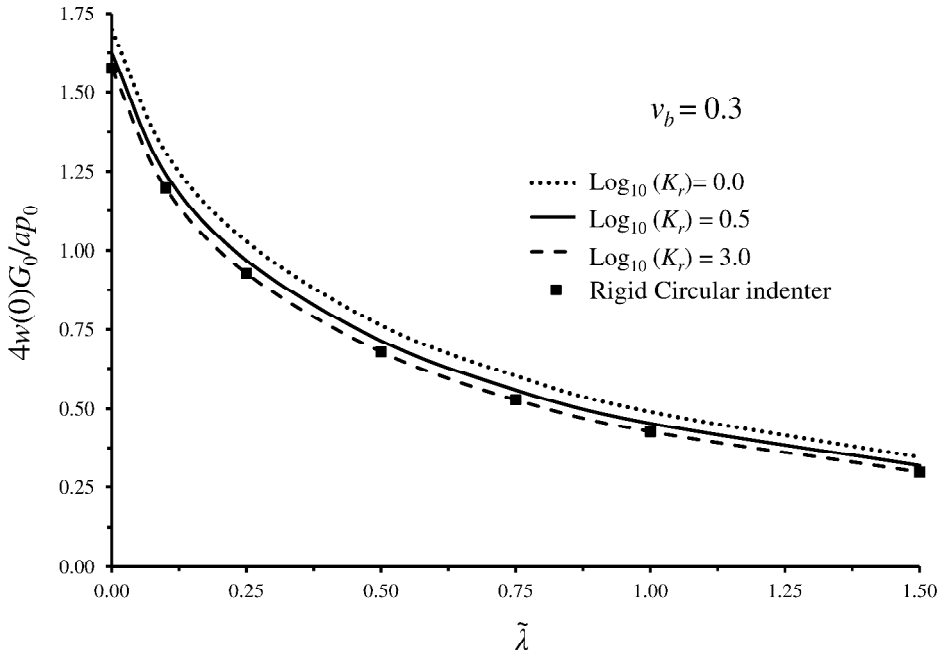

Figure 5.11: Variation of central displacement of the circular plate for different $\tilde{\lambda}$ and for different relative rigidity K_r

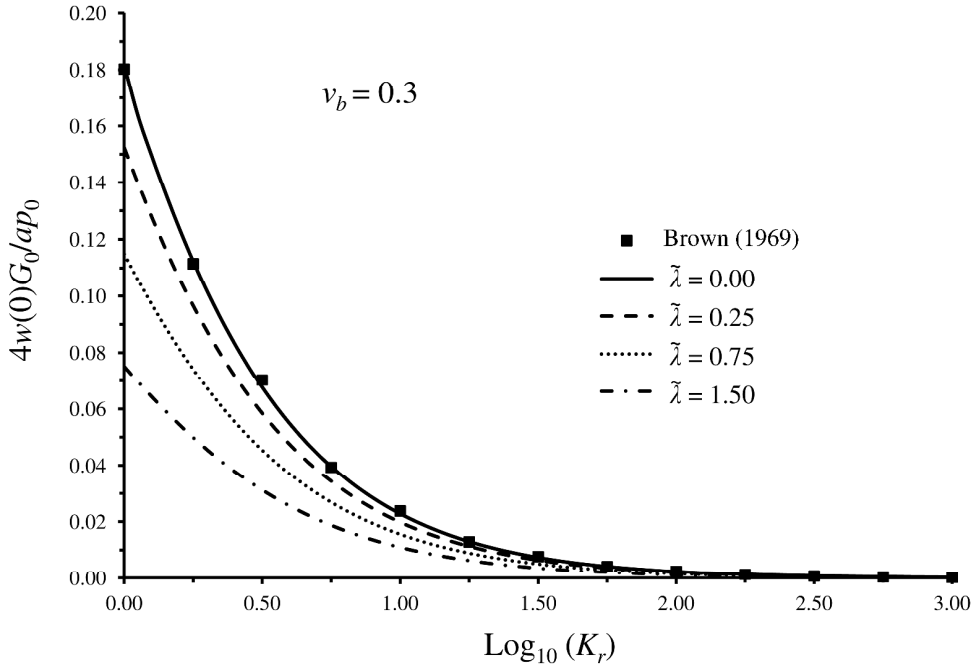

Figure 5.12: Variation of the differential deflection of the circular plate for different $\tilde{\lambda}$ and different relative rigidity K_r

Figure 5.10 shows the variation of the central displacement of a uniformly loaded circular plate for various relative rigidities for the incompressible homogeneous elastic halfspace ($\tilde{\lambda} = 0$). The current result is compared with existing solutions given in Brown (1969) and Selvadurai (1979c). The results are also compared with a finite-element analysis of the indentation problem of smooth indentation of a rigid circular plate on an isotropic homogeneous halfspace using COMSOL Multiphysics^{TM} software. It can be seen from Figure 5.10 that there is good correlation between the results presented by Brown (1969), Selvadurai (1979c), COMSOL and the variational method presented here.

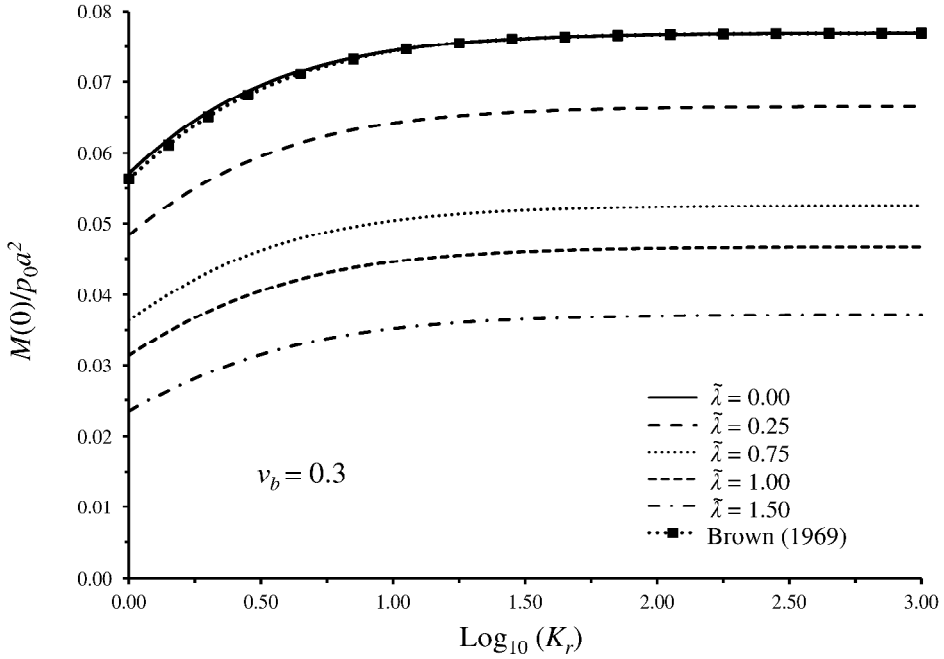

Figure 5.13: Variation of the central flexural moment for different $\tilde{\lambda}$ and different relative rigidity K_r

Figure 5.11 shows the variation in the central displacement of a uniformly loaded circular plate for different $\tilde{\lambda}$ and for different relative rigidity K_r. It is evident that the presence of non-homogeneous conditions has a significant effect on the central displacement of the plate. The results are compared with the smooth

indentation problem of a rigid circular plate and an incompressible non-homogeneous elastic halfspace presented in section 5.2. In this comparison, the flexible plate with $\log_{10} K_r = 3$ is considered to be a nearly rigid plate. As can be seen, there is good correlation between the two results.

The variation in the differential deflection of a uniformly loaded circular plate for different $\tilde{\lambda}$ and different relative rigidity is shown in Figure 5.12. The current results for homogenous case ($\tilde{\lambda} = 0$) are compared with numerical results presented by Brown (1969).

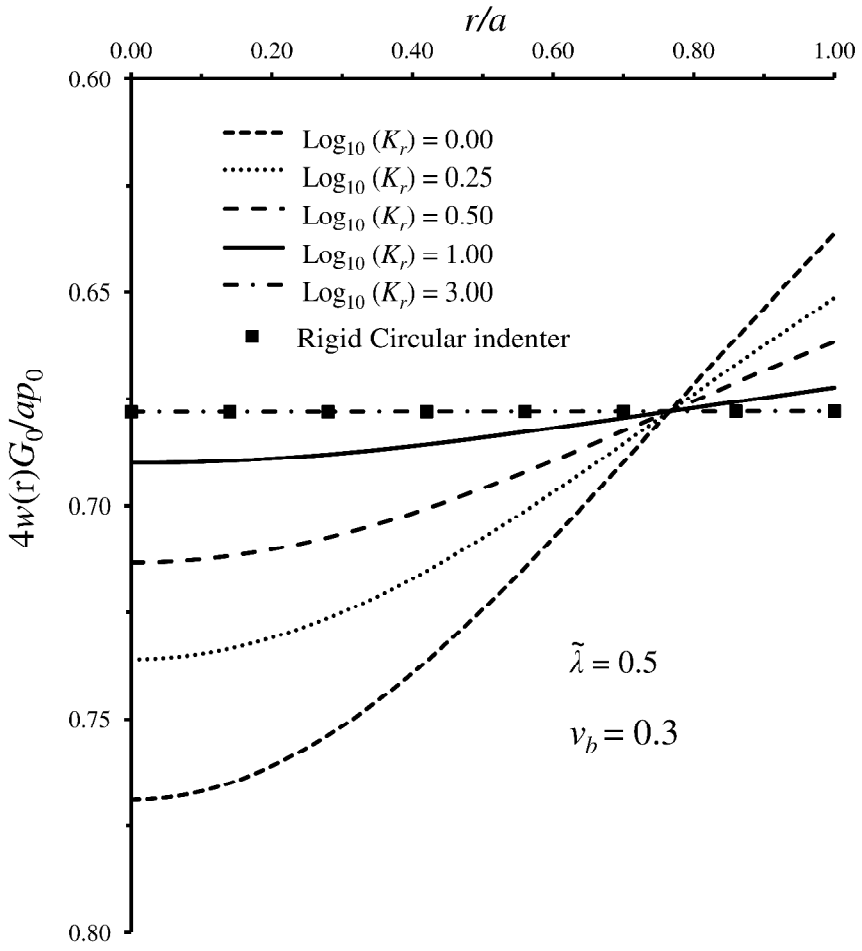

Figure 5.14: Variation of vertical surface displacement along the *r*-axis for different relative rigidities of the plate; $\tilde{\lambda} = 0.5$

The central flexural moment for different $\tilde{\lambda}$ and different relative rigidity of the plate K_r is shown in Figure 5.13 and it is compared with Brown's results (1969) for homogeneous case. There is good correlation between the two results.

Figure 5.14 shows the variation in the vertical surface displacement along the *r*-axis for different relative rigidities of the plate. The effect of the relative rigidity on the shape of the plate deflection is investigated; when $R \to \infty$ (or $K_r \to \infty$), the problem reduces to the indentation of the circular rigid plate on an incompressible elastic halfspace and the results are compared with the known solutions presented by Boussinesq (1885) and the results given in Section 5.2 for smooth contact of a rigid circular plate for $\tilde{\lambda} = 0.5$.

CHAPTER 6

CONCLUSIONS AND SCOPE FOR FUTURE RESEARCH

6.1 Summary and concluding remarks

The research presented in this thesis deals with the analytical and numerical solutions to traction and mixed boundary value problems for an incompressible non-homogeneous medium with applications to geomechanics. The geomechanics types of non-homogeneities that can be examined are many and varied and largely governed by experimentally derived observation. Experimental investigations of geological media such as London Clay deposits show that the modulus of elasticity of soils generally increases with depth, although the variation is neither linear nor exponential. The exponential variation in the shear modulus has an advantage in that the governing partial differential equations of elasticity for a non-homogeneous medium are considerably simplified through the use of this approximation. In this thesis, the non-homogeneity has an exponential variation either over the entire halfspace, or over a finite depth beyond which it considered to be constant. The numerical results have been presented to show the influence of the non-homogeneity on the response of an incompressible elastic

halfspcae. The following is a summary of the basic finding and conclusions of the research:

- A mathematical treatment was presented for the displacements corresponding to axisymmetric interior loading of a non-homogeneous incompressible isotropic elastic half-space where the linear elastic modulus varies exponentially over the entire depth. The interior loading of an elastic half-space can serve as a useful model for examining the interior loading of geologic media with predominantly isochoric or volume preserving deformations. The influence of non-homogeneity on the response of the half-space was clearly illustrated by the numerical results presented in the thesis. The analysis of the traction boundary value problem related to the interior loading of a non-homogeneous elastic halfspace was obtained in a form where results of practical interest can be derived through the evaluation of infinite integrals. The study can also be used as a benchmarking solution for examining the accuracy of computational approaches that can ultimately be used to examine more complicated variations of the shear modulus with depth.

- The problem of the interior loading of a non-homogeneous incompressible elastic halfspace was also considered where the linear elastic modulus varies exponentially over a finite depth, beyond which it is constant. The influence of this type of non-homogeneity on displacements and stresses of the halfspace was discussed by the numerical results presented. These results have been compared with two existing solutions for both linear and exponential variations of the shear modulus.

- The problem of the surface loading of a non-homogeneous incompressible halfspace was extended for the case where the medium is a layer of finite depth d and of infinite lateral extent. The elastic layer is assumed to be incompressible and that its shear modulus increases exponentially with depth. The influence of the non-homogeneity as well as the depth of the finite layer on the response of the halfspace was shown by the numerical results presented.

- Axisymmetric distributed radial loading on a surface of an incompressible elastic halfspace with an exponential variation in the linear elastic shear modulus was considered in last section of chapter 4. The results developed in this section have been used to model the adhesive contact problem presented in chapter 5.

- The mechanics of indentation is visualized as a technique for the estimation of deformability characteristics of materials as well as for the estimation of settlements of geotechnical structures. The interface conditions between the deformable region and the rigid indenter can influence the indentational stiffness. In the classical problem for the adhesive indentation of an isotropic homogeneous elastic halfspace, the indentational stiffness is controlled by Poisson's ratio for the deformable medium and, in the case of an *incompressible homogeneous elastic halfspace region*, the interface conditions (either frictionless or fully bonded) have no influence on the elastic stiffness. This is due to the zero radial displacement at the surface of the halfspace associated with Boussinesq's solution for the loading of the halfspace by a concentrated normal force. This thesis examines the problem of the axisymmetric adhesive indentation by an indenter with a flat base, of an incompressible *non-homogeneous elastic halfspace*, with an exponential variation of the shear modulus with depth. The formulation of the integral equations for the normal and shear stresses at the adhesive zone indicates that the solution cannot be readily accomplished using integral equation techniques commonly employed in the study of adhesive contact problems. A numerical scheme has been developed where the contact normal stresses and shear stresses are represented by discretized equivalents and the unknown values are evaluated by considering the kinematic and mechanical constraints on the adhesive zone. These results are used to estimate the axial stiffness of the adhesive indentation of a rigid circular indenter with an inhomogeneous elastic halfspace that has an exponential variation in the shear modulus. The results were also compared with estimates for the indentational stiffness when the contact is frictionless and when the entire surface of the non-homogeneous halfspace is considered to be radially inextensible. It is observed that for the exponential variation in shear modulus in an incompressible elastic halfspace, the contact

constraints, either adhesive contact or frictionless contact, have very little influence on the indentational stiffness of the rigid circular indenter and for the exponent in the exponential variation $\tilde{\lambda} \in (0, 0.25)$. The discrepancy is of the order of 10% for $\tilde{\lambda} \approx 2$. The discretization technique offers a convenient solution scheme for the adhesive contact problem for the non-homogeneous incompressible elastic halfspace problem.

- The contact problem was extended to examine axisymmetric smooth contact between a flexible plate and an incompressible isotropic non-homogeneous elastic halfspace in which the shear modulus varies exponentially with depth. The analysis uses a variational approach in which the deflected shape of the plate is approximated by a power series in the radial coordinates. The coefficients in the series are evaluated by making use of the principle of minimum potential energy. Using energy method, the maximum deflection, the relative deflection, and the maximum flexural moment in the circular plate were presented. The effect of relative rigidity of the plate as well as the non-homogeneity of the incompressible elastic halfspace on the response was clearly shown by numerical results presented. The results have been compared with existing solutions to validate the accuracy of the solution.

6.2 Scope for future research

In the current research, the influence of non-homogeneity were investigated on traction boundary value problems and mixed boundary value problems for an incompressible non-homogeneous medium. The following investigation can be suggested as future work:

- In this research, it was assumed that the material of the halfspace is incompressible, which simulates immediate (undrained) deformation of saturated elastic soils. Any future research can be extended to examine the general problem involving the compressible non-homogeneous elastic halfspace.

- The representation of the contact stress distribution in terms of a discretized distribution is a convenient mathematical approximation for the solution of a contact problem where the analytical solution would otherwise be intractable. The

discretization techniques which were discussed in chapter 5, can be extended to examine indenters with arbitrary-shaped plan forms that will not be amenable to exact solution. In situations where processes such as indentational fracture needs to be examined (e.g. Selvadurai, 2000e), the singularity at the boundary of the indenter needs to be incorporated in the discretization scheme, so that the stress state can be more precisely defined to generate stress intensity factors and energy release rates important to crack extension analysis can be accurately determined.

- The contact problems, both rigid indenter and flexible plate, can be extended to examine the influence of elastic non-homogeneity on the undrained elastic displacement of the test plate under the combined action of the external load and the internal anchor loads.

REFRENCES

Abbiss, C.P. (1979) A comparison of the stiffness of the chalk at Mundford from a seismic survey and a large scale tank test. *Geotechnique* 29, 461-468.

Alexander, L.G. (1977) Discussions to some results concerning displacements and stresses in a non-homogenous elastic half-space. *Geotechnique* 27, 253–4.

Aleynikov, S.M. (2011) *Spatial Contact Problems in Geomechanics. Boundary Element Method*, *Found. Engng. Mech.* Springer-Verlag, Berlin.

Aliabadi, M.H. and Brebbia, C.A. (1993) *Computational Methods in Contact Mechanics*. Computational Mechanics Publications, London, New York, Elsevier Applied Science, Southampton, Boston.

Atkinson, J.H. (1975) Anisotropic elastic deformations in laboratory tests on undisturbed London Clay. *Geotechnique* 25, 357-374.

Awojobi, A.O and Gibson, R.E. (1973) Plane strain and axially symmetric problems of a linearly nonhomogeneous elastic half-space. *Q. J. Mech. Appl. Math.* 26, 285–302.

Barber J.R. (2010) *Elasticity: Solid Mechanics and Its Applications*. 3rd ed, Springer-Verlag, Berlin.

Belik, G.I. and Protsenko, V.S. (1967) The contact problem of a half-plane for which the modulus of elasticity of the material is expressed by a power function of the depth. *Prikl. Mekhanika* 3, 80-82 .

Booker, J.R. (1991) Analytical methods in geomechanics, *Proceedings of the 7th International Conference on Computer Methods and Advances in Geomechanics*, Cairns, Australia, 1, 3-14.

Borowicka, H. (1936) Influence of rigidity of a circular foundation slab on the distribution of pressurc over the contact surface. *Proceedings of the 1st International Conference on Soil Mechanics and Foundation Engineering*, 2, 144-149.

Boussinesq, J. (1885) *Application des Potentiels à l'Etude de l'Equilibre et du Mouvement des Solides*, Gauthier-Villars, Paris, France.

Brown, P.T. (1969) Numerical analyses of uniformly loaded circular rafts on deep elastic foundations. *Georechnique* 19, 399-404.

Brown P.T. and Gibson R.E. (1972) Surface settlement of a deep elastic stratum whose modulus increases linearly with depth. *Can. Geotech. J.* 9, 467–76.

Burland, J.B. and Lord, J.A. (1969) The Load-Deformation Behaviour of the Middle Chalk at Mundford, Norfolk: A Comparison Between Full-Scale Performance and In-Situ Laboratory Measurements. *Building Research Station* CP, 6/70.

Burland, J.B., Longworth, T.I. and Moore, J.F.A. (1977) A study of ground movement and progressive failure caused by a deep excavation in Oxford Clay. *Geotechnique* 27, 557-591.

Butler, F.G. (1974) Heavily over-consolidated clays. *Proceedings BGS Conference on Settlement of Structures*, Wiley, London, pp. 531–578.

Calladine, C.R. and Greenwood, J.A. (1978) Line and point loads on a nonhomogeneous incompressible elastic half-space. *Q. J. Mech. .Appl. Math.* 31, 507–29.

Carrier III, W.D. and Christian J.T. (1973a) Analysis of an inhomogeneous elastic half-space. *J. Soil Mech. Found. Div ASCE* 99, 301–6.

Carrier III, W.D. and Christian J.T. (1973b) Rigid circular plate resting on a non-homogeneous elastic half-space. *Geotechnique* 23, 67–84.

Cerruti, V. (1882) Ricerche intorno all'equilibrio de' corpi elastici isotropi. *Rend Accad Lincei* 3, 13, 81-122

Chow, Y.K. (1987) Vertical deformation of rigid foundations of arbitrary shape on layered soil media. *Int. J. Numer. Anal. Meth. Geomech.* 11, 1–15.

Cooke, R.W. and Price, G. (1973) Strains and displacements around friction piles, *Proceedings of the 8th Conference Soil Mechanics and Foundation Engineering*, Moscow, 2, 52-60.

Costa Filho, L.F. and Vaughan, P.R. (1980) A computer model for the analysis of ground movements in London Clay. *Geotechnique* 30, 336-339.

Cripps, J.C. and Taylor, R.K. (1981) The engineering properties of mudrocks. *Q. J. Eng.Geol.London* 14, 325-346.

Cripps, J.C. and Taylor, R.K. (1986) Engineering characteristics of British over-consolidated clays and mudrocks I. Tertiary deposits. *Engng. Geology* 22, 349–376.

De Pater, A.D. and Kalker, J.J. (1975) The mechanics of contact between deformable bodies. *Proceedings of the IUTAM Conference*, Enschede. Delft University Press, The Netherlands.

Dempsey, J.P. and Li, H. (1995) A flexible rectangular footing on a Gibson soil: required rigidity for full contact. *Int. J. Solids Struct.* 32, 357–73.

Dhaliwal, R.S. and Singh, B.M. (1978) Torsion by a circular die of a nonhomogeneous elastic layer bonded to a nonhomogeneous halfspace. *Int. J. Engng. Sci.* 16, 649-658.

Eason, G., Noble, B. and Sneddon, I.N. (1955) On certain integrals of Lipschitz–Hankel type involving products of Bessel functions. *Phil Trans Roy Soc London. Ser A. Math. Phys. Sci.* 247, 529–551.

Flamant, A. (1892) Sur la répartition des pressions dans un solide rectangulaire chargé transversalement. *Compte. Rendu. Acad. Sci. Paris*, 114, 1465-1468.

Galin, L.A. (1961) *Contact Problems in the Theory of Elasticity*. North Carolina State College. (Translated from Russian by Mrs. Moss).

Gibson R.E. (1967) Some results concerning displacements and stresses in a non-homogeneous elastic halfspace. *Geotechnique* 17, 58–67.

Gibson, R.E. and Brown, P.T. (1979) Surface settlement of a finite elastic layer whose modulus increases linearly with depth. *Int. J. Numer. Analyt. Meth. Geomech.* 3, 37-47.

Gibson, R.E., Brown, P.T., Andrews, K.R.F. (1971) Some results concerning displacements in a non-homogeneous elastic layer. *Z. Angew. Math. Phys.* 22, 855–64.

Gladwell, G.M.L. (1980) *Contact Problems in the Classical Theory of Elasticity*. Sijthoff and Noordhoff , The Netherlands.

Goodman, R.E. (1974) Developments of the three-dimensional theory of elasticity. In: *R.D. Mindlin and Applied Mechanics* (G. Herrmann, Ed), Pergamon press, Oxford, UK, pp. 25–64.

Goodier, J.N. (1958) *Elasticity and Plasticity: The mathematical theory of elasticity*. (J.N. Goodier and P. G. Hodge, Jr., eds.) , John Wiley, New York.

Gorbunov-Posadov, M.I. (1940) Design of beams and plates on an elastic halfspace. *PMM* 2, 4, 61–80 [in Russian].

Gunn, D.A., Jackson, P.D., Entwisle, D.C., Armstrong, R.W. and Culshaw, M.G. (2003) Predicting subgrade shear modulus from existing ground models. *NDT&E International* 36, 135–144.

Gurtin, M.E. (1972) *The Linear Theory of Elasticity*, *Mechanics of Solids II, Encyclopaedia of Physics* (S. Flügge, ed.), Vol. VIa/2, 1–295, Springer-Verlag, Berlin, Germany.

Habel, A. (1937) Die auf dem elastisch-isotropen halbraum auf ruhende zentral symmetrisch belastete elastische kreisplatte. *Bauingenieur* 18, 188-193.

Hertz, H. (1882) On the contact of firm elastic bodies (in German: Ueber die Berührung fester elastischer Körper). *J. Reine Angewandte Mathematik* 92, 156-171.

Hetényi, M. (1946) *Beams on Elastic Foundations*, University of Michigan Press, Ann Arbor

Hobbs, N.B. (1974) Factors affecting the prediction of settlement on rock with particular reference to chalk and trias. *BGS Conference on Settlement of Structures*, Cambridge, pp. 579–560.

Holmberg, A. (1946) Cirkulara plattor med jamnt fordelad last pa elastiskt underlag. *Betong*, 107.

Hooper, J.A. (1973) Observations on the behaviour of a pile raft foundation on London Clay. *Proc. Inst. Civ. Eng.*, Pt. 2, 55, 855-877.

Hooper, J.A. and Butler, F.G. (1966) Some numerical results concerning the shear strength of London Clay. *Geotechnique* 16, 282-304.

Hooper, J.A. and Wood, L.A. (1977) Comparative behaviour of raft and piled foundations. *Proceedings of the 9th Conference Soil Mechanics and Foundation Engineering*, Tokyo, 1, 545-550.

Ishkova, A.G. (1951)Bending of a circular plate on the elastic halfspace under the action of a uniformly distributed axisymmetrical load. *Uch. Zap. Mosk. Gos. Univ.* 3, 202-225 (in Russian).

Jeng, D.S. and Lin, Y.S (1999) Wave-induced pore pressure around a buried pipeline in Gibson soil: finite element analysis. *Int. J. Numer. Anal. Meth. Geomech.* 23, 1559–78.

Johnson, K.L. (1985) *Contact Mechanics*. Cambridge University Press, Cambridge.

Kassir, M.K. (1970) The Reissner-Sagoci problem for a non-homogeneous solid. *Int. J. Engng. Sci.* 8, 875-885.

Kassir, M.K. and Chuapresert, M.F. (1974) A rigid punch in contact with a non-homogeneous elastic solid. *J. Appl. Mech.* 41, 1019–1024.

Katebi, A., Rahimian, M., Khojasteh, A. and Pak, R.Y.S. (2010) Axisymmetric interaction of a rigid disc with a transversely isotropic half-space. *Int. J. Numer. Analyt. Meth. Geomech.* 34, 1211-1236.

Klein, G.K. (1956) Study of non-homogeneity of discontinuities in deformations and of other mechanical properties of the soil in the design of structures on solid foundations. *Sb. Trud. Mosk. inzh-stroit. Inst.*14.

Koronev, B.G. (1957) A die resting on elastic halfspace, the modulus of elasticity of which is an exponential function of depth. *Dokl. Akad. Nauk.* SSSR 112, 5.

Koronev, B.G. (1960) *Structures Resting on an Elastic Foundation*. Pergamon Press, Oxford, 160-190 (Translated from Russian, edited by G. Herrmann).

Lekhnitskii, S.G. (1962) Radial distribution of stresses in a wedge and in a half-plane with variable modulus of elasticity. *PMM* 26, 146-151.

Love, A.E.H. (1927) *A Treatise on the Mathematical Theory of Elasticity*. Cambridge University Press, Cambridge, UK.

Lur'e, A.I. (1964) *Three-Dimensional Problems of the Theory of Elasticity*. Wiley-Interscience, New York.

Marsland, A. (1973a) Large in-situ tests to measure the properties of stiff fissured clays. Current Paper 1/73, *Building Research Establishment*, 12 pp.

Marsland, A. (1973b) In-situ plate tests in lined and unlined boreholes in highly fissured clay. Current Paper 5/73, *Building Research Establishment*, 32 pp.

Marsland, A. (1973c) Laboratory and in-situ measurements of the deformation moduli of London Clay. Current Paper 24/73, *Building Research Establishment*, 12 pp.

Marsland, A. and Randolph, M.F. (1978) Comparison of the results from pressuremeter tests and large in situ plate tests in London Clay. Current Paper 10/78, *Building Research Establishment*, 26 pp.

Michell, J. H. (1900) Some elementary distributions of stress in three-dimensions. *Proc. London Math. Soc.* 32, pp. 23–35.

Mindlin, R.D. (1936) Force at a point in the interior of a semi-infinite solid. *Physics* 7, 195-202

Mossakovskii, V.I. (1954) The fundamental mixed problem of the theory of elasticity for a halfspace with a circular line separating the boundary conditions. *J. Appl. Math. Mech.* 18, 187–196 (in Russian.).

Mossakovskii, V.I. (1958) Pressure of a circular punch on an elastic halfspace whose modulus of elasticity is an exponential function. *Prikl. Mat. Mekh.* 22, 168-171.

Oliveira, M.F.F., Dumont, N.A. and Selvadurai, A.P.S. (2012) Boundary element formulation of axisymmetric problems for an elastic half-space. *Eng. Analysis Bound. Elem.* 36, 1478-1492.

Olszak, W. (1959) *Non-Homogeneity in Elasticity and Plasticity*. Pergamon Press, Oxford.

Plevako, V.P. (1971) On the theory of elasticity of an inhomogeneous media. *J. Appl. Math. Mech.* 35, 1566–1573.

Plevako, V.P. (1972) On the possibility of using harmonic functions for solving problems of the theory of elasticity of non-homogeneous media. *PMM* 36, 834–842.

Plevako, V.P. (1973a) Equilibrium of a nonhomogeneous half-plane under the action of forces applied to the boundary. *Appl. Math. Mech.* 37, 858–866.

Plevako, V.P. (1973b) The deformation of a nonhomogeneous halfspace under the action of a surface load. *PMM* 9, 593-598.

Plevako, V.P. (1973c) A problem concerned with the action of shear forces applied to the surface of an inhomogeneous halfspace. *PMM* 9, 1191-1195.

Plevako, V.P. (1974) Inhomogeneous layer bonded to a halfspace under the action of internal and external forces. *PMM* 38, 865-875.

Podio-Guidugli, P. (2004) Examples of concentrated contact interactions in simple bodies. *J. Elast.* 75, 67 186.

Popov, G.Ia. (1959) Bending on an unbounded plate supported by an elastic halfspace with a modulus of elasticity varying with depth. *J. Appl. Math. Mech.* 23, 1566-1573.

Popov, G.Ia. (1973) Axisymmetric contact problem for an elastic inhomogeneous half-space in the presence of cohesion. *PMM* 37, 1109-1116.

Poulos, H.G. and Davis, E.H. (1975) Prediction of downdrag forces in end-bearing piles. *J. Geotech. Eng. Div. ASCE* 101(2), 189- 204.

Puro, A. E. (1973) Application of Hankel transforms to the solution of axisymmetric problems when the modulus of elasticity is a power function of depth. *PMM*, 37, Ng5, 945-948.

Rahimian, M., Eskandari-Ghadi, M., Pak, R.Y.S. and Khojasteh, A. (2007) Elastodynamic potential method for transversely isotropic solid. *J. Eng. Mech. ASCE* 133, 1134–1145.

Rajapakse, R.K.N.D. (1990a) A vertical load in the interior of a non-homogeneous incompressible elastic half-space. *Q. J. Mech. App. Math.* 43(1), 1-14.

Rajapakse, R.K.N.D. (1990b) Rigid inclusion in nonhomogeneous incompressible elastic half-space. *J. Eng. Mech.* ASCE 116, 399–410.

Rajapakse, R.K.N.D. and Selvadurai, A.P.S. (1986) On the performance of Mindlin plate elements in modelling plate elastic medium interaction, *In. J. Num. meth. Engng.* 23, 1229-1244.

Rajapakse, R.K.N.D. and Selvadurai, A.P.S. (1989) Torsion of foundations embedded in non-homogeneous soil in a weathered crust. *Géotechnique* 39, 485-496.

Rajapakse, R.K.N.D. and Selvadurai, A.P.S. (1991) Response of circular footings and anchor plates in non-homogeneous elastic soils. *Int. J. Num. Analyt. Meth. Geomech.* 15, 457-470.

Rakov, A.Kh. and Rvachev, V.L. (1961) Contact problems of the theory of elasticity for a half-space whose modulus is a power function of depth. *Dopov. Akad. Nauk. Ukr. SSR* 3: 286–290.

Rostovtsev, N.A. (1961) An integral equation encountered in the problem of a rigid foundation bearing on non-homogeneous soil, *J. Appl. Math. Mech.* 25, 238–246.

Rostovtsev, N.A. (1964) On the theory of elasticity of a nonhomogeneous medium. *PMM* 28, 745–757.

Rostovtsev, N.A. and Khranevskaia, I.E.(1971) The solution of the Boussinesq problem for a halfspace whose modulus of elasticity is a power function of the depth. *PMM* 35, 1053-1061.

Selvadurai, A.P.S. (1979a) *Elastic Analysis of Soil-Foundation Interaction*. Developments in Geotechnical Engineering, Vol. 17, Elsevier Scientific, Amsterdam, The Netherlands.

Selvadurai, A.P.S. (1979b) An energy estimate of the flexural deflections of a circular foundation embedded in an elastic medium. *Int. J. Numer. Analyt. Meth. Geomech.* 3, 285-292.

Selvadurai, A.P.S. (1979c) The interaction between a uniformly loaded circular plate and an isotropic elastic halfspace: a variational approach. *J. Struct. Mech.* 7, 231-246.

Selvadurai, A.P.S (1980) Elastic contact between a flexible circular plate and a transversely isotropic elastic halfspace. *Int. J. Solid. Struct.* 16, 167-176.

Selvadurai, A.P.S. (1981) The displacements of a flexible inhomogeneity embedded in a transversely isotropic elastic medium. *Fibre Sci. Technol.* 14, 251-259.

Selvadurai, A.P.S. (1984a) The flexure of an infinite strip of finite width embedded in an isotropic elastic medium of infinite extent. *Int. J. Numer. Analyt. Meth. Geomech.* 8, 157-166.

Selvadurai, A.P.S. (1984b) Elastostatic bounds for the stiffness of an elliptical disc inclusion embedded at a transversely isotropic bimaterial interface. *ZAMP* 35, 13-23.

Selvadurai A.P.S. (1989) The influence of a boundary fracture on the elastic stiffness of a deeply embedded anchor plate. *Int. J. Num. Analyt. Meth. Geomech.* 13, 159-170.

Selvadurai, A.P.S. (1993) The axial loading of a rigid circular anchor plate embedded in an elastic half-space. *Int. J. Num. Analyt. Meth. Geomech.* 17, 343-353.

Selvadurai A.P.S. (1994) On the problem of a detached anchor plate embedded in a crack. *Int. J. Solids. Struct.* 31, 1279-1290.

Selvadurai, A.P.S. (1996) The settlement of a rigid circular foundation resting on a halfspace exhibiting a near surface elastic non-homogeneity. *Int. J. Numer. Analyt. Meth. Geomech.* 20, 351-364.

Selvadurai, A.P.S. (2000a) *Partial Differential Equations in Mechanics*. Vol.2 The Biharmonic Equation, Poisson's Equation, Springer-Verlag, Berlin.

Selvadurai, A.P.S. (2000b) On the mathematical modelling of certain fundamental elastostatic contact problems in geomechanics. In: *Modelling in Geomechanics*, (M. Zaman, G. Gioda and J.R. Booker, Ed.) Chapter 13, John Wiley, New York, 301-328.

Selvadurai, A.P.S. (2000c) An inclusion at a bi-material elastic interface. *J. Engng Math.* 37, 155-170

Selvadurai, A.P.S. (2000d) Boussinesq's problem for an elastic halfspace reinforced with a rigid disk Inclusion. *Math. Mech. Solids* 5, 483-499.

Selvadurai, A.P.S. (2000e) Fracture evolution during indentation of a brittle elastic solid. *Mech. Cohes. Frict. Mat.* 5, 325-339.

Selvadurai, A.P.S. (2001a) On the displacements of an elastic halfspace containing a rigid inhomogeneity. *Int. J. Geomech.* 1, 149-174.

Selvadurai, A.P.S. (2001b) Mindlin's problem for a halfspace with a bonded flexural surface constraint. *Mech. Res. Comm.* 28, 157-164.

Selvadurai, A.P.S. (2003) On an invariance principle for unilateral contact at a bi- material elastic interface. *Int. J. Engng. Sci.* 41, 721-739.

Selvadurai A.P.S. (2007) The analytical method in geomechanics. *Appl. Mech. Rev.* 60, 87-107

Selvadurai, A.P.S. (2009) Boussinesq indentation of an isotropic elastic halfspace reinforced with an inextensible membrane. *Int. J. Engng. Sci.* 47, 1339-1345.

Selvadurai, A.P.S. and Au, M.C. (1986) Generalized displacements of a rigid elliptical anchor embedded at a bi-material geological interface. *Int. J. Numer. Analyt. Meth. Geomech.* 10, 633-652.

Selvadurai, A.P.S., Dumont, N.A. (2011) Mindlin's problem for a halfspace indented by a flexible plate, *J. Elasticity* 105, 253-269.

Selvadurai, A.P.S. and Lan, Q. (1997) A disc inclusion at a non-homogeneous elastic interface, *Mech. Res. Commun.* 24, pp. 473-488.

Selvadurai, A.P.S. and Lan, Q. (1998) Axisymmetric mixed boundary value problems for an elastic halfspace with a periodic nonhomogeneity. *Int. J. Solids Struct.* 35, 1813-1826.

Selvadurai, A.P.S. and Rajapakse, R.K.N.D. (1985) On the load transfer from a rigid cylindrical inclusion into an elastic half space. *Int. J. Solids. Struct.* 21, 1213–1229.

Selvadurai, A.P.S. and Spencer, A.J.M. (1972) Second-order elasticity with axial symmetry. I. General theory. *Int. J. Eng. Sci.* 10, 97-114.

Selvadurai, A.P.S., Bauer, G.E. and Nicholas T.J. (1980) Screw plate testing of a soft clay. *Can. Geotech. J.* 17, 465-472.

Selvadurai, A.P.S., Singh, B.M. and Vrbik, J. (1986) A Reissner-Sagoci problem for a non-homogeneous elastic solid. *J. Elasticity* 16, 383-391.

Shibuya, S., Tatsuoka, F., Teachavorasinkun, S., Kong, X.J., Abe, F., Kim, Y.S. and Park, C.S. (1992) Elastic deformation properties of geomaterials. *Soil and Foundations* 32, 26-46.

Simons, N.E. and Som, N.N. (1969) The influence of lateral stresses on the stress deformation characteristics of London Clay, *Proceedings of the 7th Conference Soil Mechanics and Foundation Engineering*, Mexico, 1, 369-377.

Simpson, B., O'Riordan, N.J. and Croft, D.D. (1979) A computer model for the behaviour of London Clay, *Geotechnique*. 29, 149-175.

Skempton, A.W. and Henkel, D.J. (1957) Tests on London Clay from deep borings at Paddington, Victoria and the South Bank, *Proceedings of the 4th International Conference on Soil Mechanics and Foundation Engineering*, London, Vol. 1, pp. 100–106.

Sneddon, I. N. (1951) *Fourier Transforms*, McGraw–Hill, New York.

Sneddon, I.N. (1965) The relation between load and penetration in the axisymmetric Boussinesq problem for a punch of arbitrary profile. *Int. J. Engng. Sci.* 3, 45-47.

Sokolnikoff, I.S. (1956) *The Mathematical Theory of Elasticity*, McGraw–Hill, New York.

Spencer, A.J.M (1970) The static theory of finite elasticity. *J. Inst. Math. Appl.* 6, 164-200.

Spencer, A.J.M (1980) *Continuum Mechanics*, Longman Mathematical Texts, London.

Spencer, A.J.M. and Selvadurai, A.P.S. (1998) Some generalized anti-plane strain problems for an inhomogeneous elastic halfspace. *J. Engng. Math.* 34, 403-416.

Ter-Mkrtch'ian, L.N. (1961) Some problems in the theory of elasticity of non homogeneous elastic media. *PMM* 25, 1120-1225.

Timoshenko, S.P., Woinowsky-Krieger, S. (1959) *Theory of Plates and Shells*, McGraw-Hill, New York.

Timoshenko, S. P., and Goodier, J. N. (1970) *Theory of Elasticity*. McGraw–Hill, New York.

Ufliand, Ia.S. (1956) The contact problem of the theory of elasticity for a die, circular in its plane, in the presence of adhesion. *J. Appl. Math. Mech.* 20, 578–587.

Ward, W.H., Marsland, A. and Samuels, S.G. (1965) Properties of the London Clay at the Ashford Common Shaft, *Geotechnique* 15, 324–344.

Westergaard, H.M. (1952) *Theory of Elasticity and Plasticity*. Harvard University Press, Cambridge, MA.

Windle, D. and Wroth, C.P. (1977) In-situ measurement of the properties of stiff clays. *Proceedings of the 9th Conference Soil Mechanics and Foundation Engineering,* Tokyo, 1, 347-352.

Winkler, E. (1867) *Die Lehre von der Elastizität und Festigkeit,* Dominicus, Prague.

Yue, Z.Q., Yin J.H. and Zhang, S.Y. (1999) Computation of point load solutions for geo-materials exhibiting elastic non-homogeneity with depth. *Comput Geotech.* 25,75–105.

Zaman, M.M., Kukreti, A.R. and Issa, A. (1988) Analysis of circular plate-elastic half-space interaction using an energy approach. *Appl. Math. Modeling* 12, 285–292.

Zaretsky, Y.K. and Tsytovich, N.A. (1965) Considerations of heterogeneity and non-linear deformations of the base in the design of rigid foundations. *Proceedings of the 6th Conference Soil Mechanics and Foundation Engineering*, Montreal, Canada 2, 222–5.

Zemochkin, B.N. (1939) *Analysis of Circular Plates on Elastic Foundation*. Mosk. Izd. Voenno. Lnzh. Akad., Moscow.

APPENDIX A

The explicit solutions for the arbitrary functions A_1, B_1, C_1, D_1, A_2 and B_2 from Eqs. (4.11-4.16) can be expressed as follows:

$$A_1 = (e^{-dk_1} f_1 \delta_1 \eta_4)/(\eta_1 \vartheta) - (e^{-dk_1} f_1 \eta_3 \delta_2)/(\eta_1 \vartheta) + \frac{\eta_2}{\eta_1}[(e^{-dk_1} f_1 \delta_2 \gamma_2)/(\gamma_1 \vartheta) - (e^{-dk_1} f_1 \delta_1 \gamma_3)/(\gamma_1 \vartheta)] \quad \text{(A1)}$$

$$B_1 = -(e^{-dk_1} f_1 \delta_2 \gamma_2)/(\gamma_1 \vartheta) + (e^{-dk_1} f_1 \delta_1 \gamma_3)/(\gamma_1 \vartheta) \quad \text{(A2)}$$

$$C_1 = (e^{-dk_1} f_1 \delta_2)/\vartheta \quad \text{(A3)}$$

$$D_1 = -(e^{-dk_1} f_1 \delta_1)/\vartheta \quad \text{(A4)}$$

$$B_2 = (e^{-dk_1} f_3 \delta_1)/\vartheta - (e^{-dk_1} f_2 \delta_2)/\vartheta - (e^{-dk_1} f_1 \delta_2 \gamma_2)/(\gamma_1 \vartheta) + (e^{-dk_1} f_1 \delta_1 \gamma_3)/(\gamma_1 \vartheta) \quad \text{(A5)}$$

$$\begin{aligned} A_2 = {} & -(e^{dk_4} f_1 \delta_1)/\vartheta + (e^{-dk_1} f_1 \delta_1 \eta_4)/(\eta_1 \vartheta) + (e^{+dk_3} f_1 \delta_2)/\vartheta - (e^{-dk_1} f_1 \eta_3 \delta_2)/(\eta_1 \vartheta) \\ & - e^{dk_1 - dk_2}[(e^{-dk_1} f_1 \delta_2 \gamma_2)/(\gamma_1 \vartheta) - (e^{-dk_1} f_1 \delta_1 \gamma_3)/(\gamma_1 \vartheta)] + \frac{\eta_2}{\eta_1}[(e^{-dk_1} f_1 \delta_2 \gamma_2)/(\gamma_1 \vartheta) \\ & - (e^{-dk_1} f_1 \delta_1 \gamma_3)/(\gamma_1 \vartheta)] + e^{dk_1 - dk_2}[-(e^{-dk_1} f_3 \delta_1)/\vartheta + (e^{-dk_1} f_2 \delta_2)/\vartheta + (e^{-dk_1} f_1 \delta_2 \gamma_2)/(\gamma_1 \vartheta) \\ & - (e^{-dk_1} f_1 \delta_1 \gamma_3)/(\gamma_1 \vartheta)] \end{aligned} \quad \text{(A6)}$$

where

$$f_1 = (-\beta_1 e^{-dk_1 - dk_2} + \beta_2 e^{-dk_1 - dk_2}); \qquad f_2 = (\beta_1 e^{-dk_1 + dk_3} + \beta_3 e^{-dk_1 + dk_3});$$

$$f_3 = (\beta_1 e^{-dk_1 + dk_4} + \beta_4 e^{-dk_1 + dk_4}); \qquad f_4 = (-\eta_1 e^{-dk_1 - dk_2} + \eta_2 e^{-dk_1 - dk_2})$$

$$f_5 = (\eta_1 e^{-dk_1 + dk_3} - \eta_3 e^{-dk_1 + dk_3}); \qquad f_6 = (\eta_1 e^{-dk_1 + dk_4} - \eta_4 e^{-dk_1 + dk_4})$$

$$f_7 = (-\theta_1 e^{-dk_1 - dk_2} + \theta_2 e^{-dk_1 - dk_2}); \qquad f_8 = (\theta_1 e^{-dk_1 + dk_3} - \theta_3 e^{-dk_1 + dk_3})$$

$$f_9 = (\theta_1 e^{-dk_1 + dk_4} - \theta_4 e^{-dk_1 + dk_4})$$

(A7)

and

$$\delta_1 = (-f_2 f_4 + f_1 f_5); \qquad \delta_2 = (-f_3 f_4 + f_1 f_6)$$

$$\gamma_1 = (-\eta_2 \theta_1 + \eta_1 \theta_2); \qquad \gamma_2 = (-\eta_3 \theta_1 + \eta_1 \theta_3); \qquad \gamma_3 = (-\eta_4 \theta_1 + \eta_1 \theta_4)$$

$$\vartheta = \left(G(d) / \tilde{p}(\xi)\right)(-\delta_2(-f_2 f_7 + f_1 f_8) + \delta_1(-f_3 f_7 + f_1 f_9))$$

(A8)

APPENDIX B

The system of linear simultaneous equations for the arbitrary functions A_1, B_1, C_1, D_1, A_2 and B_2 , …, etc., resulted by substituting Eqs. (4.24-4.26) into boundary and continuity conditions (4.20-4.23), can be expressed as follow:

$$A_1\theta_1 + B_1\theta_2 + C_1\theta_3 + D_1\theta_4 = 0 \tag{B1}$$

$$A_1\eta_1 + B_1\eta_2 + C_1\eta_3 + D_1\eta_4 = 0 \tag{B2}$$

$$A_1k_1e^{-k_1d} + B_1k_2e^{-k_2d} - C_1k_3e^{k_3d} - D_1k_4e^{k_4d} = [A_2\xi + B_2(d\xi - 1)]e^{-\xi d} \tag{B3}$$

$$A_1e^{-k_1d} + B_1e^{-k_2d} + C_1e^{k_3d} + D_1e^{k_4d} = [A_2 + B_2d]e^{-\xi d} \tag{B4}$$

$$A_1\eta_1e^{-k_1d} + B_1\eta_2e^{-k_2d} + C_1\eta_3e^{k_3d} + D_1\eta_4e^{k_4d} = [2\xi A_2 + 2\xi B_2d - 2B_2]e^{-\xi d} \tag{B5}$$

$$A_1\theta_1e^{-k_1d} + B_1\theta_2e^{-k_2d} + C_1\theta_3e^{k_3d} + D_1\theta_4e^{k_4d} + 2[A_2\xi + B_2d\xi]e^{-\xi d} = \frac{\tilde{p}(\xi)}{G(d)} \tag{B6}$$

where

$$\eta_i = \xi + \frac{k_i^2}{\xi} \quad ; \quad i = 1,2,3,4$$

$$\theta_i = q_i - 2k_i \quad ; \quad \theta_{i+2} = q_{i+2} + 2k_{i+2} \; ; \quad i = 1,2$$

$$G(d) = G_0e^{\tilde{\lambda}d}$$

$$\tilde{p}(\xi) = \int_0^\infty rp(r)J_0(\xi r)dr \tag{B7}$$

The explicit solutions for the arbitrary functions A_1, B_1, C_1, D_1, A_2 and B_2 can be expressed as follows:

$$A_1 = \frac{\gamma\ell_3\chi_4}{\vartheta_3} \tag{B8}$$

$$B_1 = -\frac{\gamma \ell_3}{\vartheta_2} - \frac{\gamma \ell_3 \chi_4 \vartheta_1}{\vartheta_2 \vartheta_3} \tag{B9}$$

$$C_1 = \frac{\gamma \ell_2}{\vartheta_2} - \frac{\gamma \ell_3 \chi_4 (\ell_1 / \ell_3 - \ell_2 \vartheta_1 / \ell_3 \vartheta_2)}{\vartheta_3} \tag{B10}$$

$$D_1 = \frac{\gamma \ell_5}{\vartheta_2} - \frac{\gamma \ell_3 \chi_4 (\ell_4 / \ell_3 - \ell_5 \vartheta_1 / \ell_3 \vartheta_2)}{\vartheta_3} \tag{B11}$$

$$A_2 = \frac{\gamma \ell_3 \delta_2}{\vartheta_2} - \frac{\gamma \ell_3 \chi_4 (\delta_1 - \delta_2 \vartheta_1 / \vartheta_2)}{\vartheta_3} \tag{B12}$$

$$B_2 = \frac{\gamma \ell_3 R_1}{\vartheta_2} - \frac{\gamma \ell_3 \chi_4 (R_1 - R_2 \vartheta_1 / \vartheta_2)}{\vartheta_3} \tag{B13}$$

Where

$$\ell_i = \eta_4 \theta_i - \eta_i \theta_4;\ i = 1,2,3;\ \ell_{i+3} = -\eta_3 \theta_i + \eta_i \theta_4;\ i = 1,2$$

$$I_i = e^{-d(\xi + k_i)}(\xi - k_i);\ I_{i+2} = e^{-d(\xi - k_{i+2})}(\xi + k_{i+2});\ i = 1,2$$

$$J_i = e^{-2d\xi - d(\xi + k_i)}(2\xi - \eta_i);\ J_{i+2} = e^{-2d\xi - d(\xi - k_i)}(2\xi - \eta_{i+2});\ i = 1,2$$

$$h_i = -e^{-d(\xi + k_i)}(2\xi + \theta_i);\ h_{i+2} = -e^{-d(\xi - k_{i+2})}(2\xi + \theta_{i+2});\ i = 1,2$$

$$\omega_i = e^{d(\xi - k_i)}(-1 + d\xi - dk_i);\ \omega_{i+2} = e^{d(\xi + k_{i+2})}(-1 + d\xi + dk_{i+2});\ i = 1,2$$

$$f_1 = e^{d(\xi - k_i)}(e^{d(k_i + k_4)}\xi\eta_2 + e^{d(k_i + k_4)}k_4\eta_2 - \xi\eta_4 - k_1\eta_4);$$

$$f_2 = e^{d\xi}(-e^{dk_4}\xi\eta_3 - e^{dk_4}k_4\eta_3 + e^{dk_3}\xi\eta_4 + e^{dk_3}k_3\eta_4)$$

$$\chi_i = ((-2e^{-2d\xi}I_i - J_i)\eta_4 + \eta_i(-2e^{-2d\xi}I_4 - J_4));\ i = 1,2,3;\ \chi_4 = (-\chi_2\ell_2 + \chi_1\ell_3)$$

$$\vartheta_i = (\ell_3(\eta_4 h_i - \eta_i h_4) - \ell_i(\eta_4 h_3 - \eta_3 h_4));\ i = 1,2;\ \vartheta_3 = (-\chi_4\vartheta_1 + (\chi_1\ell_3 - \chi_3\ell_1)\vartheta_2)$$

$$\delta_i = \omega_i - (\omega_4\eta_i / \eta_4) - ((\omega_3 - (\omega_4\eta_3 / \eta_4)\ell_2) / \ell_3);\ i = 1,2$$

$$R_i = f_1 / \eta_4 + f_2\ell_i / \eta_4\ell_3;\ i = 1,2;\ \gamma = e^{-d\xi}\eta_4(\tilde{p}(\xi) / G(d))$$

(B14)

APPENDIX C

The w_{ij}, w'_{ij}, u_{ij} and u'_{ij} in Eqs. (5.30), (5.42) and (5.43) can be calculated by using superposition technique, we have:

w_{ij} : by using Eq. (5.23) we have:

for j=1 and i=1, 2, …, n:

$$w_{ij}(r_{mi},0)=\int_0^{\infty}\left(\frac{(k_1^2-k_2^2)}{(2k_1-q_1)(\xi^2+k_2^2)+(q_2-2k_2)(\xi^2+k_1^2)}\right) J_0(r_{mi}\xi)\frac{r_1}{a}J_1(r_1\xi)d\xi \tag{C1}$$

and for j=2,3,…,n and i=1,2,…,n:

$$w_{ij}(r_{mi},0)=\int_0^{\infty}\left(\frac{(k_1^2-k_2^2)}{(2k_1-q_1)(\xi^2+k_2^2)+(q_2-2k_2)(\xi^2+k_1^2)}\right) J_0(r_{mi}\xi)[\frac{r_j}{a}J_1(r_j\xi)-\frac{r_{j-1}}{a}J_1(r_{j-1}\xi)]d\xi \tag{C2}$$

w'_{ij} : by using Eq. (5.44) we have:

for j=1 and i=1, 2, …, n:

$$w'_{i1}(r_{mi},0)=\int_0^{\infty}\left(\frac{(q_1-2k_1)+(2k_2-q_2)}{(2k_1-q_1)(\xi^2+k_2^2)+(q_2-2k_2)(\xi^2+k_1^2)}\right) \xi^2 J_0(r_{mi}\xi)\left[\int_0^{r_1}\frac{r}{a}J_1(\xi r)dr\right]d\xi \tag{C3}$$

and for j=2,3,…,n and i=1,2,…,n:

$$w'_{ij}(r_{mi},0)=\int_0^{\infty}\left(\frac{(q_1-2k_1)+(2k_2-q_2)}{(2k_1-q_1)(\xi^2+k_2^2)+(q_2-2k_2)(\xi^2+k_1^2)}\right)\xi^2 J_0(r_{mi}\xi)\left[\int_{r_{j-1}}^{r_j}\frac{r}{a}J_1(\xi r)dr\right]d\xi \tag{C4}$$

u_{ij} : by using Eq. (5.24) we have:

for j=1 and i=1, 2, …, n:

$$u_{i1}(r_{mi},0)=\int_0^{\infty}\left(\frac{k_2(\xi^2+k_1^2)-k_1(\xi^2+k_2^2)}{\xi(2k_1-q_1)(\xi^2+k_2^2)+\xi(q_2-2k_2)(\xi^2+k_1^2)}\right)J_1(r_{mi}\xi)\frac{r_1}{a}J_1(r_1\xi)d\xi \tag{C5}$$

and for j=2,3,…,n and i=1,2,…,n:

$$u_{ij}(r_{mi},0)=\int_0^{\infty}\left(\frac{k_2(\xi^2+k_1^2)-k_1(\xi^2+k_2^2)}{\xi(2k_1-q_1)(\xi^2+k_2^2)+\xi(q_2-2k_2)(\xi^2+k_1^2)}\right)J_1(r_{mi}\xi)[\frac{r_j}{a}J_1(r_j\xi)-\frac{r_{j-1}}{a}J_1(r_{j-1}\xi)]d\xi \tag{C6}$$

u'_{ij} : by using Eq. (5.45) we have:

for j=1 and i=1, 2, …, n:

$$u'_{i1}(r_{mi},0)=\int_0^{\infty}\left(\frac{k_2q_1-k_1q_2}{(2k_1-q_1)(\xi^2+k_2^2)+(q_2-2k_2)(\xi^2+k_1^2)}\right)\xi J_1(r_{mi}\xi)\left[\int_0^{r_1}\frac{r}{a}J_1(\xi r)dr\right]d\xi \tag{C7}$$

and for j=2,3,…,n and i=1,2,…,n:

$$u'_{ij}(r_{mi},0)=\int_0^{\infty}\left(\frac{k_2q_1-k_1q_2}{(2k_1-q_1)(\xi^2+k_2^2)+(q_2-2k_2)(\xi^2+k_1^2)}\right)\xi J_1(r_{mi}\xi)\left[\int_{r_{j-1}}^{r_j}\frac{r}{a}J_1(r\xi)dr\right]d\xi \tag{C8}$$